HOKKAIDO UNIVERSITY

Title	Development of Caged Phosphine Ligands for Transition Metal Catalysis
Author(s)	小西, 菖太
Citation	北海道大学. 博士(理学) 甲第13276号
Issue Date	2018-06-29
DOI	10.14943/doctoral.k13276
Doc URL	http://hdl.handle.net/2115/71328
Type	theses (doctoral)
File Information	Shota_Konishi.pdf

Instructions for use

Hokkaido University Collection of Scholarly and Academic Papers : HUSCAP

Development of Caged Phosphine Ligands for Transition Metal Catalysis

Shota Konishi

2018

Table of Contents

General Introduction

1. Phosphorus Ligands for Transition Metal Catalysis

1.1. Introduction

Trivalent phosphorus compounds are widely used as ancillary ligands in transition metal catalysts (Figure 1). They strongly coordinate to many transition metals to form complexes. Ligands on the transition metal catalysts greatly influence their reactivity by changing electronic and steric conditions[1]. Therefore, ligand design is important for producing highly active catalysts and for developing new reactions.

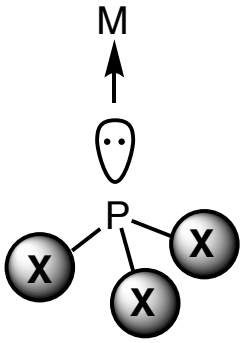

Figure 1. Coordination of trivalent phosphorus compounds

1.2. Electronic Parameters of Phosphorus Ligands

Parameters to judge the electron donating ability of the ligands are reported. Strohmeier and Müller reported that wave numbers of A_1 stretching vibration of CO (ν_{CO}) in IR spectrum of the 1:1 type complex $Ni(CO)_3(PX_3)$ synthesized from a phosphorus ligand and $Ni(CO)_4$ correlate to the donor ability (Figure 2a)[2]. The parameter was further developed by Tolman[3]. Ligands with stronger donating ability have stronger back donations from Ni to CO, which weaken CO bonds, showing lower ν_{CO} value. This value of ν_{CO} is called Tolman Electronic Parameter. Values for representative phosphorus ligands are shown in Figure 2c.

Donor abilities of phosphines also correlate to the $^1J_{P-Se}$ coupling constant of corresponding phosphine selenide on ^{31}P NMR (Figure 2b)[3,4]. However, the $^1J_{P-Se}$ value is influenced by steric factors. Thereby, applicability of this method is limited.

(a)

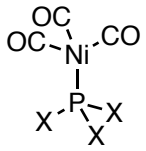

(b)

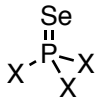

(c)

L	ν_{CO} (cm^{-1})	$^1J_{P\text{-}Se}$ (Hz)
P*t*Bu$_3$	2056.1	687
PEt$_3$	2061.7	684
P(4-MeO-C$_6$H$_4$)$_3$	2066.1	714
P(4-Me-C$_6$H$_4$)$_3$	2066.7	720
P(2-Me-C$_6$H$_4$)$_3$	2066.6	706
P(4-F-C$_6$H$_4$)$_3$	2071.3	743

Figure 2. (a) Nickel–Phosphine 1:1 type complex $Ni(CO)_3(PX_3)$. (b) Phosphine selenides (c) Tolman electronic parameter (ν_{CO}) and $^1J_{P-Se}$ coupling constant of representative phosphines.

1.3. Steric Parameters of Phosphorus Ligands

Bulkiness of the ligand is a factor that influences not only a steric environment around the metal but also dissociation equilibrium of the ligand. Tolman proposed an index called "cone angle" to compare bulkiness of phosphorus ligands. Cone angle is calculated using a space-filling model of phosphorus ligands. Tolman defined cone angle as "apex angle of a cylindrical cone, centered 2.28 Å from the center of the P atom, which just touches the van der Waals radii of the outermost atoms of the model"[5]. Cone angle of $PX_1X_2X_3$ can be measured as indicated in Figure 3 and Eq 1, by using a model to minimize the sum of half-angles.

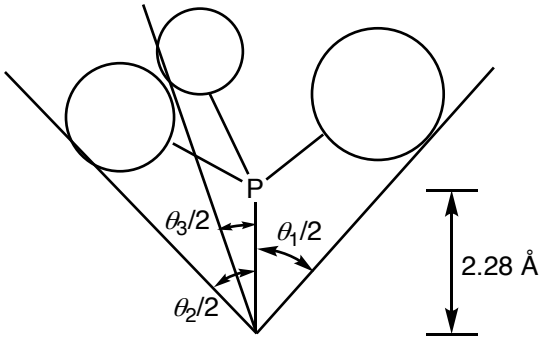

Figure 3. Method of measuring cone angles for phosphine ligands.

$$\Theta = (2/3) \sum_{i=1}^{2} \theta_i/2 \qquad (1)$$

2. Design of Highly Active Palladium Catalysts for Cross-coupling reactions

Pd-catalyzed cross-coupling reactions are useful reactions capable of forming carbon-carbon and carbon-heteroatom bonds from aryl halides and various nucleophiles. Early Pd-catalyzed cross-coupling reactions did not proceed efficiently with aryl chlorides, which are poor in reactivity as compared with aryl bromides or iodides. A remarkable development of the ligand enabled the reaction of aryl chloride. In 1998, Fu and co-workers reported that the combination of P*t*Bu$_3$ and palladium efficiently catalyze Suzuki–Miyaura coupling of aryl chlorides[6]. In the same year, Buchwald and co-workers reported that *o*-(dialkylphosphino)biphenyl derivatives are also effective[7]. Since these breakthroughs, various Pd catalysts capable of cross-coupling reaction of aryl chlorides have been reported. Herein, the development of phosphorus ligands to produce highly active Pd catalysts is shown by taking the Suzuki–Miyaura coupling reaction of aryl chloride as an example.

2.1. Alkylphosphines for Pd-catalyzed cross-coupling

These days, bulky and electron donating alkyl phosphines became common ligands for producing highly active palladium catalysts. The high electron donating ability increases the electron density of Pd (0) to promote rate-limiting oxidative addition (Scheme 1). In addition, it was found by computational[8] and experimental methodology[9] that the formation of coordinatively unsaturated Pd(0):P = 1:1 complex is important for the oxidative addition process of aryl chloride. Bulkiness of the ligand is favorable for the formation of Pd(0):P = 1:1 complex because excess coordination is suppressed.

Scheme 1. The mechanism of palladium catalyzed Suzuki-Miyaura cross-coupling of chloroarenees.

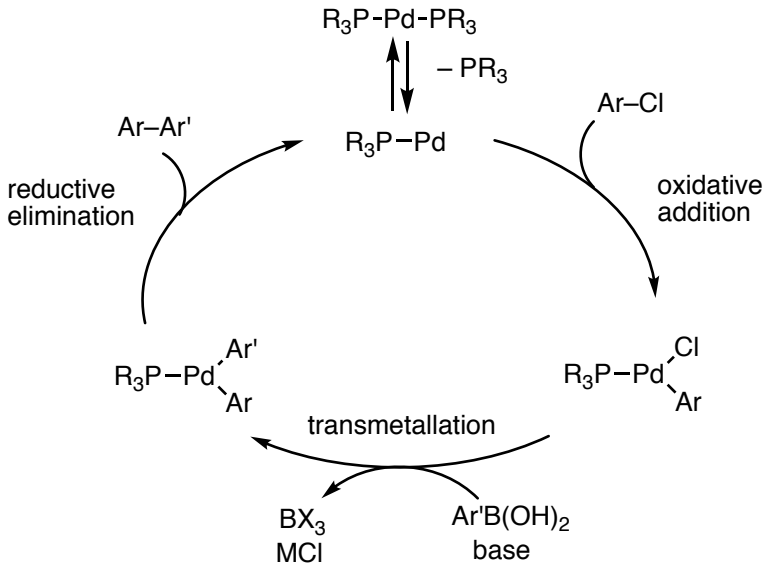

2.1.1. Tri-tert-butylphosphine

Fu *et al.* reported that tri-tert-butylphosphine is an effective ligand for Suzuki–Miyaura coupling catalyzed by Pd catalyst. Tri-tert-butylphosphine has bulky tert-butyl group on phosphorus atom, which not only increase donor ability but also prevent overcoordination. This catalyst can promote the coupling reaction even with electron deficient or rich aryl chloride (scheme 2).

Scheme 2. Suzuki-Miyaura coupling of chloroarene with tri-tert-butylphosphine.

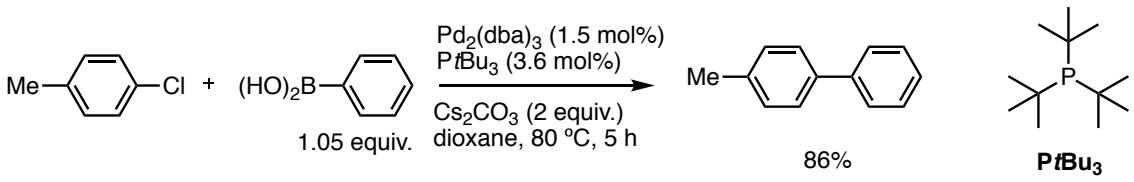

2.1.2. Buchwald-type biarylphosphines

In 1998, Buchwald found that a Pd catalyst with biarylphosphine **L1** caused Suzuki –Miyaura coupling of aryl chloride at room temperature. After that, Buchwald and colleagues have developed various biarylphosphine derivatives widely used for various coupling reactions (scheme3).

Scheme 3. Suzuki-Miyaura coupling of chloroarene with **L1**

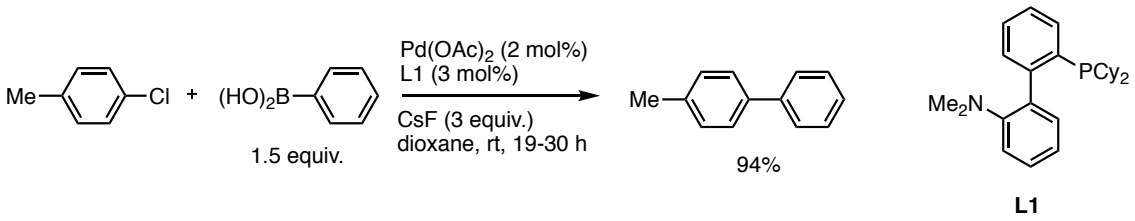

Figure 4 shows features of these ligands. The bulky alkyl substituents on the phosphorus atom increase the electron-donating ability of the ligand. Formation of a 1:1 complex with Pd is also preferred due to its bulkiness. The aryl group at the ortho position interacts with Pd to stabilize the complex and promote reductive elimination (figure 4).

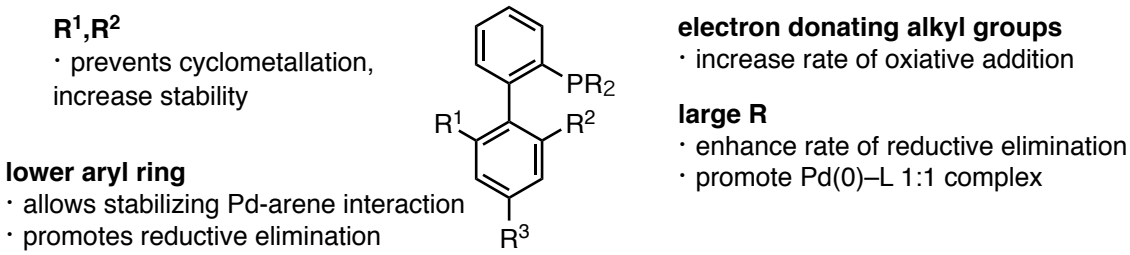

Figure 4. Schematic illustration of the features of *o*-biarylphosphines

2.2. Triarylphosphines for Pd-catalyzed cross coupling

Triarylphosphines are moderately electron donating. Although they are generally not effective in palladium-catalyzed cross coupling of aryl chloride, Fu *et al.* found the bulky phosphine **L2** is effective ligand for Suzuki-Miyaura coupling of chloroarenes (scheme 4).[10] This example indicates strong electron donor ability is not an essential factor.

Scheme 4. Suzuki-Miyaura coupling of chloroarene with **L2**

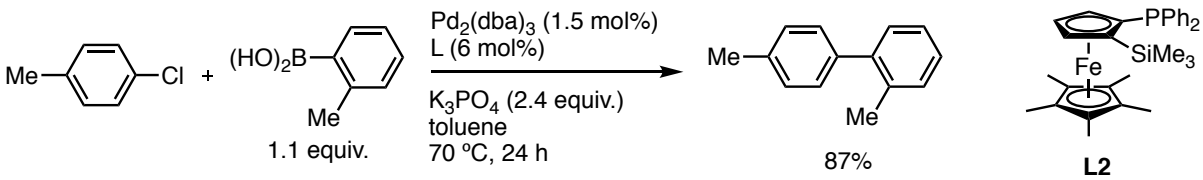

2.2.1. Bowl-Shaped Phosphines

Bowl-shaped phosphines have bulky substituents at the periphery of the phosphine.[11a] The steric hindrance in the vicinity of the coordination point is small, while it has large cone angle. Because of steric repulsion, this ligand suppresses excessive coordination with respect

to metals and preferentially forms a 1:1 complex with a metal[11b]. Tsuji reported that the ligand **L3** is effective for Suzuki–Miyaura coupling of aryl chlorides despite triarylphosphine (Scheme 5)[11c].

Scheme 5. Suzuki-Miyaura coupling of chloroarene with the bowl-shaped phosphine.

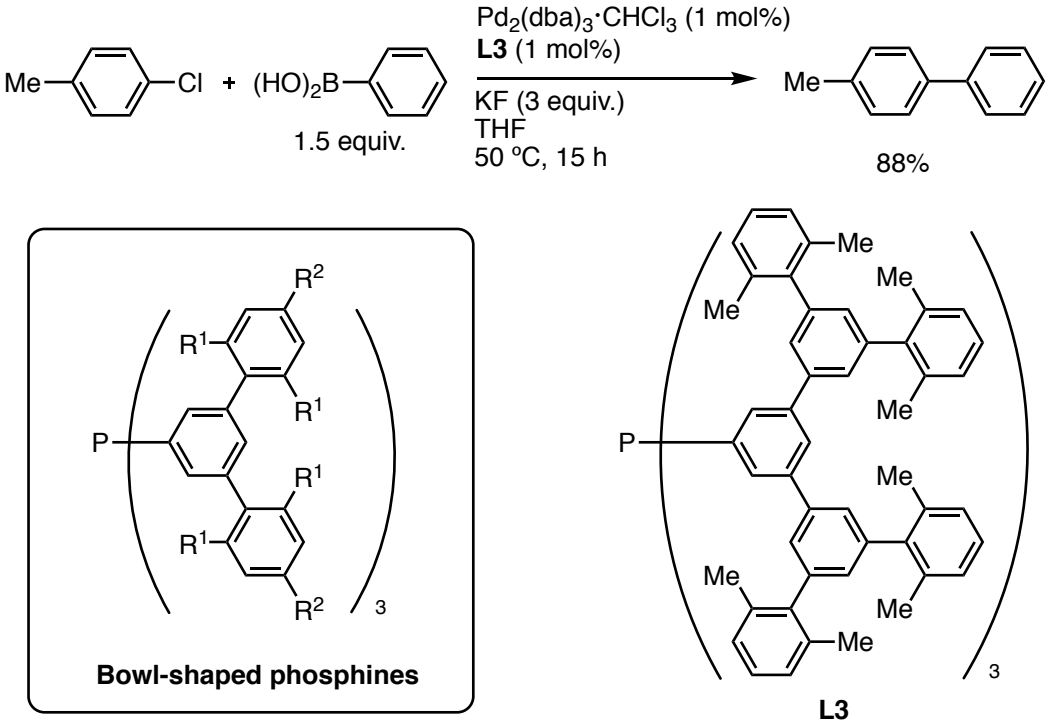

2.2.2. Triarylphosphines with dendritically arranged tetraethylene glycol moieties

Tsuji synthesized a triarylphosphine (**L4**, scheme 6) whose periphery was dendritically functionalized with tetraethylene glycol (TEG) moiety[12]. The Pd catalyst with **L4** is effective for Suzuki-Miyaura coupling of aryl chlorides in THF (scheme 6). It is considered that coordinatively unsaturated catalytically active species are generated due to the steric size around the ligand.

Scheme 6. Suzuki-Miyaura coupling of chloroarene with **L4**.

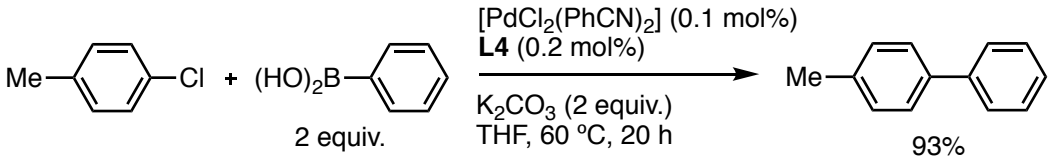

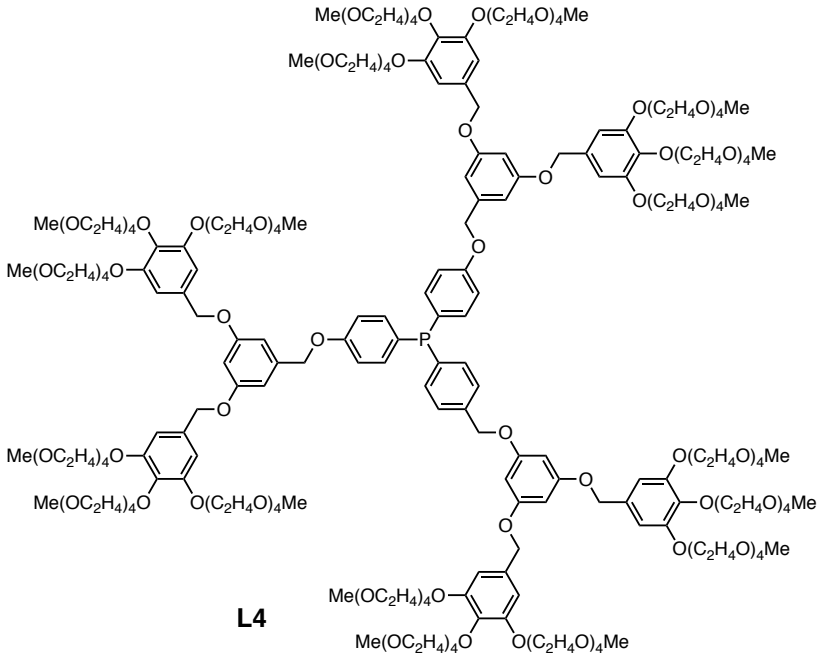

2.2.3. Threefold Cross-Linked Polystyrene–Triphenylphosphane Hybrids

Sawamura *et al.* developed heterogenious triarylphosphine ligands. A phosphine unit was introduced as the threefold cross-linker in the polystyrene resin[13]. Complexation experiments using CP/MAS solid state NMR showed that this ligand can selectively form a 1: 1 complex with Pd. In the vicinity of the triple crosslinking site part, the density of the polymer chain is high, and it is considered that multiple coordination does not occur because the phosphine moieties are difficult to approach each other. The Suzuki–Miyaura coupling of 4-chlorotoluene proceeded with a yield of 95% with a Pd complex having threefold crosslinked PS-3p-TPP. On the other hand, PS-2p-TPP with two-point crosslinking PS-1p-TPP with a single point grafting gave only 52% and 6% yields, respectively. The selective formation of 1:1 complexes by three-point-crosslinking is important for high activity (scheme 7)

Scheme 7. Suzuki-Miyaura coupling of 4-chlorotoluene and phenylboronic acid with polystyrene-crosslinking phosphines**.**

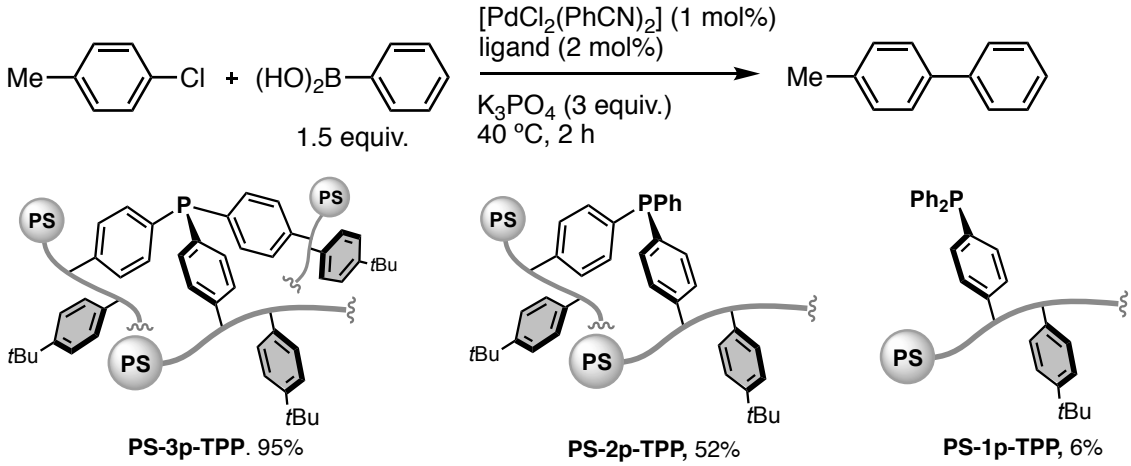

PS-3p-TPP. 95% **PS-2p-TPP**, 52% **PS-1p-TPP**, 6%

3. Caged Phosphorous Ligands

3.1. Features of caged molecule

This section deals with ligands having a phosphorus atom at the bridgehead position of the cage structures. Bicyclic cage structures give caged phosphorus ligands unique features owing to limited degree of freedom. First, steric effects and three-dimensional environment of the ligand can easily be controlled. Second, electronic properties of the phosphorus atom can be potentially tuned by the bridgehead atom at the side opposite to the phosphorus atom because its location is fixed near the phosphorus atom, it can affect the reactivity of the phosphorus atom. Examples of ligands having these features are shown below.

3.2. Sterical features of caged ligands

3.2.1. Phosphabarrelenes

Breit and co-workers developed benzophosphabarelenes via a [4+2] cycloaddition reaction of the phosphabenzene with benzyne (scheme 8). Due to the rigid cage structure, the substituent at the α position gives an adequate and rigid stereo environment near the central metal[14].

Scheme 8. The synthesis of **L5**.

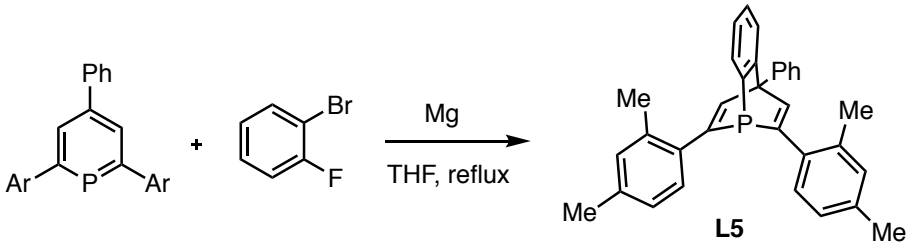

L5

A Rh catalyst with this ligand showed a high catalytic activity on hydroformylation of the internal alkene without causing isomerization of the alkene (Scheme 9).

Scheme 9. Rhodium–**L5**-catalyzed hydroformylation of the internal alkene.

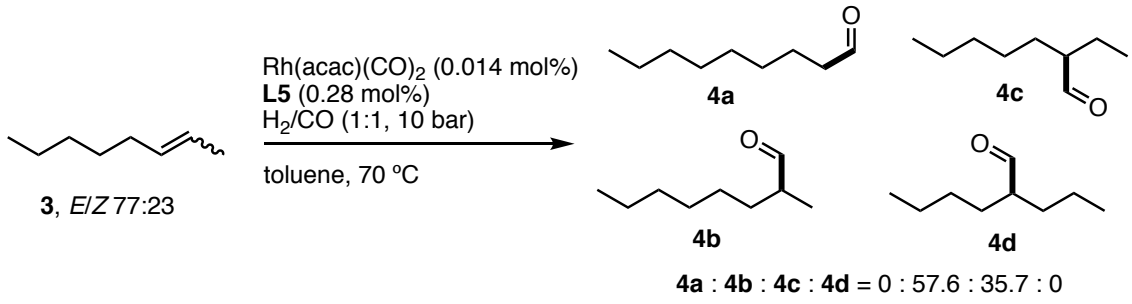

3.2.2. Bicyclic Phosphites

Caged phosphites with a [2.2.2]-fused structure are synthesized by Verkade, Reynolds et al. (Figure 5) in 1960[15a]. The substituents on the phosphorus are constrained in the cage structure. As a result, this phosphorus ligand has a smaller cone angle than trimethylphosphite[5].

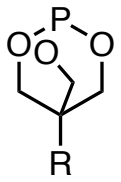

Figure 5. The structure of [2.2.2] fused bicyclic phosphites.

3.3. Effects of bridgehead atoms

3.3.1. Proazaphosphatranes

Verkade and co-workers developed proazaphosphatranes, which have a [3.3.3]-fused triaminophosphine structure.[16a] The three nitrogen atoms attached to the bridgehead phosphorus atom adopt nearly planar geometry, indicating significant donation of the N lone pair to the phosphorus atom. The bridgehead N atom is bound at the backside of the phosphorus atom, so that the nitrogen atom can donate electrons through a transannular orbital interaction with the phosphorus atom (figure 6). As a result, these phosphorus compounds show extremely high basicities and are used as organic superbases.[16b] These compounds are excellent ligands for Pd-catalyzed cross-coupling of chloroarenes, such as Suzuki–Miyaura coupling[16c], Stille coupling[16d], Buchwald–Hartwig amination[16e] and α-arylation of nitriles[16f].

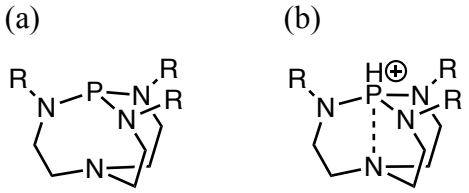

Figure 6. Free (a) and protonated form (b) of proazaphosphatranes.

3.3.2. Phosphatriptycenes

A tryptycene-type molecule having phosphorus atom at the bridgehead have been reported. Azaphosphatriptycene was reported by Hellwinkel *et al.* in 1969 (Figure 7a). [17a] Diphosphatriptycene (Figure 7b)[17b] and phosphatriptycene (Figure 7c)[17c] were reported in 1971 and 1974, respectively. Kawashima synthesized an oxy-functionalized phosphatriptycene derivative (Figure 7d), This ligand has lower σ-donor property than triphenylphosphine as proved by the CO stretching vibration of the tungsten carbonyl complex and $^{1}J_{\text{P-Se}}$ value of corresponding phosphine selenide.[17d] Tamao and Tsuji synthesized various 9-sila-10-phosphatriptycene derivatives (Figure 7d). The substituents on the bridgehead-silicon atom did not influence the σ-donor ability of the phosphines.[17e]

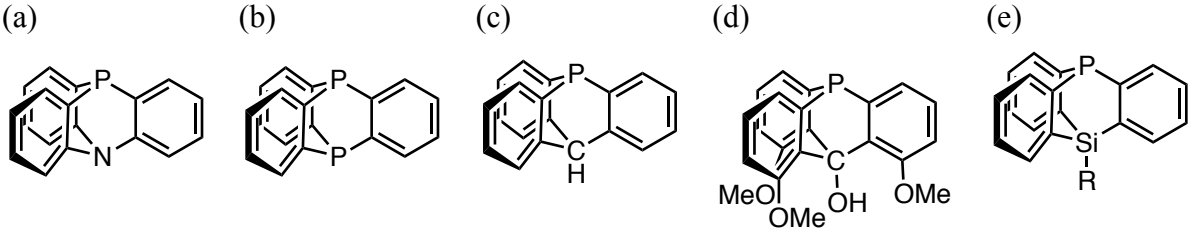

Figure 7. Examples of phosphatriptycene derivatives.

3.3.3. Silicon-constrained caged trialkylphosphines

Sawamura reported cage shaped trialkylphosphine constrained by a silicon atom.[18a] Having a cage shape, it is as compact as PMe_3 (figure 8a). The substituent on the silicon is fixed to the opposite side of the lone electron pair of the bridgehead phosphorus. Substituents at the bridgehead Si atom of the SMAP derivatives had significant impact on electron-donor power of the P lone pair due to long range orbital interactions in the rigid cage system. (figure 8b).[18b]

(a) (b)

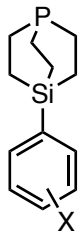

X	$^1J_{P\text{-}Se}$ (Hz)
4-NMe_2	729.3
H	735.4
3,5-$(CF_3)_2$	739.1

Figure 8. (a) Structure of SMAPs. (b) $^1J_{P\text{-}Se}$ coupling constants of corresponding SMAP selenides.

3.3.4. Immobilization of caged trialkylphosphines on solid supports

3.3.4.1. Immobilization on gold surface

Caged trialkylphosphine (SMAP) immobilized on gold surface ([Au]-SMAP) was developed by Hara, Sawamura and co-workers[19]. The phosphine molecules with an alkanethiolate linkers form a self-assembled monolayer on the gold surface.

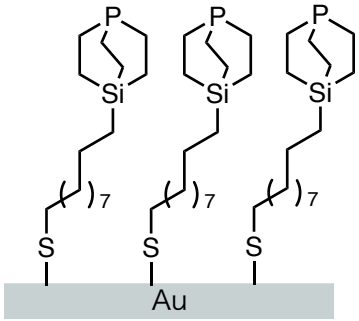

Figure 9. The structure of [Au]-SMAP.

The Au-SMAP–rhodium complex showed high catalytic activity to dehydrogenative silylation of alcohols with hydrosilane(table 1). The catalyst was easy to separate from the reaction mixture after the reaction, and could be recycled at least four times. The silylation reaction proceeded selectively with primary alcohols in the presence of secondary alcohols. The highly selectivity is attributed to the steric congestion of the catalytic environment, which exists in a densely packed rhodium–phosphane assembly.

Table 1. [Au]-SMAP–Rh-catalyzed primary alcohol selective silylation.

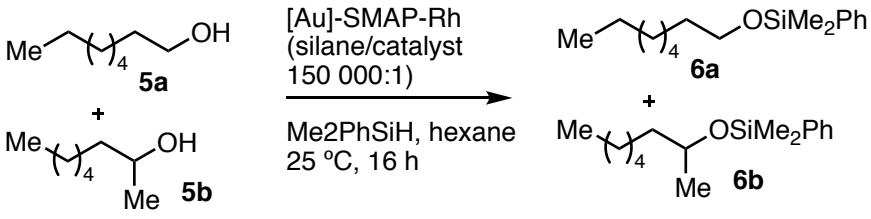

	yield (%)	TON	**6a/6b**
1st run	60	90000	>99.5:0.5
2nd run	58	87000	>99.5:0.5
3rd run	55	83000	>99.5:0.5
4th run	50	75000	>99.5:0.5

3.3.4.2. Immobilization on silica gel

Sawamura *et al.* reported a ligand in which the silicon moiety of cage type trialkylphosphine was immobilized on silica gel.[20] Since the cage-type skeleton is rigid, the lone pair of the phosphorus atom is always fixed upward with respect to the silica surface, so that the transition metal complex is not sterically hindered by the silica surface (Figure 10). In addition, it was shown that silica-SMAP can selectively form a complex with Rh:P = 1:1 even though it is a compact ligand. Since the steric hindrance of the ligand is small, the coordination unsaturated complex obtained is considered to have an open reaction space.

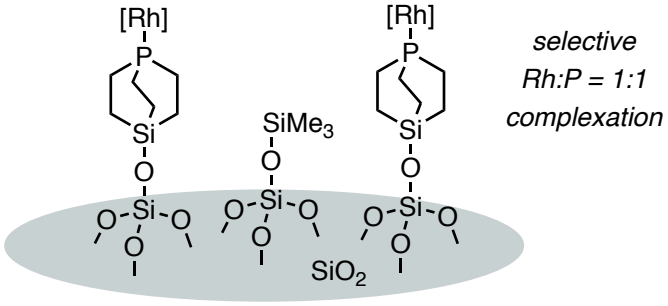

Figure 10. The structure of Silica-SMAP.

3.3.4.2.1. Silica-SMAP–Pd Catalyzed Borylation of Chloroarenes

Silica-SMAP-palladium catalyst was effective for palladium-catalyzed Miyaura borylation reaction of aryl chlorides (Eq. 2).[21] Selective formation of a Pd:P = 1:1 complex is considered to be the key for high reactivity on the activation of C–Cl bond. Even very bulky aryl chlorides were applicable for this catalyst system. The substrates are accessible to the reaction center due to the very compact nature of Silica-SMAP.

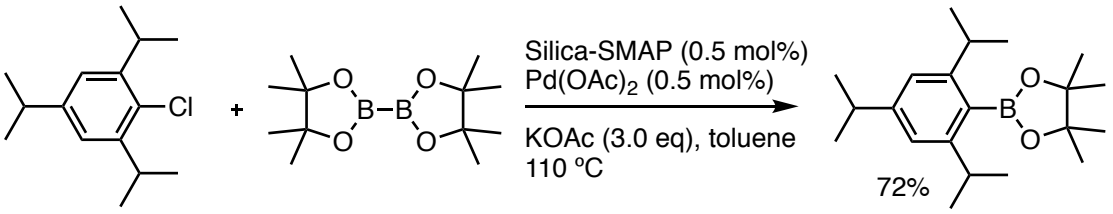

3.3.4.2.2. Silica-SMAP–Ir Catalyzed Direct Borylation of C–H bonds

In 2002, Ishiyama, Miyaura, Hartwig *et al.* reported direct borylation reaction of C(sp^2)–H bonds of aromatic compounds with iridium–bipyridine based catalyst.[22a-b] This reaction proceeds preferentially at the C–H bonds with less steric hindrance react. Sawamura and co-workers found that selective C–H borylation at the position ortho to the coordinative functional groups proceed with Silica-SMAP-Ir complex (eq. 3).[23a-c]

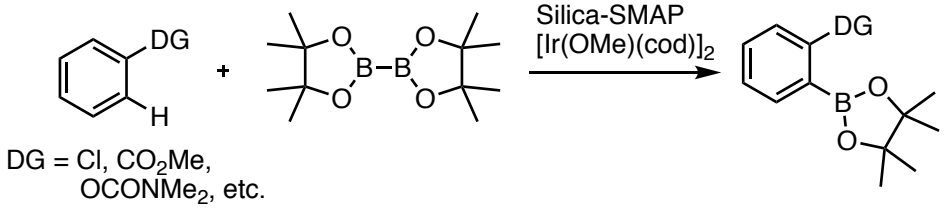

It is proposed that triboryl iridium complex is an active species in the reaction using Ir-bipyridine type catalyst (Figure 11a).[22b] On the other hand, when using monodentate phosphine Silica-SMAP, one more vacant coordination site is formed, and cleavage of the C–H bond and the coordination of a functional group occars at the same time, resulting in regioselectivite reaction at the position ortho to the functional group (figure 11b).

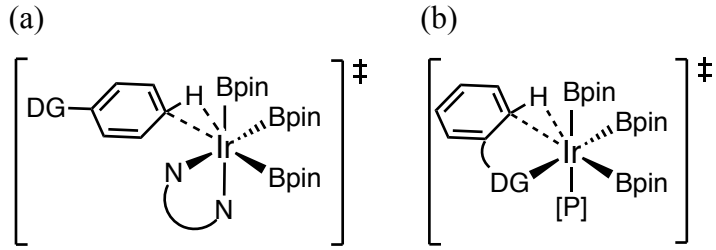

Figure 11. Proposed C–H bond activating transition states with triboryliridium complexes.

It was also found that the silica-SMAP-Ir catalyst undergoes a selective borylation reaction of inactive C(sp^3)–H bond. In 2-alkylpyridines, the primary or secondary C(sp^3)–H bond located γ to the pyridine nitrogen atom was selectively borylated (eq4).[23d]

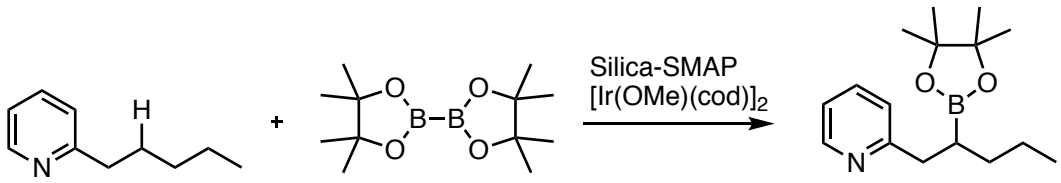

4. Overview of This Thesis

The author focused on the structural feature of caged phosphine ligands. Caged phosphine-based transition metal catalysts and its reactions were investigated. In chapter 1, Silica-SMAP–Ir catalyst system was applied for the site-selective borylation of quinoline derivatives. In chapter 2, synthesis and coordination property of a silica-supported triptycene-type caged phosphine ligand and its application to Suzuki-Miyaura coupling are described. Chapter 3 describes the synthesis of a caged phosphine containing a borate moiety and its reactivities.

Chapter 1 describes C-8 selective direct C–H borylation of quinolines using Silica-SMAP–iridium catalyst system. This reaction enabled direct, regioselective introduction of the boron functional group into the quinoline ring to give various 8-quinoline boronic acids, which can be used as versatile synthetic intermediate for 8-substituted quinoline derivatives. This method could be used for shortened synthesis of the highly functionalized quinoline compound, which is reported as a CRF1 receptor antagonist.

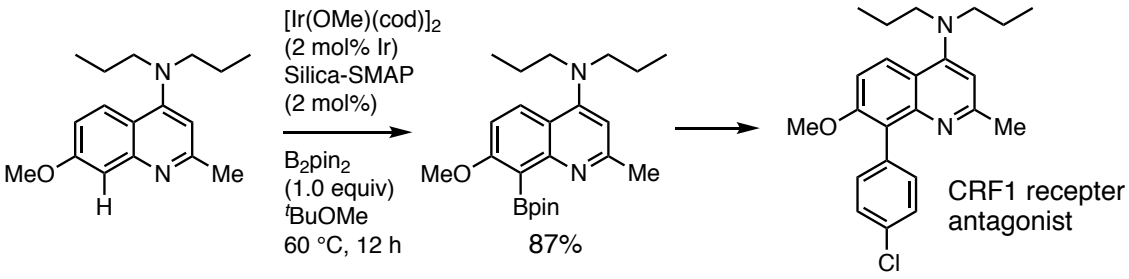

Chapter 2 describes Silica-TRIP with cageed triarylphosphine immobilized on silica. The complexation behavior of Silica-TRIP ligand with Pd was analyzed. Silica-TRIP was used for complexation with a Pd complex and the resulting complex was analyzed by solid state ^{31}P CP/MAS NMR. The Pd:P = 1:1 type complex was selectively formed even when excess Silica-TRIP was applied. Silica-TRIP found out to be effective ligand to promomote the Pd-catalyzed cross-coupling between arylchlorides and arylboronic acids. The reaction did not proceed in the corresponding homogeneous ligand.

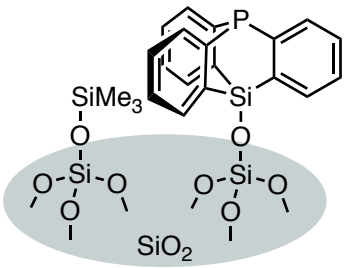

Silica-TRIP

Chapter 3 describes synthesis, property and catalytic application of a triptycene-type anionic borate-phosphine ligand **L-X** (X = Na or NBu_4). A negative charge at the bridgehead boron atom affected the donor-power of the phosphorus center. The coordination property of **L-X** to [PdCl(η^3-allyl)] was dependent on the counter cation, giving a neutral Pd complex [PdCl(η^3-allyl)(**L-NBu$_4$**)] from **L-NBu$_4$** in CH_2Cl_2 or a zwitterionic Pd complex [Pd(η^3-allyl)(MeCN)(**L**)] from **L-Na** in MeCN/CH_2Cl_2. Utility of **L-X** as a ligand for metal catalysis was demonstrated in the Pd-catalyzed Suzuki–Miyaura cross-coupling of aryl chlorides.

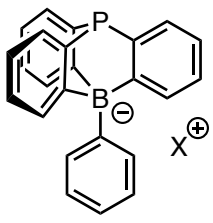

References

(1) Dias, P. B.; de Piedade, M. E. M.; Simões, J. A. M. *Coord. Chem. Rev.* **1994**, *135*, 737–807.

(2) Strohmeier, W.; Müller, F.-J. *Chem. Ber.* **1967**, 100, 2812–2821.

(3) Tolman, C. *J. Am. Chem. Soc.* **1970**, *92*, 2953–2956.

(4) (a) Pinnell, R. P.; Megerle, C. A.; Manatt, S. L.; Kroon, P. A. *J. Am. Chem. Soc.* **1973**, *95*, 977–978. (b) Allen, D. W.; Taylor, B. F. *J. Chem. Soc., Dalton Trans.* **1982**, 51–54.

(5) Tolman, C. *Chem. Rev.* **1977**, *77*, 313–348.

(6) Fu, G.C. *Acc. Chem. Res.* **2008**, *41*, 1555–1564.

(7) (a) Old, D. W.; Wolfe, J. P.; Buchwald, S. L. *J. Am. Chem. Soc.* **1998**, *120*, 9722–9723. (b) Martin, R.; Buchwald, S. *Acc. Chem. Res.* **2008**, *41*, 1461–1473.

(8) (a) Lam, K.; Marder, T.; Lin, Z. *Organometallics* **2007**, *26*, 758–760. (b) Ahlquist, M.; Norrby, P.O. *Organometallics* **2007**, *26*, 550–553.

(9) (a) Amatore, C. and Jutand, A. *J. Organomet. Chem.* **1999**, 576, 254–278. (b) Barrios-Landeros, F. and Hartwig, J. F. *J. Am. Chem. Soc.* **2005**, 127, 6944– 6945. (c) Barrios-Landeros, F., Carrow, B. P., and Hartwig, J. F. *J. Am. Chem. Soc.* **2009**, 131, 8141– 8154.

(10) Liu, S.-Y.; Choi, M.; Fu, G. *Chem. Commun.* **2001**, 2408–2409.

(11) (a) Goto, K.; Ohzu, Y.; Sato, H.; Kawashima, T. *Phosphorus, Sulfur, Silicon Relat. Elem.* **2002**, *177*, 2179. (b) Niyomura, O.; Iwasawa, T.; Sawada, N.; Tokunaga, M.; Obora, Y.; Tsuji, Y. *Organometallics* **2005**, *24*, 3468–3475. (c) Ohta, H.; Tokunaga, M.; Obora, Y.; Iwai, T.; Iwasawa, T.; Fujihara, T.; Tsuji, Y. *Org. Lett.* **2007**, *9*, 89–92.

(12) Fujihara, T.; Yoshida, S.; Ohta, H.; Tsuji, Y. *Angew. Chem. Int. Ed.* **2008**, *47*, 8310–8314.

(13) Iwai, T.; Harada, T.; Hara, K.; Sawamura, M. *Angew. Chem. Int. Ed.* **2013**, *52*, 12322–13226.

(14) (a) Breit, B.; Fuchs, E. *Chem. Commun.* **2004**, 694–695. (b) Fuchs, E.; Keller, M.; Breit, B. *Chem. Eur. J.* **2006**, *12*, 6930–6939.

(15) Verkade, J. G.; Reynolds, L. T. *J. Org. Chem.* **1960**, *25*, 663–665.

(16) (a) Laramay, M. A. H.; Verkade, J. G. *Z. Anorg. Allg. Chem.* **1991**, *605*, 163–174. (b) Arumugam, S; Verkade, J. G. *J. Org. Chem.* **1997**, *62*, 4827–4828. (c) Urgaonkar, S.; Nagarajan, M.; Verkade, J. G. *Tetrahedron Lett.* **2002**, *43*, 8921–8924. (d) Su, W.; Urgaonkar, S.; McLaughlin, P. A.; Verkade, J. G. *J. Am. Chem. Soc.* **2004**, *126*, 16433–16439. (e) Urgaonkar, S; Verkade, J. G. *Org. Lett.* **2003**, *5*, 815–818. (f) You, J.; Verkade, J. G. *Angew. Chem. Int. Ed.* **2003**, *42*, 5051 –5053.

(17) (a) Hellwinkel, D.; Schenk, W. *Angew. Chem. Int. Ed.* **1969**, *8*, 987–988. (b) Weinberg, K. B.; Whipple, E. G. *J. Am. Chem. Soc.* **1971**, *93*, 1801–1802. (c) Jongsma, C.; De Kleijn, J. P.; Bickelhaupt, F. *Tetrahedron* **1974**, *30*, 3465. (d) Kobayashi, J.; Agou, T.; Kawashima, T. *Chem Lett* **2003**, *32*, 1144–1145. (e) Tsuji, H.; Inoue, T.; Kaneta, Y.; Sase, S.; Kawachi, A.; Tamao, K. *Organometallics* **2006**, *25*, 6142–6148.

(18) (a) Ochida, A.; Hara, K.; Ito, H.; Sawamura, M. *Org. Lett.* **2003**, *5*, 2671–2674. (b) Ochida, A.; Ito, S.; Miyahara, T.; Ito, H.; Sawamura, M. *Chem. Lett.* **2006**, *35*, 294–295.

(19) Hara, K.; Akiyama, R.; Takakusagi, S.; Uosaki, K.; Yoshino, T.; Kagi, H.; Sawamura, M. *Angew. Chem. Int. Ed.* **2008**, *47*, 5627–5630.

(20) Hamasaka, G.; Ochida, A.; Hara, K.; Sawamura, M. *Angew. Chem. Int. Ed.* **2007**, *46*, 5381–5383.

(21) Kawamorita, S.; Ohmiya, H.; Iwai, T.; Sawamura, M. *Angew. Chem. Int. Ed.* **2011**, *50*, 8363–8366.

(22) (a) Ishiyama, T.; Takagi, J.; Ishida, K.; Miyaura, N.; Anastasi, N. R.; Hartwig, J. F. *J. Am. Chem. Soc.* **2002**, *124*, 390–391. (b) Ishiyama, T.; Takagi, J.; Hartwig, J. F.; Miyaura, N. *Angew. Chem., Int. Ed.* **2002**, *41*, 3056–3058.

(23) (a) Kawamorita, S.; Ohmiya, H.; Hara, K.; Fukuoka, A.; Sawamura, M. *J. Am. Chem. Soc.* **2009**, *131*, 5058–5059. (b) Kawamorita, S.; Ohmiya, H.; Sawamura, M. *J. Org. Chem.* **2010**, *75*, 3855–3858. (c) Yamazaki, K.; Kawamorita, S.; Ohmiya, H.; Sawamura, M. *Org. Lett.* **2010**, *12*, 3978–3981. (d) Kawamorita, S.; Murakami, R.; Iwai, T.; Sawamura, M. *J. Am. Chem. Soc.* **2013**, *135*, 2947–2950.

(24) Konishi, S.; Kawamorita, S.; Iwai, T.; Steel, P. G.; Marder, T. B.; Sawamura, M. *Chem. Asian J.* **2014**, *9*, 434–438.

(25) Iwai, T.; Konishi, S.; Miyazaki, T.; Kawamorita, S.; Yokokawa, N.; Ohmiya, H.; Sawamura, M. *ACS Catal.* **2015**, *5*, 7254–7264.

Chapter 1

C-8 Selective C–H Borylation of Quinolines Catalyzed by Silica-Supported Caged Trialkylphosphosphine–Iridium Complex

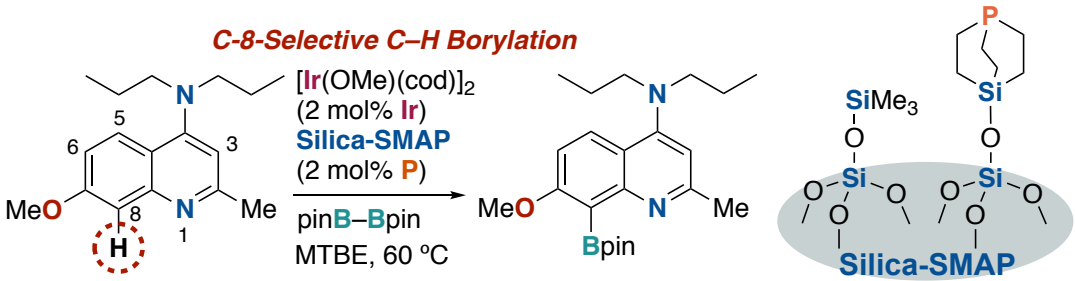

Site-selective C–H borylation of quinoline derivatives at the C8 position has been achieved by using a heterogeneous Ir catalyst system based on a silica-supported cage-type monophosphine ligand Silica-SMAP. The efficient synthesis of a corticotropin-releasing factor 1 (CRF_1) receptor antagonist based on a late-stage C–H borylation strategy demonstrates the utility of the C8 borylation reaction.

1. Introduction

The quinoline heterocyclic scaffold is an important structural motif that is found in many natural products, bioactive compounds, dyes, and other functional molecules, for example, Alq3 for OLEDs.[1-3] Accordingly, the development of efficient methods for accessing substituted quinolines is a subject of considerable importance. In particular, streamlining the synthetic process through the introduction of site selective direct functionalization of a quinoline C–H bond is highly desirable. Several methods that allow direct C–C bond formation at the C2 position of quinolines or quinoline N-oxides, using Rh,[4] Pd,[5] Ni,[6] Cu,[7] and Ag[8] catalyst systems, have been reported in recent years. The C2 selectivity of these catalysts is based on the inherent reactivity of the C=N bond or the N-adjacent C–H bond. In contrast, site-selective catalytic C–H transformation at the C8 position was only reported by Chang and coworkers. In their work, Rh–NHC (NHC = N-heterocyclic carbene) catalytic systems were used for C8 arylation with aryl bromides.[9–10]

Miyaura, Ishiyama, and co-workers reported that direct C–H borylation of quinoline occurred preferentially at the C3 position when an Ir–bipyridine-type (Ir–dtbpy; Hartwig–Ishiyama–Miyaura catalyst; dtbpy = 4,4-di-tert-butylbipyridine) catalyst was used, with a large excess of the quinoline substrate (10 equiv).[11] More recently, Marder and co-workers provided guidelines for achieving selective borylation at the C3, C4, C6, or C7 positions of disubstituted quinolines.[12] In contrast, access to the much desired quinoline-8-boronic acid has required multiple steps, which involve generation of the corresponding halide as an immediate precursor.[13]

In this chapter, Ir-catalyzed site-selective C–H borylation of quinoline derivatives with bis(pinacolato)diboron (pinB–Bpin, 2) is described. C8-selective borylation was effected by choosing silica-supported trialkylphosphine (Silica-SMAP) as a monodentate P ligand for Ir.[14–16] The borylation reaction proceeded under mild reaction conditions with excellentsite selectivity toward various substrates with different substitution patterns.

2. Results and Discussion

The reaction of quinoline **1a** (0.30 mmol) and diboron **2** (1.1 equiv) in methyl tert-butyl ether (MTBE) in the presence of an immobilized catalyst precursor (Ir, 2 mol%), prepared in situ from Silica-SMAP, and $[Ir(OMe)(cod)]_2$ (P/Ir, 1:1; cod = cycloocta-l,5-diene) proceeded at 60 ºC over 12 h with 94% consumption of **1a** (Scheme 1). The ^{1}H NMR spectrum of the crude product indicated that the major product was C8-borylated quinoline **3a**, which was contaminated with small amounts of reduced products, such as 1,2,3,4-tetrahydroquinoline (**4a**, 13% yield, analysis based on ^{1}H NMR

spectroscopy).[17] As the quinoline-8-boronic acid pinacol ester (**3a**) was unstable to hydrolysis,[18] the crude product was subjected to oxidation with $NaBO_3 \cdot 4H_2O$, followed by treatment with $(Boc)_2O$ (Boc = tert-butoxycarbonyl). This method afforded *O*-tert-butoxycarbonyl-8-hydroxyquinoline (**6a**) in 68% yield after purification by silica-gel chromatography. No other isomers were detected in the crude reaction mixture.

Scheme 1. Silica-SMAP–Ir catalyzed C–H borylation of quinoline.

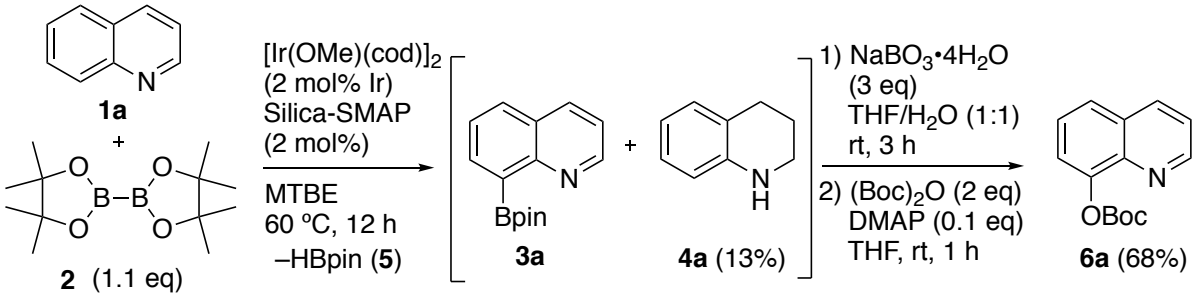

Based on the fact that the reaction of 2-substituted quinolines (see below) proceeded with exclusive selectivity, we assumed that Ir-catalyzed addition of the pinBH (**5**) byproduct across the C=N bond (hydroboration) of **1a** triggered reductive side reactions.[19] In fact, the reaction of **1a** with **5** (1.1 equiv) instead of **2**, under otherwise identical conditions, produced the C8-borylated product **3a** in only 17% yield, while giving the reduced product **4a** in an increased yield of 30% with 67% conversion of **1a** (analysis based on ^{1}H NMR spectroscopy).

The selective borylation at the C8 position is thought to be due to coordination of the ring nitrogen atom to the Ir catalyst center. This contrasts with previous directed (hetero) arene C–H borylation using Silica-SMAP, which required pendant functional groups as coordination-based directing moieties.[14c–e, g] The Ir center is most likely mono-P ligated and in a monomeric form because of the geometrical constraint of the directional phosphine molecule (SMAP) that is immobilized on the solid surface in a site-isolated fashion. Thus, C–H bond cleavage should occur through a four-membered iridacyclic reaction pathway. The corresponding Rh catalyst (Silica-SMAP/$[Rh(OMe)(cod)]_2$) did not yield the C8-borylated product (**3a**) with 60% consumption of **1a** under otherwise identical conditions, and instead gave a complex mixture containing the tetrahydroquinoline **4a** in 6% yield. The Ir-catalyzed borylation of **1a** did not proceed efficiently with other phosphine ligands shown in Figure 1. The use of silica-supported triarylphosphane ligand (Silica-TRIP),[20] a threefold-benzannulated analogue of Silica-SMAP, gave only a trace of **3a**. Homogeneous monodentate phosphine ligands such as Ph-SMAP,[21] PMe_3, PBu_3, PCy_3, P*t*Bu_3, PPh_3, and

XPhos (XPhos=2-dicyclohexylphosphino- 2',4',6'-triisopropylbiphenyl) induced no reaction or only trace reactions. No reaction occurred when a phosphine-free Ir system was used. These ligand effects indicate the crucial importance of both the SMAP structure and its immobilization on a solid surface. The method using the Silica–SMAP–Ir system was broadly applicable to substituted quinolines. The results of borylation of monosubstituted quinolines are summarized in Table 1.

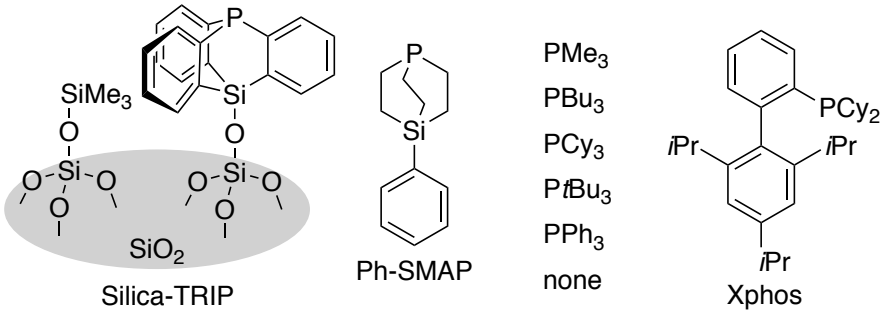

Figure 1. The ligands induced trace of no reaction.

C2 substituted substrates generally resulted in very clean C(8)–H borylation reactions without giving reduced side products. For example, 2-methylquinoline (**1b**, quinaldine) was converted into 8-borylquinaldine (**3b**) in 99% yield (86% yield after purification) without formation of a reduced heterocyclic compound (**4**) (Table 1, entry 1). In contrast, the reaction of **1b** with the Ir–dtbpy catalyst system gave the C4, C6, and C7 borylation products in 16%, 27%, and 20% yields, respectively, along with diborylation products.[11,12] It was possible to reduce the catalyst loading of the Silica–SMAP–Ir system to 0.05 mol% (Ir) upon scaling up this transformation (Table 1, entry 2). C8 borylation also proceeded cleanly, even with the sterically more demanding *n*Pr group (**1c**) at the C2 position (Table 1, entry 3). Furthermore, substitution with methoxy (**1d**) or N,N-diethylamino (**1e**) groups at the terminus of the C2 pendant chain was tolerated (Table 1, entries 4 and 5). In contrast, monosubstitution with Me or MeO groups at the C3 (**1f**), C4 (**1g**), and C6 (**1h**) positions, leaving the C2 position unsubstituted, did not cause a significant effect on the reaction profile of the parent quinoline **1a** (Table 1, entries 6–8).[22] These results strongly support the above-mentioned assumption that the C2 substituents blocked the undesired C=N reduction with **5**.

Table 1. Silica-SMAP-Ir catalyzed borylation of monosubstituted quinolines.[a]

entry	substrate	product	temp. (ºC)	yield (%)
1	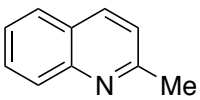 **1b**	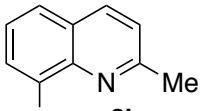 Bpin **3b**	50	86[b] (99)[c]
2[d]			80	91[b] (99)[c]
3	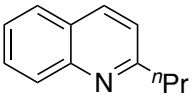 **1c**	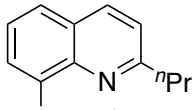 Bpin **3c**	50	80[b] (99)[c]
4	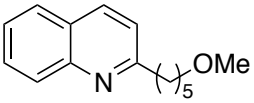 **1d**	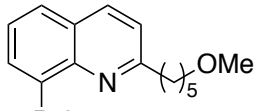 Bpin **3d**	50	74[b] (88)[c]
5	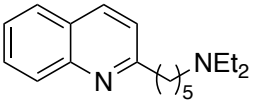 **1e**	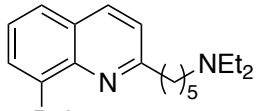 Bpin **3e**	50	81[b] (99)[c]
6	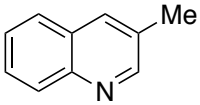 **1f**	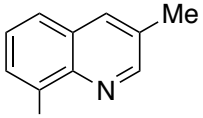 OBoc **6f**	60	61[e]
7	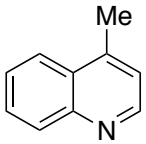 **1g**	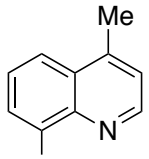 OBoc **6g**	60	71[e]
8	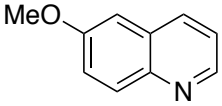 **1h**	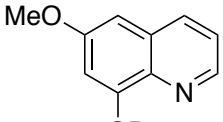 OBoc **6h**	60	60[e]

[a] The reaction was carried out with **1** (0.30 mmol), **2** (0.33 mmol), $[Ir(OMe)(cod)]_2$ (1 mol%) and Silica-SMAP (2 mol%) in MTBE (1.5 mL) for 12 h. Yields of purified boronates (**3**) are shown in parentheses. [b] Yield of isolated C8-borylated product **3**. [c] Yield of **3**, as determined by ^1H NMR spectroscopy of the crude product. [d] **1b** (6 mmol), **2** (6.6 mmol), $[Ir(OMe)(cod)]_2$ (0.025 mol%), and Silica-SMAP (0.05 mol%) in MTBE (1.5 mL), at 80 ºC for 12 h. [e] Yield of the isolated O-tert-butoxycarbonyl-8-hydroxyquinoline **6**.

The results of C8 borylation of mono- or disubstituted quinaldines (di- or trisubstituted quinolines) are summarized in Table 2. Reflecting the substituent effect at the 2-position, these substrates were converted cleanly into the corresponding C8 borylation products in high yields. Ring substitution with chlorine (Table 2, entries 1, 3, 6) or Boc-protected oxygen atoms (Table 2, entry 4) was not detrimental to the reaction. Importantly, the steric effects of substituents (Me, MeO, Cl) at the adjacent C7 position did not hamper C8 borylation (Table 2, entries 6–8).

Table 2. Silica-SMAP-Ir-catalyzed borylation of di- or trisubstituted quinolines.[a]

entry	substrate	product	temp. (ºC)	yield (%)[b]
1	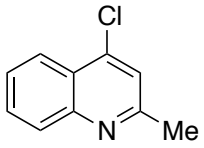 **1i**	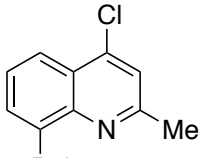 **3i**	60	81 (94)
2	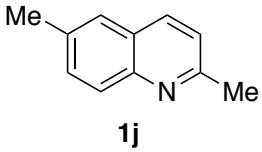 **1j**	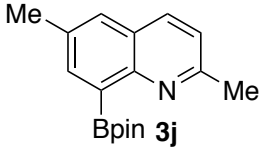 **3j**	50	86 (99)
3	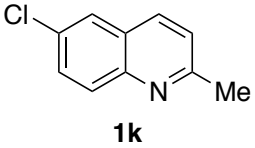 **1k**	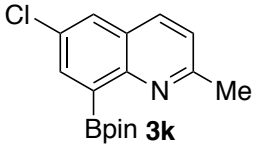 **3k**	60	79 (91)
4	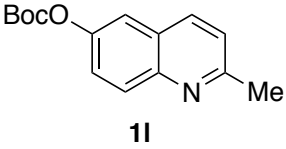 **1l**	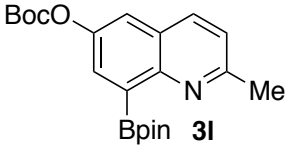 **3l**	50	76[c]
5	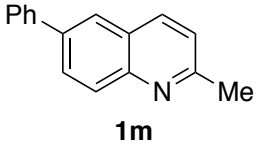 **1m**	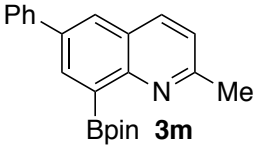 **3m**	60	71 (86)
6[d]	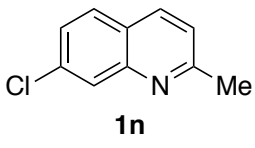 **1n**	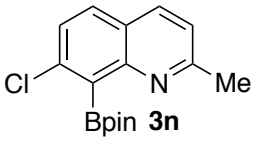 **3n**	60	84 (96)
7	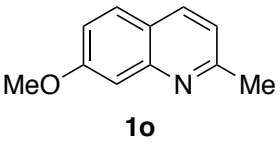 **1o**	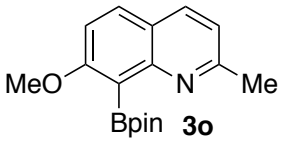 **3o**	50	86 (92)

8	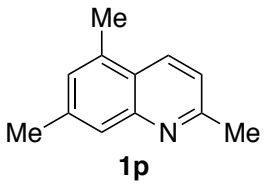 **1p**	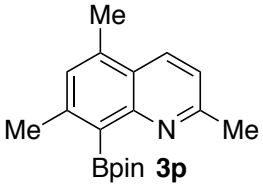 Bpin **3p**	50	84 (99)

[a] The reaction was carried out with **1** (0.30 mmol), **2** (0.33 mmol), $[Ir(OMe)(cod)]_2$ (1 mol%) and Silica-SMAP (2 mol%) in MTBE (1.5 mL) for 12 h. Yields of purified boronates (**3**) are shown in parentheses. [b] Yields of the purified boronates (**3**). Yields of **3** based on ^{1}H NMR analysis of crude products are shown in parentheses. [c] Yield of isolated arylation product **9l**. As the boronate **3l** was unstable, it was transformed into **9l** through Suzuki–Miyaura coupling with methyl 4-bromobenzoate under the conditions described in Scheme 2. [d] One equivalent of 2 was employed.

The molecular structure of **3n** was determined by single crystal X-ray diffraction analysis (Figure 2). No intra- or intermolecular interaction between the *N* lone pair and the boron atom was found in the solid-state structure.

Figure 2. Molecular structure of **3n**.

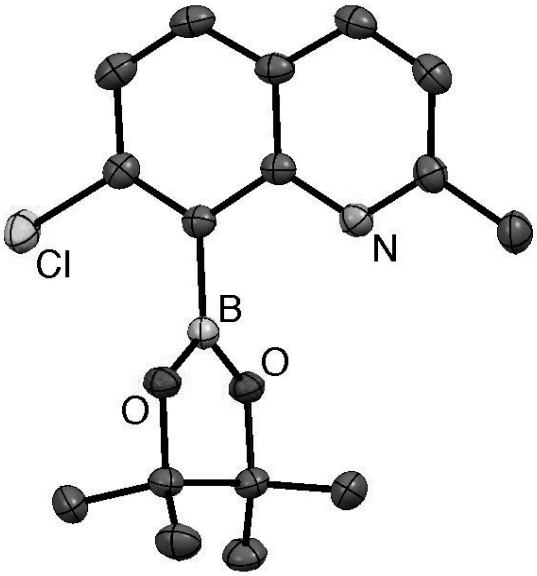

The reaction of 2,3-dimethylquinoxaline (**1q**) with 2.2 equivalents of **2**, catalyzed by the Silica–SMAP–Ir system, afforded the 5,8-diborylation-product **3q** in 62% yield, as shown in eq 1. The quinoxaline heterocyclic scaffold is a versatile structural motif found in various functional molecules with potential applications in the development of electronic and luminescent devices.[23]

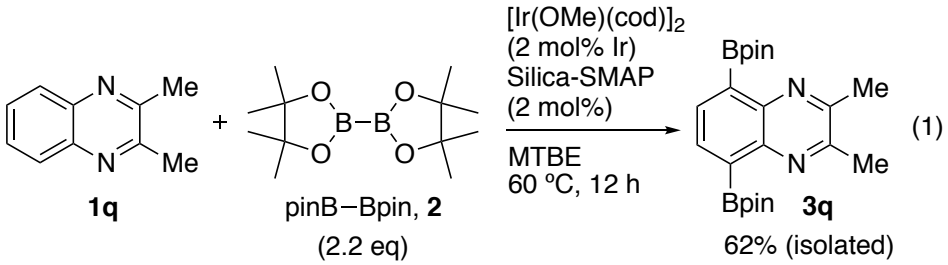

(1)

The C8-borylated quinaldine **3b** can be used for various transformations including oxidation,[24] one-carbon-homologation/oxidation sequence,[25] Rh-catalyzed Heck-type reaction,[26] and Suzuki–Miyaura coupling[27] (Scheme 2). The excellent yields of these transformations show the utility of C8-borylated quinoline derivatives as a point of structural diversification.

Scheme 2. Transformations of the C-8 borylation product **3b**.

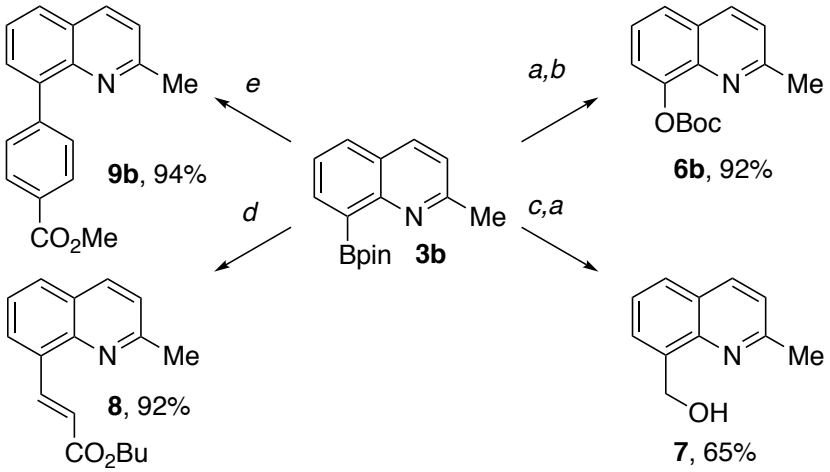

Conditions: [a] $NaBO_3 \cdot 4H_2O$ (3 eq) in THF/H_2O (1:1), rt, 3 h. [b] $(Boc)_2O$ (2 eq), DMAP (0.1 eq) in THF, rt, 1 h. [c] bromochloromethane (2 eq), *n*-BuLi (1.7 eq) in THF, –78 °C to rt, 1 h. [d] *n*-Butyl acrylate (5 eq), $[Rh(OH)(cod)]_2$ (2.5 mol%) in dioxane/H_2O (50:1), 90 °C, 16 h. [e] Methyl 4-bromobenzoate (1.5 eq), $Pd(PPh_3)_4$ (5 mol%), K_3PO_4 (3 eq) in THF/H_2O (5:1), 60 °C, 12 h.

The Silica-SMAP–Ir–catalyzed C8 Borylation showed a utility for late-stage functionalization of quinoline ring. A corticotropin-releasing factor 1 (CRF_1) receptor antagonist (**14**) was synthesized based on a late-stage C–H borylation strategy, as outlined in Scheme 3.[28] Commercially available 3-methoxyaniline (**10**) was transformed into 4-chloro-7-methoxyquinaldine (**11**) according to the literature.[29] Treatment of **11** with excess dipropylamine in the presence of TsOH furnished 4-dipropylamino-7-methoxyquinalidine (**12**) as a substrate for Ir-catalyzed C–H borylation. The reaction of **12** with one equivalent of diboron reagent **2** in the presence of the Silica–SMAP–Ir catalyst system (2 mol%) at 60 ºC over 12 h cleanly produced the desired C8-borylation product **13** (unpurified) with good site selectivity. Remarkably, the C–H bonds at the C3 and C5 positions, which are proximal to the dipropylamino group, were intact. Finally, Suzuki–Miyaura coupling between the boronate **13** and 4-bromochlorobenzene gave the CRF_1 receptor antagonist **14** (57% yield from **12**). The highly functionalized boronate **13** has the potential to be a versatile precursor for analogous 8- substituted quinoline derivatives.

Scheme 3. Synthesis of CRF_1 receptor antagonist based on a late-stage C–H borylation strategy.

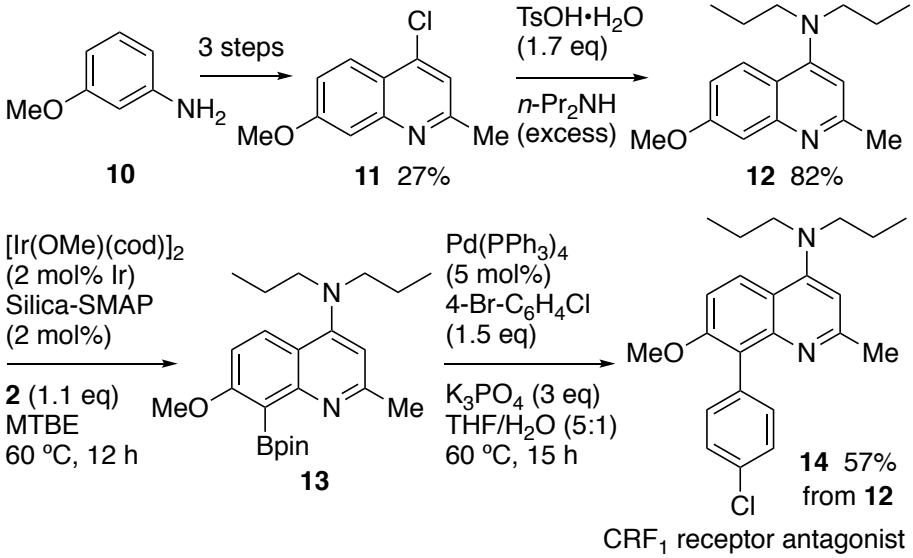

3. Conclusion

A heterogeneous Ir catalyst system based on the silica-supported cage-type monophosphane ligand Silica-SMAP enabled catalytic site-selective C–H borylation of quinolines at the C8 position, thereby complementing existing quinoline borylation methods using Ir–bipyridine-type catalysts. The synthesis of a CRF_1 receptor antagonist based on a late-stage C–H borylation strategy demonstrated the utility of the C8 borylation.

4. Experimental Section

4.1. Instrumentation and Chemicals

^1H (300 MHz) and ^{13}C (75.4 MHz) NMR spectra were recorded on a Varian Gemini 2000 spectrometer. ^{11}B (128 MHz) NMR spectra were recorded on a JEOL JNM-ECA spectrometer. Chemical shift values for ^1H, ^{13}C and ^{11}B are referenced to Me_4Si, the residual solvent resonances and BF_3•OEt_2, respectively. Chemical shifts are reported in δ ppm. High-resolution mass spectra were recorded on a Thermo Fisher Scientific Exactive, JEOL JMS-T100LP mass spectrometer or JEOL JMS-T100 GC mass spectrometer at the Instrumental Analysis Division, Equipment Management Center, Creative Research Institution, Hokkaido University. TLC analyses were performed on commercial glass plates bearing 0.25-mm layer of Merck Silica gel $60F_{254}$. Silica gel (Kanto Chemical Co., Silica gel 60 N, spherical, neutral) was used for column chromatography. GLC analyses were conducted on a Shimadzu GC-14B equipped with a flame ionization detector. Melting points were determined on a micro melting point apparatus (Yanaco: MP-500D) using micro cover glass.

All reactions were carried out under a nitrogen atmosphere. Materials were obtained from commercial suppliers or prepared according to standard procedures unless otherwise noted. $[Ir(OMe)(cod)]_2$ was prepared according to the literature.[30] Ph-SMAP,[21c] Silica-SMAP[14b] and Silica-TRIP[20b] were prepared with CARiACT Q-10® according to the reported procedure. CARiACT Q-10 (Catalyst grade, 75-150 μm) was purchased from Fuji Silysia Chemical Ltd. and dehydrated by heating at 150 ˚C for 10 h and stored in a glove box before use. All solvents for catalytic reactions were degassed via four freeze–pump–thaw cycles before use. Bis(pinacolato)diboron (**2**) was purchased from AllyChem Co., Ltd., and recrystallized from pentane before use.

4.2. Experimental Procedures

Typical Procedure for the Borylation of Quinoline (1a) with Immobilized Ligands (Scheme 1). In a glove box, Silica-SMAP (0.070 mmol/g, 85.7 mg, 0.006 mmol, 2 mol%),

bis(pinacolato)diboron (**2**) (83.8 mg, 0.33 mmol), and anhydrous, degassed MTBE (0.5 mL) were placed in a 10-mL glass tube containing a magnetic stirring bar. A solution of $[Ir(OMe)(cod)]_2$ (2.0 mg, 0.003 mmol, 1 mol%) in MTBE (1 mL), and quinoline (**1a**) (38.7 mg, 0.3 mmol) were added successively. The tube was sealed with a screw cap and removed from the glove box. The reaction mixture was stirred at 60 ºC for 12 h, and filtered through a glass pipette equipped with a cotton plug. Solvent was removed under reduced pressure. An internal standard (1,1,2,2-tetrachloroethane) was added to the residue to determine the yield of the product **3a** by ^{1}H NMR (51%). Next, the crude product (**3a**) and sodium perborate tetrahydrate (139 mg, 0.9 mmol) were added to a 10-mL glass tube containing a magnetic stirring bar, and the mixture was dissolved in a solution of THF (1.5 mL) and water (1.5 mL). The reaction mixture was stirred vigorously at room temperature for 3 h under air. The volatiles were removed under reduced pressure. Next, THF (3 mL), di-*tert*-butyl dicarbonate (131 mg, 0.6 mmol), and 4-(*N,N*'-dimethylamino)pyridine (3.7 mg, 0.03 mmol) were added successively to the tube. The reaction mixture was stirred for 1 h at room temperature. Solvent was removed under reduced pressure. The residue was then purified by silica gel chromatography to give **6a** (50.0 mg, 0.20 mmol in 68% isolated yield based on **1a**).

Typical Procedure for the Borylation of Quinoline (1a) with Soluble Ligands (Scheme 1). In a glove box, bis(pinacolato)diboron (**2**) (83.8 mg, 0.33 mmol) and anhydrous, degassed MTBE (0.18 mL) were placed in a 10-mL glass tube containing a magnetic stirring bar. A solution of Ph-SMAP (1.3 mg, 0.006 mmol, 2 mol%) in MTBE (0.32 mL), a solution of $[Ir(OMe)(cod)]_2$ (2.0 mg, 0.003 mmol, 1 mol%) in MTBE (1 mL), and quinoline (**1a**) (38.7 mg, 0.3 mmol) were added successively. The tube was sealed with a screw cap and removed from the glove box. The reaction mixture was stirred at 60 ºC for 12 h. Solvent was removed under reduced pressure. An internal standard (1,1,2,2-tetrachloroethane) was added to the residue to determine the yield of the product **3a** by ^{1}H NMR (<1% yield).

Typical Procedure for the Borylation of Quinoline Derivatives (Table 1, entry 1). In a glove box, Silica-SMAP (0.070 mmol/g, 85.7 mg, 0.006 mmol, 2 mol%), bis(pinacolato)diboron (**2**) (83.8 mg, 0.33 mmol), and anhydrous, degassed MTBE (0.5 mL) were placed in a 10-mL glass tube containing a magnetic stirring bar. A solution of $[Ir(OMe)(cod)]_2$ (2.0 mg, 0.003 mmol, 1 mol%) in MTBE (1 mL), and quinaldine (**1b**) (41.6 mg, 0.3 mmol) were added successively. The tube was sealed with a screw cap and removed from the glove box. The reaction mixture was stirred at 50 ºC for 12 h, and filtered through a glass pipette equipped with a cotton plug. Solvent was removed under reduced pressure. An

internal standard (1,1,2,2-tetrachloroethane) was added to the residue to determine the yield of the product **3b** by ^{1}H NMR (99%). The crude material was purified by Kugelrohr distillation to give **3b** (67.6 mg, 0.26 mmol in 86% isolated yield).

Procedure for the Borylation of 1l and the Following Suzuki-Miyaura Coupling with Methyl 4-Bromobenzoate (Table 2, entry 4). In a glove box, Silica-SMAP (0.070 mmol/g, 85.7 mg, 0.006 mmol, 2 mol%), bis(pinacolato)diboron (**2**) (83.8 mg, 0.33 mmol), and anhydrous, degassed MTBE (0.5 mL) were placed in a 10-mL glass tube containing a magnetic stirring bar. A solution of $[Ir(OMe)(cod)]_2$ (2.0 mg, 0.003 mmol, 1 mol%) in MTBE (1 mL) and **1l** (77.8 mg, 0.3 mmol) were added successively. The tube was sealed with a screw cap and removed from the glove box. The reaction mixture was stirred at 50 ºC for 12 h, and filtered through a glass pipette equipped with a cotton plug. Solvent was removed under reduced pressure. An internal standard (1,1,2,2-tetrachloroethane) was added to the residue to determine the yield of the C-8-borylated product **3l** by ^{1}H NMR (80%). Next, the crude product (**3l**), methyl 4-bromobenzoate (96.8 mg, 0.45 mmol), $Pd(PPh_3)_4$ (17.3 mg, 0.015 mmol), and K_3PO_4 (191 mg, 0.9 mmol) were added successively to a 10-mL two-necked round-bottom flask containing a magnetic stirring bar under an Ar atmosphere, and the mixture was dissolved in a solution of THF (3 mL) and H_2O (0.6 mL). The reaction mixture was stirred at 60 ºC for 12 h, and then cooled to room temperature. After addition of water, the crude mixture was extracted with Et_2O. The organic layer was washed with brine, dried over $MgSO_4$, filtered and concentrated. The residue was then purified by silica gel chromatography (1:9 EtOAc/hexane) to give **9l** (90.0 mg, 0.23 mmol in 76% isolated yield).

Procedure for the Oxidation of 3b and the Following Boc-Protection (Scheme 2, upper right). Under an air atmosphere, **3b** (53.8 mg, 0.2 mmol) and sodium perborate tetrahydrate (92.3 mg, 0.6 mmol) were successively added to a 10-mL glass tube containing a magnetic stirring bar, and the mixture was dissolved in a solution of THF (1 mL) and H_2O (1 mL). The reaction mixture was stirred vigorously at room temperature for 3 h. The volatiles were removed under reduced pressure. Next, THF (2 mL), di-*tert*-butyl dicarbonate (87.3 mg, 0.4 mmol) and 4-(*N,N*'-dimethylamino)pyridine (2.4 mg, 0.02 mmol) were added successively to the tube. The reaction mixture was stirred for 1 h at room temperature. Solvent was removed under reduced pressure. The residue was then purified by silica gel chromatography (1:9 EtOAc/hexane) to give **6e** (47.6 mg, 0.18 mmol in 92% isolated yield).

Procedure for the One-Carbon Homologation of 3b and the Following Oxidation

(Scheme 2, lower right). Under an Ar atmosphere, **3b** (54.1 mg, 0.2 mmol), bromochloromethane (51.8 mg, 0.4 mmol), and anhydrous THF (2 mL) were placed in a 10-mL glass tube containing a magnetic stirring bar. The tube was sealed with a screw cap having a Teflon-coated silicone rubber septum. After cooling to –78 ˚C, ^{n}BuLi in hexane (1.64 M, 207 μL, 0.34 mmol) was added to the mixture. The reaction mixture was stirred at –78 ˚C for 5 min, and allowed to stir at room temperature for 1 h. Solvent was removed under reduced pressure. An internal standard (1,1,2,2-tetrachloroethane) was added to the residue to determined the yield of the product 2-methyl-8-((4,4,5,5-tetramethyl-1,3,2-dioxaborolan-2-yl)methyl)quinoline by ^{1}H NMR (68%). Next, the crude material and sodium perborate tetrahydrate (138 mg, 0.9 mmol) were placed in a 10-mL glass tube containing a magnetic stirring bar, and the mixture was dissolved in a solution of THF (1.5 mL) and H_2O (1.5 mL) under air. The reaction mixture was stirred vigorously at room temperature for 3 h. Solvent was removed under reduced pressure. The residue was then purified by silica gel chromatography (3:7 EtOAc/hexane) to give **7** (21.4 mg, 0.12 mmol in 61% isolated yield based on **3b**).

Procedure for the Rh-Catalyzed Heck-Type Reaction of 3b (Scheme 2, lower left). Under an Ar atmosphere, **3b** (26.9 mg, 0.1 mmol), butyl acrylate (51.7 mg, 0.4 mmol), and $[Rh(OH)(cod)]_2$ (1.1 mg, 0.0025 mmol) were placed in a 10-mL vial containing a magnetic stirring bar, and the mixture was dissolved in a solution of dioxane (1 mL) and H_2O (0.1 mL). The reaction mixture was stirred at 90 ºC for 16 h. Solvent was removed under reduced pressure. The residue was then purified by silica gel chromatography (1:9 EtOAc/hexane) to give **8** (24.8 mg, 0.09 mmol in 92% isolated yield).

Procedure for the Pd-Catalyzed Suzuki-Miyaura Coupling of 3b (Scheme 2, upper left). Under an Ar atmosphere, **3b** (80.7 mg, 0.3 mmol), methyl 4-bromobenzoate (96.8 mg, 0.45 mmol), $Pd(PPh_3)_4$ (17.3 mg, 0.015 mmol), and K_3PO_4 (191 mg, 0.9 mmol) were successively added to a 10-mL glass tube containing a magnetic stirring bar, and the mixture was dissolved in a solution of THF (3 mL) and H_2O (0.6 mL). The reaction mixture was stirred at 60 ºC for 12 h. After addition of water, the mixture was extracted with Et_2O. The organic layer was washed with brine, dried over $MgSO_4$, filtered and concentrated. The residue was then purified by silica gel chromatography (1:19 EtOAc/hexane) to give **9b** (78.9 mg, 0.28 mmol in 94% isolated yield).

Procedure for the Ir-Catalyzed Borylation of 12 and the Following Pd-Catalyzed

Suzuki-Miyaura Coupling (Scheme 3). In a glove box, Silica-SMAP (0.070 mmol/g, 85.7 mg, 0.006 mmol, 2 mol%), bis(pinacolato)diboron (**2**) (83.8 mg, 0.33 mmol), and anhydrous, degassed MTBE (0.5 mL) were placed in a 10-mL glass tube containing a magnetic stirring bar. A solution of $[Ir(OMe)(cod)]_2$ (2.0 mg, 0.003 mmol, 1 mol%) in MTBE (1 mL), and **12** (82.4 mg, 0.3 mmol) were added successively. The tube was sealed with a screw cap and removed from the glove box. The reaction mixture was stirred at 60 ºC for 12 h, and filtered through a glass pipette equipped with a cotton plug. Solvent was removed under reduced pressure. An internal standard (1,1,2,2-tetrachloroethane) was added to the residue to determine the yield of the C-8-borylated product **13** by ^{1}H NMR (84%). Next, the crude product (**13**), methyl 4-bromobenzoate (96.8 mg, 0.45 mmol), $Pd(PPh_3)_4$ (17.3 mg, 0.015 mmol), and K_3PO_4 (191 mg, 0.9 mmol) were placed in a 10-mL glass tube containing a magnetic stirring bar under an Ar atmosphere, and the mixture was dissolved in a solution of THF (3 mL) and H_2O (0.6 mL). The reaction mixture was stirred at 60 ºC for 10 h. Solvent was removed under reduced pressure. The residue was then purified by silica gel chromatography (99:1 hexane/Et_3N) to give **14** with trace amounts of impurities (68.7 mg, 0.18 mmol in 57% isolated yield based on **12**). Further purification was carried out by recrystallization from hexane to obtain the analytically pure compound.

4.3. Compound Characterization

The substrates for borylation **1a**, **1b**, **1f–1k**, **1n** and **1q** were obtained from commercial suppliers. The substrates **1c**,[31] **1o**[29] and **11**[29] were prepared according the literature. The substrate **1m**[32] was prepared via the Pd-catalyzed Suzuki-Miyaura coupling of 6-bromoquinaldine and phenylboronic acid.

2-(5-Bromopentyl)quinoline (15). Under an Ar atmosphere, ^{n}BuLi (1.64 M in hexane, 29 mL, 47 mmol) was added dropwise to a solution of quinaldine (5.73 g, 40 mmol) in THF (200 mL) at –78 ºC. The reaction mixture was allowed to stir at 0 ºC for 1 h. The resulting solution was added dropwise to a solution of 1,4-dibromobutane (48.2 g, 200 mmol) in THF (200 mL) at –78 ºC via a cannula. The reaction mixture was allowed to stir at room temperature for 12 h. After quenching with aqueous NH_4Cl, the crude mixture was extracted with EtOAc. The organic layer was washed with brine, dried over $MgSO_4$, filtered, and concentrated. The residue was purified by silica gel chromatography to give **15**. (10.3 g, 37.2 mmol in 93% yield).

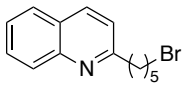

15

Pale yellow oil. **^{1}H NMR** ($CDCl_3$) δ 1.57 (quin, *J* = 7.5 Hz, 2H), 1.81–1.98 (m, 4H), 2.99 (t, *J* = 7.8 Hz, 2H), 3.42 (t, *J* = 6.9 Hz, 2H), 7.30 (d, *J* = 8.4 Hz, 1H), 7.49 (dd, *J* = 8.2, 7.6 Hz, 1H), 7.69 (dd, *J* = 8.4, 7.6 Hz, 1H), 7.79 (d, *J* = 8.2 Hz, 1H), 8.04 (d, *J* = 8.4 Hz, 1H), 8.08 (d, *J* = 8.4 Hz, 1H). **^{13}C NMR** ($CDCl_3$) δ 27.78, 28.79, 32.40, 33.53, 38.81, 121.24, 125.66, 126.65, 127.45, 128.76, 129.33, 136.22, 147.89, 162.43. **HRMS–ESI** (*m/z*): $[M+H]^+$ Calcd for $C_{14}H_{17}N^{79}Br$, 278.05389; found, 278.05399.

2-(5-Methoxypentyl)quinoline (1d). A solution of 2-(5-bromopentyl)quinoline (**15**, 1.39 g, 5 mmol) and KO^{t}Bu (1.32 g, 10 mmol) in MeOH (10 mL) were refluxed for 21 h under an Ar atmosphere. After quenching with aqueous NH_4Cl, the crude mixture was extracted with Et_2O. The organic layer was washed with brine, dried over $MgSO_4$, filtered and concentrated. The residue was purified by Kugelrohr distillation to give **1d** (720 mg, 3.15 mmol in 63% yield).

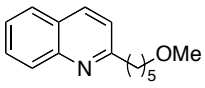

1d

Pale yellow oil. **^{1}H NMR** ($CDCl_3$) δ 1.45–1.53 (m, 2H), 1.60–1.69 (m, 2H), 1.85 (quin, *J* = 7.8 Hz, 2H), 2.99 (t, *J* = 7.8 Hz, 2H), 3.33 (s, 3H), 3.38 (t, *J* = 6.6 Hz, 2H), 7.31 (d, *J* = 8.2 Hz, 1H), 7.49 (ddd, *J* = 8.2, 7.6, 1.5 Hz, 1H), 7.69 (ddd, *J* = 8.2, 7.6, 1.5 Hz, 1H), 7.78 (dd, *J* = 8.2, 1.5 Hz, 1H), 8.04 (d, *J* = 8.2 Hz, 1H), 8.08 (d, *J* = 8.2 Hz, 1H). **^{13}C NMR** ($CDCl_3$) δ 25.85, 29.27, 29.57, 39.03, 58.29, 72.51, 121.25, 125.54, 126.62, 127.39, 128.75, 129.21, 136.10, 147.89, 162.77. **HRMS–ESI** (*m/z*): $[M+H]^+$ Calcd for $C_{15}H_{20}NO$, 230.15394; found, 230.15424.

***N,N*-Diethyl-5-(quinolin-2-yl)pentan-1-amine (1e).** A mixture of 2-(5-bromopentyl)quinoline (**15**, 1.39 g, 5 mmol) and diethylamine (10 mL) were refluxed for 22 h under an Ar atmosphere. After quenching with aqueous NH_4Cl, the crude mixture was extracted with Et_2O. The organic layer was washed with brine, dried over $MgSO_4$, filtered and concentrated. The residue was purified by Kugelrohr distillation to give **1e** (1.22 g, 4.5 mmol in 90% yield).

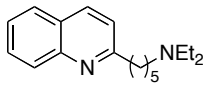

1e

Pale yellow oil. **^{1}H NMR** ($CDCl_3$) δ 1.01 (t, *J* = 7.2 Hz, 6H), 1.38–1.55 (m, 4H), 1.84 (quin, *J* = 7.8 Hz, 2H), 2.41 (t, *J* = 7.5 Hz, 2H), 2.51 (q, *J* = 7.2 Hz, 4H), 2.98 (t, *J* = 7.8 Hz, 2H), 7.31 (d, *J* = 8.4 Hz, 1H), 7.49 (dd, *J* = 8.5, 7.5 Hz, 1H), 7.69 (dd, *J* = 8.4, 7.5 Hz, 1H), 7.79 (d, *J* = 8.5 Hz, 1H), 8.04 (d, *J* = 8.4 Hz, 1H), 8.08 (d, *J* = 8.4 Hz, 1H). **^{13}C NMR** ($CDCl_3$) δ 11.37 (2C), 26.63, 27.32, 29.70, 39.04, 46.57 (2C), 52.61, 121.16, 125.44, 126.53, 127.30, 128.70, 129.11, 135.98, 147.83, 162.78. **HRMS–ESI** (*m/z*): $[M+H]^+$ Calcd for $C_{18}H_{27}N_2$, 271.21688; found, 271.21716.

***tert*-Butyl (2-Methylquinolin-6-yl) Carbonate (1l).** The title compound (**1l**) was prepared through the Boc-protection of 6-hydroxy-2-methylquinoline.[33]

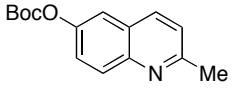

1l

White solid. **M.p.** 89–91 ˚C. **^{1}H NMR** ($CDCl_3$) δ 1.59 (s, 9H), 2.74 (s, 3H), 7.30 (d, *J* = 8.5 Hz, 1H), 7.51 (dd, *J* = 8.5, 2.7 Hz, 1H), 7.60 (d, *J* = 2.7 Hz, 1H), 8.02 (d, *J* = 8.5 Hz, 1H), 8.02 (d, *J* = 8.5 Hz, 1H). **^{13}C NMR** ($CDCl_3$) δ 25.14, 27.56 (3C), 83.82, 117.77, 122.54, 124.26, 126.62, 130.15, 135.92, 145.88, 148.31, 151.90, 158.95. **HRMS–ESI** (*m/z*): $[M+H]^+$ Calcd for $C_{15}H_{18}NO_3$, 260.12812; found, 260.12833.

2,5,7-Trimethylquinoline (1p).[34] The title compound (**1p**) was prepared through the Doebner-Miller reaction of 3,5-dimethylaniline and crotonaldehyde.[35]

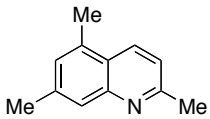

1p

Colorless liquid. **^{1}H NMR** ($CDCl_3$) δ 2.47 (s, 3H), 2.56 (s, 3H), 2.69 (s, 3H), 7.09 (s, 1H), 7.16 (d, *J* = 8.7 Hz, 1H), 7.65 (s, 1H), 8.06 (d, *J* = 8.7 Hz, 1H). **^{13}C NMR** ($CDCl_3$) δ 18.14, 21.52, 24.91, 120.56, 123.68, 125.88, 128.37, 132.23, 133.79, 139.97, 148.38, 158.25.

7-Methoxy-2-methyl-*N*,*N*-dipropylquinolin-4-amine (12). 11 (831 mg, 4 mmol), *p*-toluenesulfonic acid monohydrate (1.3 g, 7.5 mmol), and dipropylamine (5 mL) were placed in a 50-mL glass tube containing a magnetic stirring bar. The reaction mixture was stirred at 160 ºC for 16 h, and then cooled to room temperature. After addition of water, the

mixture was extracted with CH_2Cl_2. The organic layer was washed with brine, dried over $MgSO_4$, filtered and concentrated. The residue was purified by silica gel chromatography (50:49:1 EtOAc/hexane/Et_3N) followed by Kugelrohr distillation to give **12** (895 mg, 3.28 mmol in 82% yield).

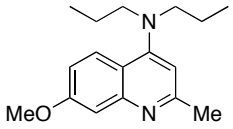

12

Pale yellow viscous liquid. **^{1}H NMR** ($CDCl_3$) δ 0.87 (t, *J* = 7.5 Hz, 6H), 1.59 (sext, *J* = 7.5 Hz, 4H), 2.62 (s, 3H), 3.23 (t, *J* = 7.5 Hz, 4H), 3.92 (s, 3H), 6.63 (s, 1H), 7.03 (dd, *J* = 9.0, 2.7 Hz, 1H), 7.30 (d, *J* = 2.7 Hz, 1H), 7.90 (d, *J* = 9.0 Hz, 1H). **^{13}C NMR** ($CDCl_3$) δ 11.40 (2C), 20.05 (2C), 25.42, 54.48 (2C), 55.28, 107.33, 109.32, 116.44, 117.67, 125.28, 151.59, 156.53, 159.20, 160.31. **HRMS–ESI** (*m/z*): $[M+H]^+$ Calcd for $C_{17}H_{25}N_2O$, 273.19614; found, 273.19617.

8-(4,4,5,5-Tetramethyl-1,3,2-dioxaborolan-2-yl)quinaldine (3b)[36]

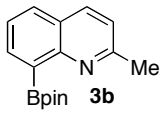

3b

^{1}H NMR ($CDCl_3$) δ 1.48 (s, 12H), 2.71 (s, 3H), 7.23 (d, *J* = 8.4 Hz, 1H), 7.44 (dd, *J* = 7.9, 6.9 Hz, 1H), 7.77 (dd, *J* = 7.9, 1.5 Hz, 1H), 7.89 (dd, *J* = 6.9, 1.5 Hz, 1H), 7.97 (d, *J* = 8.4 Hz, 1H). **^{13}C NMR** ($CDCl_3$) δ 24.76 (4C), 25.46, 83.98 (2C), 121.61, 125.02, 125.77, 129.20, 134.63, 135.91, 151.30, 158.93. A signal for the carbon directly attached to the boron atom was not observed. **^{11}B NMR** ($CDCl_3$) δ 32.01.

2-Propyl-8-(4,4,5,5-tetramethyl-1,3,2-dioxaborolan-2-yl)quinoline (3c)

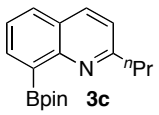

3c

Pale yellow oil. **^{1}H NMR** ($CDCl_3$) δ 1.02 (t, *J* = 7.5 Hz, 3H), 1.47 (s, 12H), 1.92 (sext, *J* = 7.5 Hz, 2H), 2.95 (t, *J* = 7.5 Hz, 2H), 7.22 (d, *J* = 8.4 Hz, 1H), 7.44 (dd, *J* = 8.1, 6.9 Hz, 1H), 7.78 (dd, *J* = 8.1, 1.5 Hz, 1H), 7.88 (dd, *J* = 6.9, 1.5 Hz, 1H), 7.98 (d, *J* = 8.4 Hz, 1H). **^{13}C NMR** ($CDCl_3$) δ 13.92, 21.62, 24.79 (4C), 40.77, 83.90 (2C), 121.29, 125.00, 126.02, 129.23, 134.56, 135.76, 151.25, 162.27. A signal for the carbon directly attached to the boron atom was not observed. **^{11}B NMR** ($CDCl_3$) δ 32.18. **HRMS–APCI** (*m/z*): $[M+H]^+$ Calcd for $C_{18}H_{25}{}^{10}BNO_2$, 297.20092; found, 297.20126.

2-(5-Methoxypentyl)-8-(4,4,5,5-tetramethyl-1,3,2-dioxaborolan-2-yl)quinoline (3d)

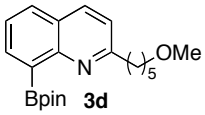

3d

Colorless oil. **^{1}H NMR** ($CDCl_3$) δ 1.42–1.52 (m, 14H), 1.66 (quin, *J* = 6.6 Hz, 2H), 1.94 (quin, *J* = 7.8 Hz, 2H), 2.98 (t, *J* = 7.8 Hz, 2H), 3.33 (s, 3H), 3.39 (t, *J* = 6.6 Hz, 2H), 7.22 (d, *J* = 8.4 Hz, 1H), 7.44 (dd, *J* = 7.8, 6.9 Hz, 1H), 7.78 (d, *J* = 7.8 Hz, 1H), 7.89 (d, *J* = 6.9 Hz, 1H), 7.98 (d, *J* = 8.4 Hz, 1H). **^{13}C NMR** ($CDCl_3$) δ 24.77 (4C), 25.80, 28.19, 29.47, 38.65, 58.42, 72.76, 83.84 (2C), 121.20, 124.98, 125.99, 129.24, 134.64, 135.80, 151.19, 162.17. A signal for the carbon directly attached to the boron atom was not observed. **^{11}B NMR** ($CDCl_3$) δ 32.13. **HRMS–APCI** (*m/z*): $[M+H]^+$ Calcd for $C_{21}H_{31}{}^{10}BNO_3$, 355.24278; found, 355.24330.

2-(5-(*N,N*-Diethylamino)pentyl)-8-(4,4,5,5-tetramethyl-1,3,2-dioxaborolan-2-yl)quinolin e (3e)

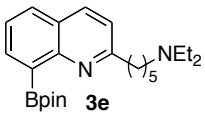

3e

Pale yellow solid. **M.p.** 123–129 ˚C. **^{1}H NMR** ($CDCl_3$) δ 1.20 (br-s, 6H), 1.39–1.60 (m, 14H), 1.68 (br-s, 2H), 1.96 (quin, *J* = 7.8 Hz, 2H), 2.80 (br-s, 6H), 2.98 (t, *J* = 7.8 Hz, 2H), 7.22 (d, *J* = 8.5 Hz, 1H), 7.45 (dd, *J* = 8.1, 6.9 Hz, 1H), 7.79 (dd, *J* = 8.1, 1.5 Hz, 1H), 7.89 (dd, *J* = 6.9, 1.5 Hz, 1H), 7.99 (d, *J* = 8.5 Hz, 1H). **^{13}C NMR** ($CDCl_3$) δ 9.51, 24.64 (4C), 26.66, 27.69, 38.31, 46.24, 51.60, 83.70 (2C), 121.09, 124.93, 125.84, 129.11, 134.47, 135.82, 150.96, 161.68. A signal for the carbon directly attached to the boron atom was not observed. **^{11}B NMR** ($CDCl_3$) δ 32.21. **HRMS–EI** (*m/z*): $[M]^+$ Calcd for $C_{24}H_{37}{}^{11}BO_2N_2$, 396.2948; found, 396.2954.

4-Chloro-8-(4,4,5,5-tetramethyl-1,3,2-dioxaborolan-2-yl)quinaldine (3i)

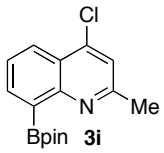

3i

White solid. **M.p.** 78–87 ˚C. **^{1}H NMR** ($CDCl_3$) δ 1.48 (s, 12H), 2.69 (s, 3H), 7.35 (s, 1H), 7.54 (dd, *J* = 8.4, 6.9 Hz, 1H), 7.92 (dd, *J* = 6.9, 1.5 Hz, 1H), 8.19 (dd, *J* = 8.4, 1.5 Hz, 1H). **^{13}C NMR** ($CDCl_3$) δ 24.71 (4C), 25.17, 84.15 (2C), 121.56, 124.04, 125.43, 126.06, 135.42,

142.11, 151.94, 158.76. A signal for the carbon directly attached to the boron atom was not observed. **^{11}B NMR** ($CDCl_3$) δ 31.91. **HRMS–APCI** (*m/z*): $[M+H]^+$ Calcd for $C_{16}H_{20}{}^{10}BClNO_2$, 303.13065; found, 303.13104.

2,6-Dimethyl-8-(4,4,5,5-tetramethyl-1,3,2-dioxaborolan-2-yl)quinoline (3j)

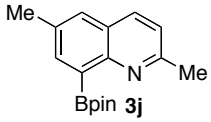

3j

Pale yellow solid. **M.p.** 122–129 ˚C. **^{1}H NMR** ($CDCl_3$) δ 1.48 (s, 12H), 2.49 (s, 3H), 2.69 (s, 3H), 7.19 (d, *J* = 8.4 Hz, 1H), 7.53 (br-s, 1H), 7.73 (br-s, 1H), 7.89 (d, *J* = 8.4 Hz, 1H). **^{13}C NMR** ($CDCl_3$) δ 21.16, 24.76 (4C), 25.39, 83.94 (2C), 121.56, 125.88, 128.27, 134.48, 135.30, 137.01, 149.90, 158.01. A signal for the carbon directly attached to the boron atom was not observed. **^{11}B NMR** ($CDCl_3$) δ 32.07. **HRMS–APCI** (*m/z*): $[M+H]^+$ Calcd for $C_{17}H_{23}{}^{10}BNO_2$, 283.18527; found, 283.18537.

6-Chloro-8-(4,4,5,5-tetramethyl-1,3,2-dioxaborolan-2-yl)quinaldine (3k)

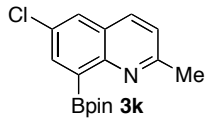

3k

White solid. **M.p.** 148–157 ˚C. **^{1}H NMR** ($CDCl_3$) δ 1.48 (s, 12H), 2.70 (s, 3H), 7.25 (d, *J* = 8.4 Hz, 1H), 7.75 (d, *J* = 2.4 Hz, 1H), 7.80 (d, *J* = 2.4 Hz, 1H), 7.90 (d, *J* = 8.4 Hz, 1H). **^{13}C NMR** ($CDCl_3$) δ 24.73 (4C), 25.40, 84.36 (2C), 122.49, 126.59, 127.69. 130.87, 135.04, 149.56, 159.32. A signal for the carbon directly attached to the boron atom was not observed. **^{11}B NMR** ($CDCl_3$) δ 31.58. **HRMS–APCI** (*m/z*): $[M+H]^+$ Calcd for $C_{16}H_{20}{}^{10}BClNO_2$, 303.13065; found, 303.13091.

6-Phenyl-8-(4,4,5,5-tetramethyl-1,3,2-dioxaborolan-2-yl)quinaldine (3m)

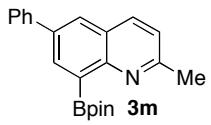

3m

White solid. **M.p.** 120–125 ˚C. **^{1}H NMR** ($CDCl_3$) δ 1.50 (s, 12H), 2.73 (s, 3H), 7.26 (d, *J* = 8.4 Hz, 1H), 7.34–7.39 (m, 1H), 7.45–7.50 (m, 2H), 7.73 (d, *J* = 7.5 Hz, 2H), 7.96 (d, *J* = 2.1 Hz, 1H), 8.03 (d, *J* = 8.4 Hz, 1H), 8.14 (d, *J* = 2.1 Hz, 1H). **^{13}C NMR** ($CDCl_3$) δ 24.79 (4C), 25.50, 84.09 (2C), 122.01, 125.99, 127.04, 127.38, 127.49 (2C), 128.81 (2C), 134.35, 136.14, 137.69, 140.75, 150.74, 158.99. A signal for the carbon directly attached to the boron

atom was not observed. **^{11}B NMR** ($CDCl_3$) δ 32.41. **HRMS–EI** (*m/z*): $[M]^+$ Calcd for $C_{22}H_{24}{}^{11}BNO_2$, 345.1900; found, 345.1895.

7-Chloro-8-(4,4,5,5-tetramethyl-1,3,2-dioxaborolan-2-yl)quinaldine (3n)

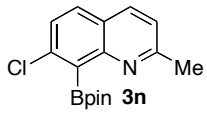

3n

White solid. **M.p.** 148–157 ˚C. **^{1}H NMR** ($CDCl_3$) δ 1.52 (s, 12H), 2.67 (s, 3H), 7.21 (d, *J* = 8.4 Hz, 1H), 7.38 (d, *J* = 8.4 Hz, 1H), 7.66 (d, *J* = 8.4 Hz, 1H), 7.94 (d, *J* = 8.4 Hz, 1H). **^{13}C NMR** ($CDCl_3$) δ 24.64 (4C), 25.14, 84.63 (3C), 121.86, 123.93, 126.49, 129.31, 135.51, 137.88, 151.77, 159.72. A signal for the carbon directly attached to the boron atom was not observed. **^{11}B NMR** ($CDCl_3$) δ 31.54. **HRMS–APCI** (*m/z*): $[M+H]^+$ Calcd for $C_{16}H_{20}{}^{10}BClNO_2$, 303.13065; found, 303.13080.

7-Methoxy-8-(4,4,5,5-tetramethyl-1,3,2-dioxaborolan-2-yl)quinaldine (3o)

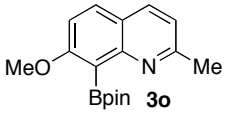

3o

White solid. **M.p.** 115–123 ºC. **^{1}H NMR** ($CDCl_3$) δ 1.50 (s, 12H), 2.64 (s, 3H), 3.93 (s, 3H), 7.06 (d, *J* = 8.1 Hz, 1H), 7.15 (d, *J* = 9.0 Hz, 1H), 7.70 (d, *J* = 9.0 Hz, 1H), 7.88 (d, *J* = 8.1 Hz, 1H). **^{13}C NMR** ($CDCl_3$) δ 24.67 (4C), 25.22, 56.12, 84.03 (2C), 112.43, 119.53, 121.08, 129.71, 135.34, 152.49, 159.27, 162.72. A signal for the carbon directly attached to the boron atom was not observed. **^{11}B NMR** ($CDCl_3$) δ 32.44. **HRMS–EI** (*m/z*): $[M]^+$ Calcd for $C_{17}H_{22}{}^{11}BO_3N$, 299.1693; found, 299.1682.

2,5,7-Trimethyl-8-(4,4,5,5-tetramethyl-1,3,2-dioxaborolan-2-yl)quinoline (3p)

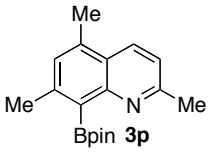

3p

White solid. **M.p.** 93–98 ˚C. **^{1}H NMR** ($CDCl_3$) δ 1.50 (s, 12H), 2.50 (s, 3H), 2.58 (s, 3H), 2.64 (s, 3H), 7.08 (s, 1H), 7.14 (d, *J* = 8.7 Hz, 1H), 8.06 (d, *J* = 8.7 Hz, 1H). **^{13}C NMR** ($CDCl_3$) δ 18.23, 21.88, 24.74 (4C), 24.87, 83.82 (2C), 120.28, 123.00, 128.42, 131.73, 134.50, 142.10, 152.18, 157.75. A signal for the carbon directly attached to the boron atom was not observed. **^{11}B NMR** ($CDCl_3$) δ 32.78. **HRMS–APCI** (*m/z*): $[M+H]^+$ Calcd for $C_{18}H_{25}{}^{10}BNO_2$, 297.20092; found, 297.20102.

2,3-Dimethyl-5,8-bis(4,4,5,5-tetramethyl-1,3,2-dioxaborolan-2-yl)quinoxaline (3q)

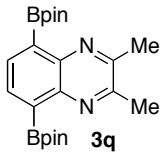

3q

White solid. **M.p.** 215–227 ˚C. **^{1}H NMR** ($CDCl_3$) δ 1.46 (s, 24H), 2.67 (s, 6H), 7.87 (s, 2H). **^{13}C NMR** ($CDCl_3$) δ 23.38 (2C), 24.72 (8C), 84.06 (4C), 134.06 (2C), 143.83 (2C), 152.86 (2C). A signal for the carbons directly attached to the boron atoms was not observed. **^{11}B NMR** ($CDCl_3$) δ 31.98. **HRMS–EI** (*m/z*): $[M]^+$ Calcd for $C_{22}H_{32}{}^{11}B_2O_4N_2$, 410.2548; found, 410.2550.

***tert*-Butyl Quinolin-8-yl Carbonate (6a)**[37]

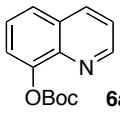

6a

White solid. **^{1}H NMR** ($CDCl_3$) δ 1.61 (s, 9H), 7.44 (dd, *J* = 8.4, 4.2 Hz, 1H), 7.52–7.54 (m, 2H), 7.70–7.74 (m, 1H), 8.18 (dd, *J* = 8.4, 1.6 Hz, 1H), 8.94 (dd, *J* = 4.2, 1.6 Hz, 1H). **^{13}C NMR** ($CDCl_3$) δ 27.52 (3C), 83.59, 120.98, 121.77, 125.75, 126.18, 129.47, 135.90, 141.34, 147.49, 150.51, 152.13.

***tert*-Butyl (2-Methylquinolin-8-yl) Carbonate (6b)**

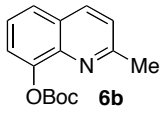

6b

White solid. **M.p.** 71–75 ˚C. **^{1}H NMR** ($CDCl_3$) δ 1.62 (s, 9H), 2.73 (s, 3H), 7.31 (d, *J* = 8.4 Hz, 1H), 7.41–7.50 (m, 2H), 7.66 (dd, *J* = 7.5, 2.1 Hz, 1H), 8.05 (d, *J* = 8.4 Hz, 1H). **^{13}C NMR** ($CDCl_3$) δ 25.48, 27.55 (3C), 83.28, 120.65, 122.71, 125.23, 125.44, 127.74, 135.95, 140.72, 147.16, 152.23, 159.29. **HRMS–ESI** (*m/z*): $[M+Na]^+$ Calcd for $C_{15}H_{17}NO_3Na$, 282.11006; found, 282.11018.

***tert*-Butyl (3-Methylquinolin-8-yl) Carbonate (6f)**[38]

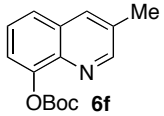

6f

White solid. **^{1}H NMR** ($CDCl_3$) δ 1.60 (s, 9H), 2.51 (s, 3H), 7.43–7.51 (m, 2H), 7.62 (dd, *J*

= 7.5, 2.2 Hz, 1H), 7.93 (br-s, 1H), 8.79 (d, *J* = 1.8 Hz, 1H). **^{13}C NMR** ($CDCl_3$) δ 18.56, 27.54 (3C), 83.51, 119.94, 125.12, 126.21, 129.43, 131.33, 134.49, 139.61, 147.51, 152.21, 152.55.

***tert*-Butyl (4-Methylquinolin-8-yl) Carbonate (6g)**

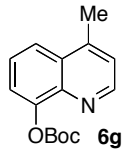

6g

White solid. **M.p.** 98–100 ˚C. **^{1}H NMR** ($CDCl_3$) δ 1.60 (s, 9H), 2.71 (s, 3H), 7.24–7.28 (m, 1H), 7.50–7.57 (m, 2H), 7.89 (dd, *J* = 6.9, 2.4 Hz, 1H), 8.79 (d, *J* = 4.4 Hz, 1H). **^{13}C NMR** ($CDCl_3$) δ 18.70, 27.51 (3C), 83.46, 120.63, 121.84, 122.51, 125.76, 129.56, 141.18, 144.34, 147.93, 150.17, 152.21. **HRMS–ESI** (*m/z*): $[M+H]^+$ Calcd for $C_{15}H_{18}NO_3$, 260.12812; found, 260.12860.

***tert*-Butyl (6-Methoxyquinolin-8-yl) Carbonate (6h)**

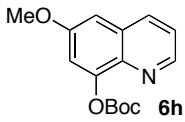

6h

White solid. **M.p.** 79–85 ˚C. **^{1}H NMR** ($CDCl_3$) δ 1.60 (s, 9H), 3.93 (s, 3H), 6.98 (d, *J* = 2.7 Hz, 1H), 7.23 (d, *J* = 2.7 Hz, 1H), 7.38 (dd, *J* = 8.4, 4.2 Hz, 1H), 8.05 (dd, *J* = 8.4, 1.5 Hz, 1H), 8.77 (dd, *J* = 4.2, 1.5 Hz, 1H). **^{13}C NMR** ($CDCl_3$) δ 27.51 (3C), 55.60, 83.73, 103.29, 114.08, 122.15, 129.99, 134.69, 137.63, 147.96, 148.29, 151.87, 157.45. **HRMS–ESI** (*m/z*): $[M+Na]^+$ Calcd for $C_{15}H_{17}NO_4Na$, 298.10498; found, 298.10552.

(2-Methylquinolin-8-yl)methanol (7)

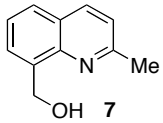

7

White solid. **M.p.** 70–73 ˚C. **^{1}H NMR** ($CDCl_3$) δ 2.73 (s, 3H), 5.17 (s, 2H), 5.76 (br-s, 1H), 7.30 (d, *J* = 8.4 Hz, 1H), 7.40 (dd, *J* = 8.4, 6.6 Hz, 1H), 7.50 (d, *J* = 6.6 Hz, 1H), 7.69 (d, *J* = 8.4 Hz, 1H), 8.07 (d, *J* = 8.4 Hz, 1H). **^{13}C NMR** ($CDCl_3$) δ 25.33, 65.23, 122.04, 125.52, 126.69, 127.10, 127.64, 137.02, 137.28, 146.89, 158.00. **HRMS–ESI** (*m/z*): $[M+H]^+$ Calcd for $C_{11}H_{12}NO$, 174.09134; found, 174.09174.

(*E*)-Butyl 3-(2-Methylquinolin-8-yl)acrylate (8)

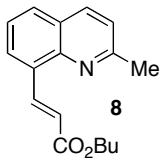

Red-brown oil. **^{1}H NMR** ($CDCl_3$) δ 0.99 (t, *J* = 7.2 Hz, 3H), 1.44–1.54 (m, 2H), 1.69–1.79 (m, 2H), 2.78 (s, 3H), 4.26 (t, *J* = 6.9 Hz, 2H), 6.84 (d, *J* = 16.2 Hz, 1H), 7.33 (d, *J* = 8.1 Hz, 1H), 7.46–7.52 (m, 1H), 7.81 (dd, *J* = 8.1, 1.2 Hz, 1H), 7.96 (dd, *J* = 7.5, 1.2 Hz, 1H), 8.04 (d, *J* = 8.1 Hz, 1H), 8.97 (d, *J* = 16.2 Hz, 1H). **^{13}C NMR** ($CDCl_3$) δ 13.66, 19.12, 25.52, 30.73, 64.28, 120.11, 122.40, 125.33, 126.68, 127.89, 129.81, 132.38, 136.28, 141.40, 145.88, 159.33, 167.57. **HRMS–ESI** (*m/z*): $[M+Na]^+$ Calcd for $C_{17}H_{19}NO_2Na$, 292.13080; found, 292.13120.

Methyl 4-(2-Methylquinolin-8-yl)benzoate (9b)

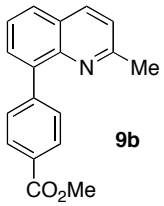

White solid. **M.p.** 98–101 ˚C. **^{1}H NMR** ($CDCl_3$) δ 2.68 (s, 3H), 3.96 (s, 3H), 7.32 (d, *J* = 8.4 Hz, 1H), 7.55 (dd, *J* = 8.1, 7.2 Hz, 1H), 7.74 (dd, *J* = 7.2, 1.5 Hz, 1H), 7.81 (dd, *J* = 8.1, 1.5 Hz, 1H), 7.87 (d, *J* = 8.4 Hz, 2H), 8.09 (d, *J* = 8.4 Hz, 1H), 8.15 (d, *J* = 8.4 Hz, 2H). **^{13}C NMR** ($CDCl_3$) δ 25.51, 51.93, 121.99, 125.33, 126.91, 127.99, 128.59, 128.99 (2C), 130.31, 131.03 (2C), 136.27, 138.76, 144.47, 145.27, 159.08, 167.41. **HRMS–ESI** (*m/z*): $[M+H]^+$ Calcd for $C_{18}H_{16}NO_2$, 278.11756; found, 278.11798.

Methyl 4-(6-((*tert*-Butoxycarbonyl)oxy)-2-methylquinolin-8-yl)benzoate (9l)

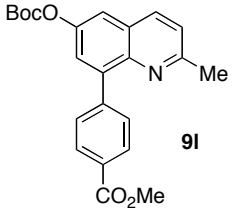

White solid. **M.p.** 106–112 ˚C. **^{1}H NMR** ($CDCl_3$) δ 1.60 (s, 9H), 2.67 (s, 3H), 3.96 (s, 3H), 7.32 (d, *J* = 8.4 Hz, 1H), 7.57 (d, *J* = 2.7 Hz, 1H), 7.62 (d, *J* = 2.7 Hz, 1H), 7.85 (d, *J* = 8.4 Hz, 2H), 8.05 (d, *J* = 8.4 Hz, 1H), 8.15 (d, *J* = 8.4 Hz, 2H). **^{13}C NMR** ($CDCl_3$) δ 25.39, 27.54 (3C), 51.96, 83.90, 118.04, 122.53, 124.81, 127.27, 128.96, 129.03 (2C), 131.02 (2C), 136.09, 140.42, 143.30, 143.40, 147.74, 151.88, 158.90, 167.28. **HRMS–ESI** (*m/z*): $[M+Na]^+$ Calcd for $C_{23}H_{23}NO_5Na$, 416.14684; found, 416.14771.

8-(4-Chlorophenyl)-7-methoxy-2-methyl-*N*,*N*-dipropylquinolin-4-amine (14)

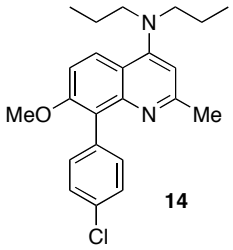

14

White solid. **M.p.** 95–98 ˚C. **^{1}H NMR** ($CDCl_3$) δ 0.90 (t, *J* = 7.5 Hz, 6H), 1.61 (sext, *J* = 7.5 Hz, 4H), 2.51 (s, 3H), 3.23 (t, *J* = 7.5 Hz, 4H), 3.88 (s, 3H), 6.65 (s, 1H), 7.26 (d, *J* = 9.3 Hz, 1H), 7.40–7.48 (m, 4H), 8.08 (d, *J* = 9.3 Hz, 1H). **^{13}C NMR** ($CDCl_3$) δ 11.51 (2C), 20.04 (2C), 25.98, 54.68 (2C), 56.36, 109.62, 110.92, 118.55, 124.70, 124.99, 127.45 (2C), 132.23, 133.52 (2C), 134.34, 148.82, 156.24, 156.31, 159.43. **HRMS–ESI** (*m/z*): $[M+H]^+$ Calcd for $C_{23}H_{28}N_2OCl$, 383.18847; found, 383.18888.

4.4. X-ray Crystallographic Analysis

Single crystal of **3n** was obtained by recrystallization from hexane. Data of **3n** were collected on a Rigaku AFC-7R diffractometer with a mercury CCD area detector, graphite monochromated Mo-Kα radiation (λ = 0.71069 Å) at 150 K, and processed using CrystalClear (Rigaku).[39] The structure was solved by a direct method (SIR2004)[40] and refined by full-matrix least-square refinement on F^2. The non-hydrogen atoms were refined anisotropically. The hydrogen atoms were located on the calculated positions and refined using a riding model. All calculations were performed using the CrystalStructure software package.[41] CCDC 943646 contains the supplementary crystallographic data for this paper. These data can be obtained free of charge from the Cambridge Crystallographic Data Centre via www.ccdc.cam.ac.uk/data_request/cif.

Crystal data for **3n**: $C_{16}H_{19}BClNO_2$, *M* = 303.59, orthorhombic, space group = Pbca (#61), *a* = 8.1914(11) Å, *b* = 12.942(2) Å, *c* = 29.341(4) Å, *V* = 3110.4(8) Å^3, *Z* = 8, density (calc.) = 1.297 g/cm^3, total reflections collected = 23343, unique reflections = 3685 (R_{int} = 0.0538), GOF = 1.108. The final *R*1 factor was 0.0504 ($I>2\sigma(I)$) (*wR*2 = 0.1325, all data).

5. References

(1) Bioactive compounds, see: (a) Eicher, T.; Hauptmann, S.; Speicher, A. *The Chemistry of Heterocycles, 2nd Ed*., Wiley-VCH, Weinheim, **2003**. (b) Michael, J. P. *Nat. Prod. Rep.* **2008**, *25*, 166–187.

(2) Dyes, See: McAteer, C. H.; Balasubramanian, M.; Murugan, R. in *Comprehensive Heterocyclic Chemistry III, Vol. 7* (Eds.: Katrizky, A. R.; Ramsden, C. A.; Scriven, E. F. V.; Taylor, R. J. K.), Elsevier, Oxford, **2008**, Chap. 7.06, pp. 309–336.

(3) OLEDs, see: (a) Shinar, J. *Organic Light-Emitting Devices: A Survey*, Springer, Berlin, **2003**. (b) Bulovic, V.; Baldo, M. A.; Forrest, S. R. in Organic Electronic Materials (Eds.: Farchioni, R.; Grosso, G.), Springer, Berlin, **2001**, pp. 391–439. (c) Chen, C. H.; Shi, J. *Coord. Chem. Rev.* **1998**, 171, 161–174.

(4) (a) Berman, A. M.; Lewis, J. C.; Bergman, R. G.; Ellman, J. A. *J. Am. Chem. Soc.* **2008**, *130,* 14926–14927. (b) Ryu, J.; Cho, S. H.; Chang, S. *Angew. Chem. Int. Ed.* **2012**, *51*, 3677–3681.

(5) (a) Cho, S. H.; Hwang, S. J.; Chang, S. *J. Am. Chem. Soc.* **2008**, *130*, 9254–9256. (b) Larivée, A.; Mousseau, J. J.; Charette, A. B. *J. Am. Chem. Soc.* **2008**, *130*, 52–54. (c) Campeau, L.-C.; Stuart, D. R.; Leclerc, J.-P.; Bertrand-Laperle, M.; Villemure, E.; Sun, H.-Y.; Lasserre, S.; Guimond, N.; Lecavallier, M.; Fagnou, K. *J. Am. Chem. Soc.* **2009**, *131*, 3291–3306. (d) Xiao, B.; Liu, Z.-J.; Liu, L.; Fu, Y. *J. Am. Chem. Soc.* **2013**, *135*, 616–619.

(6) (a) Tobisu, M.; Hyodo, I.; Chatani, N. *J. Am. Chem. Soc.* **2009**, *131*, 12070–12071. (b) Hyodo, I.; Tobisu, M.; Chatani, N. *Chem. Asian. J.* **2012**, *7*, 1357–1365.

(7) Zhao, D.; Wang, W.; Yang, F.; Lan, J.; Yang, L.; Gao, G.; You, J. *Angew. Chem. Int. Ed.* **2009**, *48*, 3296–3300.

(8) Seiple, I. B.; Su, S.; Rodriguez, R. A.; Gianatassio, R.; Fujiwara, Y.; Sobel, A. L.; Baran, P . S. *J. Am. Chem. Soc.* **2010**, *132*, 13194–13196.

(9) Kwak, J.; Kim, M.; Chang, S. *J. Am. Chem. Soc.* **2011**, *133*, 3780–3783.

(10) Knochel and co-workers reported regioselective magnesiation at the C8 position of 2-bromo-3-pivaloyl-4-ethoxycarbonylquinoline: Boudet, N.; Lachs, J. R.; Knochel, P. *Org. Lett.* **2007**, *9*, 5525–5528.

(11) Takagi, J.; Sato, K.; Hartwig, J. F.; Ishiyama, T.; Miyaura, N. *Tetrahedron Lett.* **2002**, *43*, 5649–5651.

(12) Tajuddin, H.; Harrisson, P.; Bitterlich, B.; Collings, J. C.; Sim, N.; Batsanov, A. S.; Cheung, M. S.; Kawamorita, S.; Maxwell, A. C.; Shukla, L.; Morris, J.; Lin, Z.; Marder, T. B.; Steel, P. G. *Chem. Sci.* **2012**, *3*, 3505–3515.

(13) Zhang, Y.; Gao, J.; Li, W.; Lee, H.; Lu, B. Z.; Senanayaka, C. H. *J. Org. Chem.* **2011**, *76*, 6394–6400.

(14) For the synthesis and applications of Silica-SMAP, see: (a) Hamasaka, G.; Ochida, A.; Hara, K.; Sawamura, M. *Angew. Chem. Int. Ed.* **2007**, *46*, 5381–5383. (b) Hamasaka,

G.; Kawamorita, S.; Ochida, A.; Akiyama, R.; Hara, K.; Fukuoka, A.; Asakura, K.; Chun, W. J.; Ohmiya, H.; Sawamura, M. *Organometallics* **2008**, *27*, 6495–6506. (c) Kawamorita, S.; Ohmiya, H.; Hara, K.; Fukuoka, A.; Sawamura, M. *J. Am. Chem. Soc.* **2009**, *131*, 5058–5059. (d) Kawamorita, S.; Ohmiya, H.; Sawamura, M. *J. Org. Chem.* **2010**, *75*, 3855–3858. (e) Yamazaki, K.; Kawamorita, S.; Ohmiya, H.; Sawamura, M. *Org. Lett.* **2010**, *12*, 3978–3981. (f) Kawamorita, S.; Ohmiya, H.; Iwai, T.; Sawamura, M. *Angew. Chem. Int. Ed.* **2011**, *50*, 8363–8366. (g) Kawamorita, S.; Miyazaki, T.; Ohmiya, H.; Iwai, T.; Sawamura, M. *J. Am. Chem. Soc.* **2011**, *133*, 19310–19313. (h) Kawamorita, S.; Murakami, R.; Iwai, T.; Sawamura, M *J. Am. Chem. Soc.* **2013**, *135*, 2947–2950.

(15) For the Ir-catalyzed C–H borylation of indoles at the C7 position, see: (a) Paul, S; Chotana, G. A.; Holmes, D; Reichle, R. C.; Maleczka, R. E., Jr.; Smith, M. R., III *J. Am. Chem. Soc.* **2006**, *128*, 15552–15553. (b) Robbins, D. W.; Boebel, T. A.; Hartwig, J. F. *J. Am. Chem. Soc.* **2010**, *132*, 4068–4069.

(16) For the Ir-catalyzed C–H borylation of arenes based on the directing effect of a nitrogen ring atom of pendant heteroarenes, see: (a) Ros, A.; Estepa, B.; López-Rodríguez, R.; Álvarez, E.; Fernández, R.; Lassaletta, J. M. *Angew. Chem. Int. Ed.* **2011**, *50*, 11724–11728. b) Ros, A.; López-Rodríguez, R. B. Estepa, B.; Álvarez, E.; Fernández, R.; Lassaletta, J. M. *J. Am. Chem. Soc.* **2012**, *134*, 4573–4576. For the Rh-catalyzed reaction, see Ref. [14g]. For the Ir catalysis with sp3-N-directing groups, see: c) Roering, A. J.; Hale, L. V. A.; Squier, P. A.; Ringgold, M. A.; Wiederspan, E. R.; Clark, T. B. *Org. Lett.* **2012**, *14*, 3558–3561.

(17) 1,2-Dihydroquinoline was not detected in the crude product. No trace of 2-borylation was observed.

(18) For hydrolysis and dimerization of quinoline-8-boronic acid pinacolates, see: (a) Son, J.-H.; Pudenz, M. A.; Hoefelmeyer, J. D. *Dalton Trans.* **2010**, *39*, 11081–11090. (b) Zhang, Y.; Li, M.; Chandrasekaran, S.; Gao, X.; Fang, X.; Lee, H.-W.; Hardcastle, K.; Yang, J.; Wang, B. *Tetrahedron* **2007**, *63*, 3287–3292. See also ref. 13.

(19) Hydroboration of pyridines with pinB-H (**5**) catalyzed by Mg or Rh systems: (a) Arrowsmith, M.; Hill, M. S.; Hadlington, T.; Kociok-Köhn, G.; Weetman, C. *Organometallics* **2011**, *30*, 5556–5559. (b) Oshima, K.; Ohmura, T.; Suginome, M. *J. Am. Chem. Soc.* **2012**, *134*, 3699–3702.

(20) (a) Kawamorita, S.; Miyazaki, T.; Iwai, T.; Ohmiya, H.; Sawamura, M. *J. Am. Chem. Soc.* **2012**, *134*, 12924–12927. (b) Iwai, T.; Konishi, S.; Miyazaki, T.; Kawamorita, S.; Yokokawa, N.; Ohmiya, H.; Sawamura, M. *ACS Catal.* **2015**, *5*, 7254–7264.

(21) (a) Ochida, A.; Hara, K.; Ito, H.; Sawamura, M. *Org. Lett.* **2003**, *5*, 2671–2674. (b) Ochida, A.; Ito, S.; Miyahara, T.; Ito, H.; Sawamura, M. *Chem. Lett.* **2006**, *35*, 294–295. (c) Ochida, A.; Hamasaka, G.; Yamauchi, Y.; Kawamorita, S.; Oshima, N.; Hara, K.; Ohmiya, H.; Sawamura, M. *Organometallics* **2008**, *27*, 5494–5503.

(22) Because of the instability of **3**, the borylation products (**3f**–**h**) were converted into the corresponding O-tert-butoxycarbonyl-8-hydroxyquinoline 6 through the oxidation/Boc-protection protocol.

(23) Selected examples of applications of quinoxalines: (a) Sessler, J. L.; Maeda, H.; Mizuno, T.; Lynch, V. M.; Furuta, H. *J. Am. Chem. Soc*. **2002**, *24*, 13474–13479. (b) Myers, M. R.; He, W.; Hanney, B.; Setzer, N.; Maguire, M. P.; Zulli, A.; Bilder, G.; Galzcinski, H.; Amin, D.; Needle, S.; Spada, A. P. *Bioorg. Med. Chem. Lett.* **2003**, *13*, 3091– 3095. (c) Kim, Y. B.; Kim, Y. H.; Park, J. Y.; Kim, S. K. *Bioorg. Med. Chem. Lett.* **2004**, *14*, 541–544. (d) Akai, Y.; Yamamoto, T.; Nagata, Y.; Ohmura, T.; Suginome, M. *J. Am. Chem. Soc.* **2012**, *134*, 11092–11095. (e) Li, S.; Li, A.; Yu, J.; Zhong, A.; Chen, S.; Tang, R.; Deng, X.; Qin, J.; Li, Q.; Li, Z.; *Macromol. Rapid Commun.* **2013**, *34*, 227–233.

(24) Farthing, C. N.; Marsden, S. P. *Tetrahedron Lett*. **2000**, *41*, 4235–4238.

(25) (a) Brown, H. C.; Singh, S. M.; Rangaishevi, M. V. *J. Org. Chem.* **1986**, *51*, 3150–3155. (b) Matteson, D. S. *Chem. Rev.* **1989**, *89*, 1535–1551.

(26) Lautens, M.; Roy, A.; Fukuoka, K.; Fagnou, K.; Martín-Matute, B. *J. Am. Chem. Soc.* **2001**, *123*, 5358–5359.

(27) Suzuki, A. *Angew. Chem. Int. Ed.* **2011**, *50*, 6722–6737.

(28) Huang, C. Q.; Wilcoxen, K.; McCarthy, J. R.; Haddach, M.; Webb, T. R.; Gu, J.; Xie, Y.-F.; Grigoriadis, D. E.; Chen, C. *Bioorg. Med. Chem. Lett.* **2003**, *13*, 3375–3379.

(29) Abe, Y.; Kayakiri, H.; Satoh, S.; Inoue, T.; Sawada, Y.; Inamura, N.; Asano, M.; Aramori, I.; Hatori, C.; Sawai, H.; Oku, T.; Tanaka, H. *J. Med. Chem.* **1998**, *41*, 4062–4079.

(30) Uson, R.; Oro, L. A.; Cabeza, J. A.; Bryndza, H. E.; Stepro, M. P. *Inorg. Synth.* **1985**, *23*, 126–130.

(31) Parekh, V.; Ramsden, J. A.; Wills, M. *Tetrahedron: Asymmetry* **2010**, *21*, 1549–1556.

(32) Sun, C.-L.; Li, H.; Yu, D.-G.; Yu, M.; Zhou, X.; Lu, X.-Y.; Huang, K.; Zheng, S.-F.; Li B.-J.; Shi, Z.-J. *Nat. Chem.,* **2010**, 2, 1044–1049.

(33) Zhao, H. Y.; Li, Y. M.; Gong, T. J.; Guo, Q. X. *Chin. Chem. Lett.* **2011**, *22*, 1013–1016.

(34) Karr, C.; Estep, P. A.; Papa, A. J. *J. Am. Chem. Soc.* **1959**, *81*, 152–156.

(35) Bergstrom, F. W. *Chem. Rev.* **1944**, *35*, 77–277.

(36) Murata, M.; Oyama, T.; Watanabe, S.; Masuda, Y. *J. Org. Chem.* **2000**, *65*, 164–168.

(37) Basel, Y.; Hassner, A. *J. Org. Chem*. **2000**, *65*, 6368–6380.

(38) Ziegler, E.; Haberhauer, G. *Eur. J. Org. Chem.* **2009**, 3432–3438.

(39) *CrystalClear*: (a) Rigaku Corporation, 1999. (b) CrystalClear Software User's Guide, Molecular Structure Corporation, 2000. (c) Pflugrath, J. W. *Acta Cryst. D* **1999**, *55*, 1718–1725.

(40) *SIR-2004*: Burla, M. C.; Caliandro, R.; Camalli, M.; Carrozzini, B.; Cascarano, G. L.; De Caro, L.; Giacovazzo, C.; Polidori, G.; Spagna, R. *J. Appl. Cryst.* **2005**, *38*, 381–388.

(41) (*a*) Crystal Structure Analysis Package, Rigaku and Rigaku/MSC, *CrystalStructure*, ver. 3.6.0., 9009 New Trails Dr. The Woodlands, TX 77381 USA, 2000; (*b*) Watkin, D. J.; Prout, C. K.; Carruther, J. R.; Betteridge, P. W. *Chemical Crystallography Laboratory*, Oxford, U. K., **1996**.

Chapter 2

Synthesis, Coordination Property and Reactivity of Silica-Supported Triptycene-type Phosphine

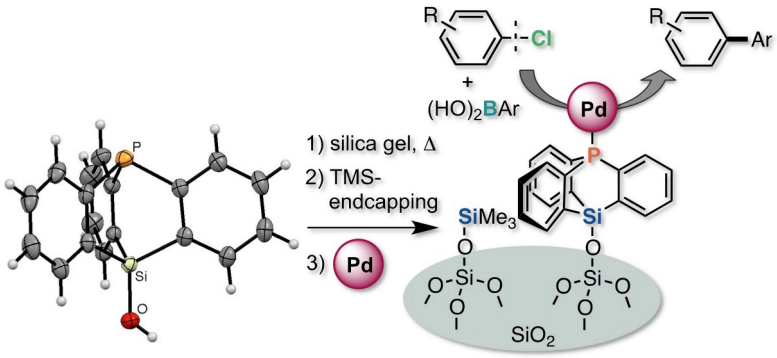

A silica-supported triptycene-type phosphine, Silica-TRIP, comprising a 9-phospha-10-silatriptycene (TRIP) and silica gel as a P-coordination center and a solid support, respectively, was synthesized and structurally characterized by nitrogen absorption measurements and solid-state CP/MAS NMR spectroscopy. Silica-TRIP exhibited a mono-P-ligating feature toward a Pd(II) complex, resulting in selective formation of a 1:1 Pd-P species even with an excess amount of the ligand. As a result, Silica-TRIP enabled Pd-catalyzed Suzuki–Miyaura cross-coupling reactions of chloroarenes under mild conditions, regardless of the moderate electron-donating nature of the triarylphosphine-based ligand.

1. Introduction

Silica-supported ligands,[1] which are generally synthesized by silane coupling between silicon-functionalized organic molecules and a silanol-containing surface, have been widely studied to prepare heterogenized transition metal catalysts with practical merits such as easy separation and reusability.[2,3] However, steric hindrance of the solid surface toward the active site often causes a decrease in catalytic performance compared to the corresponding homogeneous molecular catalysts. Moreover, commonly used flexible linkers (e.g., alkyl chains) between ligands and silica gel impart significant mobility to the coordination centers, resulting in difficulty in ligand design based on the features of the solid surface.

Recently, Sawamura *et al.* have designed and synthesized a silica-supported monophosphine, Silica-SMAP (Figure 1a), providing a novel example of increased catalytic activity by surface immobilization.[4] The rigidity of the caged trialkylphosphine (SMAP)[5] and the cage-to-surface immobilization made the P-coordination center stand upward on the surface and hence exist in isolation (Figure 1b). Thus, Silica-SMAP could form 1:1 metal-phosphine complexes exclusively with a range of transition metal species regardless of its compactness.

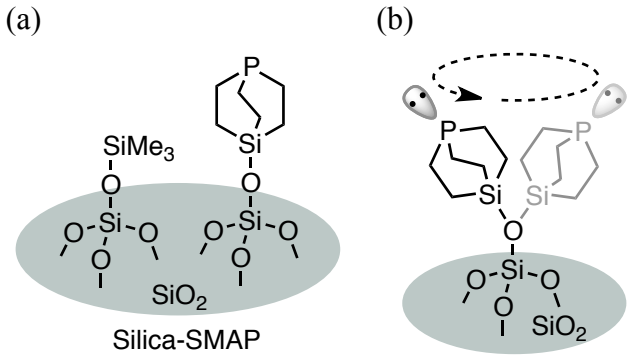

Figure 1. (a) Structure of Silica-SMAP and (b) restricted mobility of the SMAP moiety on silica surface.

The transition metal complexes prepared in this manner performed as useful heterogeneous catalysts for various reactions. On the basis of these considerations, 9-phospha-10-sila*trip*tycenes (TRIP)[6] was noticed as a new motif for silica-supported ligands. Silica-supported triptycene-type phosphine Silica-TRIP (Figure 2) was expected to function as a supported ligand complementary to Silica-SMAP-based systems. SMAP and TRIP moieties are trialkyl- and triarylphosphines, respectively, thus having contrasting electronic natures; the former should be much more electron-donating. The two ligands also differ in steric demand; the latter is significantly bulkier.

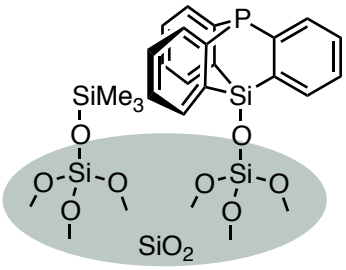

Silica-TRIP

Figure 2. Structure of Silica-TRIP.

In fact, a Silica-TRIP-Rh catalyst system realized heteroatom-directed borylation of C(sp^3)–H bonds of amides, ureas, and 2-aminopyridines at the position α to the N atom, for which Silica-SMAP was not effective, affording the corresponding primary and secondary α-aminoalkylboronates (Scheme 1, top).[7] On the other hand, both Silica-TRIP and Silica-SMAP were effective for the Ir-catalyzed N-directed C(sp^3)–H borylation of 2-alkylpyridines (Scheme 1, middle).[4j]

Scheme 1. Transformations of C(sp^3)–H and C(sp^2)–Cl bonds with Silica-TRIP-metal catalyst systems.

N-Adjacent C–H transformation *(Ref. 7)*

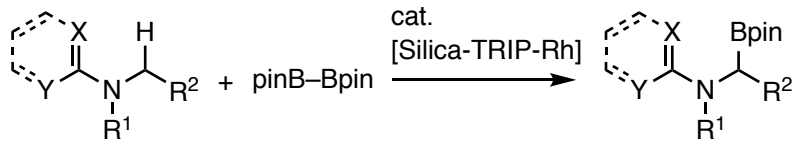

C–H transformation *(Ref. 4j)*

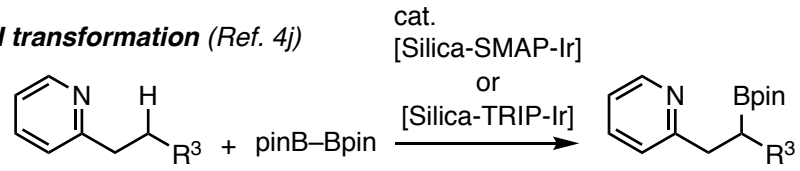

C–Cl transformation *(This work)*

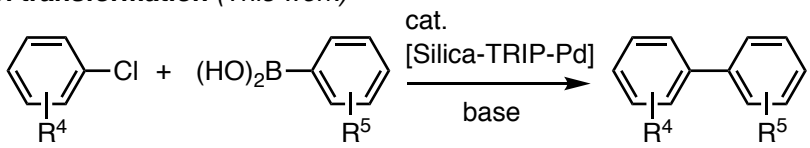

This chapter describes details of those studies on the synthesis of Silica-TRIP,[4h] its coordination properties toward Pd(II) complexes, and its catalytic application to Pd-catalyzed Suzuki–Miyaura cross-coupling of chloroarenes (Scheme 1, bottom).[8,9] The use of bulky and electron-rich monophosphine[10] or NHC[11] ligands is a common strategy for enabling the Pd-catalyzed cross-coupling of chloroarenes under mild conditions, and there are only a limited number of reports on effective catalyst systems with moderately electron-donating

triarylphosphine-based ligands; chloroarenes are more desirable but less reactive than bromoarenes and iodoarenes.[12–15]

2. Results and Discussion

The precursor for Silica-TRIP, a soluble triptycene-type phosphine **3** having a silanol group at the bridgehead, was synthesized following to Tsuji and Tamao's procedure for the synthesis of 9-phospha-10-silatriptycenes with a slight modification.[6] Thus, commercially available 1-bromo-2-iodobenzene (**1**) was converted to tris(*o*-bromophenyl)phosphine (**2**) by treatment with *i*PrMgBr for Mg-I exchange at –20 °C,[16] followed by the reaction with PCl_3 in the presence of *N*,*N*,*N*′,*N*′-tetramethylethylenediamine (TMEDA) as an additive. This procedure avoids the extremely low temperature conditions (–110 °C) employed in Tsuji and Tamao's procedure.[6] The trilithiated species generated from **2** with 6 equivalents of *t*BuLi in Et_2O/THF was reacted with $SiCl_4$. Purification by silica gel chromatography gave the silanol HO-TRIP (**3**) in 70% yield as an air- and moisture-stable solid.

Scheme 2. Preparation of silanol HO-TRIP (**3**).

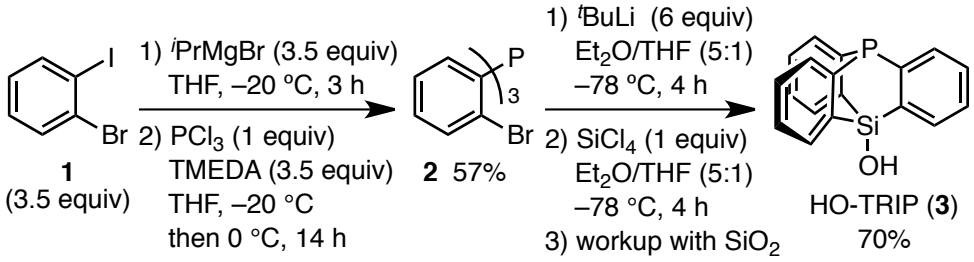

Single-crystal X-ray diffraction analysis of **3** confirmed its three-dimensional molecular structure having a triptycene cage, the bridgehead of which was substituted with P and Si atoms (Figure 3).

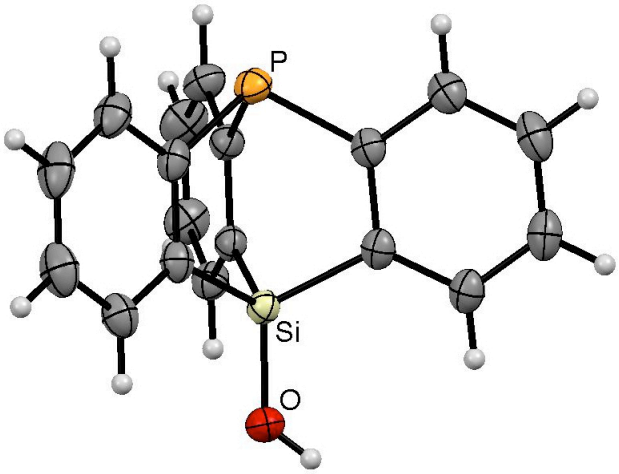

Figure 3. Molecular structure of **3** at 50% probability level; a solvent molecule ($CHCl_3$) and one of the disordered hydrogen atoms of the silanol moiety (SiO–*H*) are omitted for clarity.

Interestingly, six molecules of **3** in the crystal structure adopted a chair form hydrogen-bonding network consisting of six silanol groups as shown in Figure 4 (average distance of $Ar_3SiO\cdots OSiAr_3$; 2.651 Å).[17] The existence of the silanol group was supported by the observation of a broad absorption band at 3347 cm^{-1} by IR spectroscopy, which was assignable to an (Si)O–H stretching vibration.

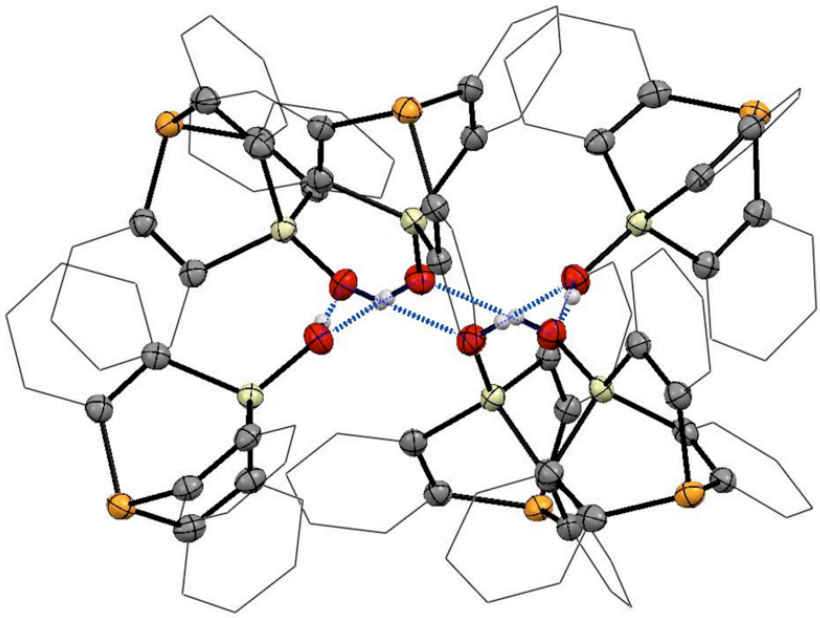

Figure 4. Chair form hydrogen-bonding network (blue-dotted lines) of **3** in the crystal structure.

The triarylsilanol **3** did not react with silica gel during the chromatography, while the purified **3** underwent slow self-condensation to form the corresponding disiloxane $(TRIP)_2O$ (**4**). The self-condensation was more rapid in the presence of a base. In fact, heating of **3** with imidazole in benzene at 80 °C caused its complete consumption, forming white precipitates (Scheme 3).[18] Filtration of the precipitates gave the disiloxane **4** in 52% isolated yield. Treatment of the silanol **3** with *N*-trimethylsilylimidazole provided the 1,1,1-trimethyl-substituted disiloxane TMSO-TRIP (**5**) in 87% yield (Scheme 4).

Scheme 3. Preparation of disiloxane $(TRIP)_2O$ (**4**).

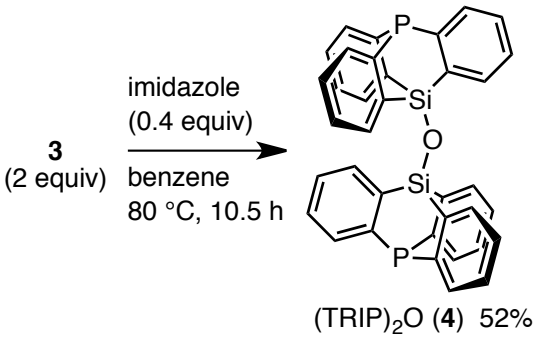

Scheme 4. Preparation of disiloxane TMSO-TRIP (**5**).

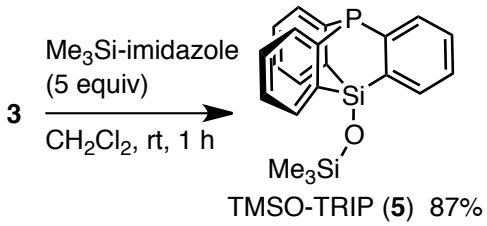

The preparation of silica-supported triptycene-type phosphine (Silica-TRIP) with a direct disiloxane linkage is shown in Scheme 5. Slight modifications were made to the procedure described in the initial report[4h] for more expeditious operation in large-scale synthesis. Specifically, the silanol phosphine **3** was grafted to a silica gel surface (CARiACT Q10, 75–150 μm) in the presence of imidazole and toluene under gentle stirring at 100 °C over 16 h. The resulting colorless solids were collected by filtration, washed successively with degassed toluene, toluene-MeOH (1:1), and MeOH, and then dried under vacuum to afford phosphine-functionalized silica-gel Silica-TRIP(SiOH). Unreacted surface silanols were Me_3Si-endcapped through treatment with excess *N*-trimethylsilylimidazole in THF at 60 °C for 24 h, to furnish Silica-TRIP. The P loading to silica gel was calculated to be 0.078 mmol/g based on the ability of the gel to bind a Pd(II) complex in a 1:1 Pd/P coordination mode (*vide infra*).

Scheme 5. Preparation of Silica-TRIP.

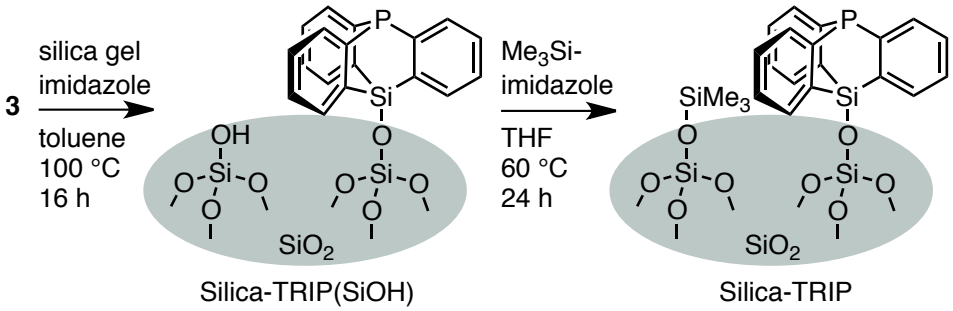

Figure 5 shows nitrogen adsorption-desorption isotherms and Barrett-Joyner-Halenda (BJH) plots for Silica-TRIP. The structural parameters (specific surface area, pore diameter and pore volume) are summarized in Table 1. Silica-TRIP exhibited a hysteresis loop, indicating the existence of mesopores with a broad pore-diameter distribution at an average of 17.2 nm. The surface modification of CARiACT Q10 silica gel (75–150 μm) for the preparation of Silica-TRIP as well as Silica-SMAP reasonably reduced their structural parameters such as surface area and pore volume.[4c] A surface P density of Silica-TRIP on the basis of the surface area (244 m^2/g) and the estimated TRIP loading (0.078 mmol/g) was calculated to be 0.19 nm^{-2}. This value was comparable to that of Silica-SMAP (0.19 nm^{-2}).

(a)

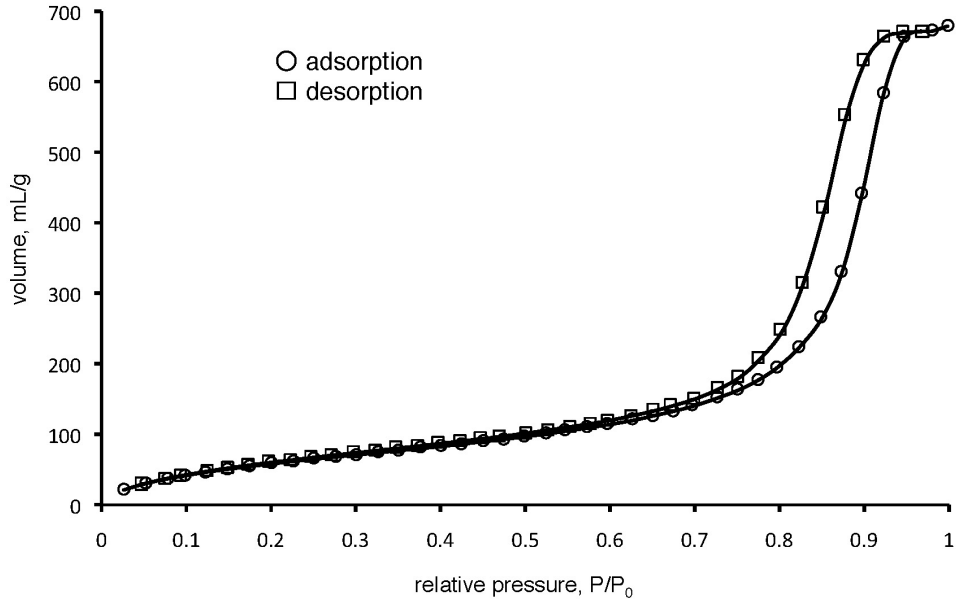

(b)

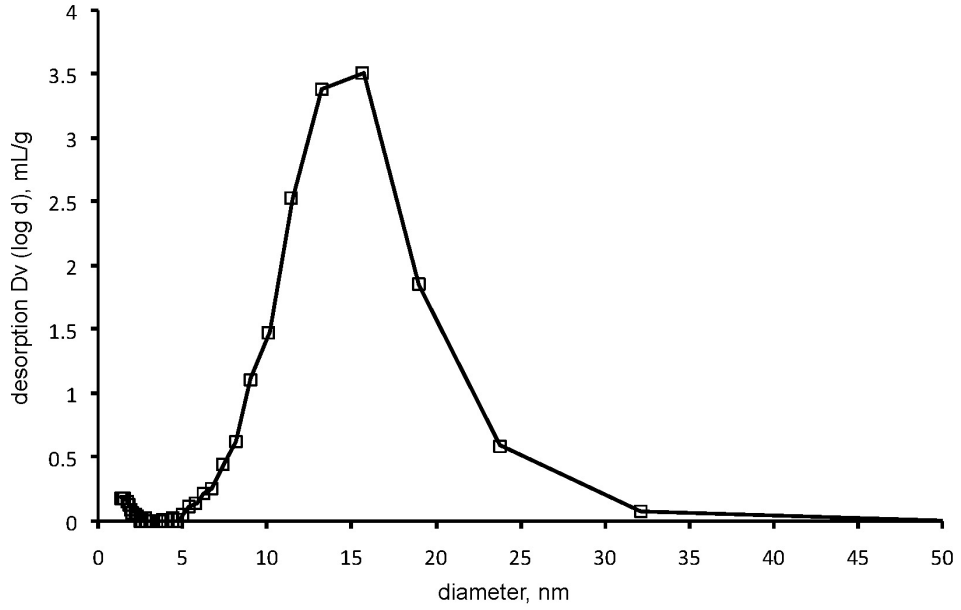

Figure 5. (a) Nitrogen adsorption–desorption isotherms and (b) BJH pore-diameter distribution plots of Silica-TRIP.

Table 1. Structural parameters.

materials	surface area (BET, m^2/g)	pore diameter (nm)	pore volume (mL/g)
Silica-TRIP	244	17.2	1.05
Silica-SMAP[a]	220	17.3	1.08
CARiACT Q10[a]	284	17.8	1.32

[a] Data were taken from ref 4c.

The silica-supported phosphine Silica-TRIP was characterized by solid-state ^{31}P, ^{13}C, and ^{29}Si NMR spectroscopies with comparison to the solution NMR spectra of the soluble disiloxane phosphine **5** in $CDCl_3$.[3] The ^{31}P CP/MAS NMR spectrum of Silica-TRIP showed a singlet signal at δ –52 (ppm) assignable to the P atom of the TRIP moiety (Figure 6a) (^{31}P NMR for **5**; δ –54.9). The ^{13}C CP/MAS spectrum showed a sharp signal at δ 2 ppm for the Me carbons of the trimethylsilyl endcaps and multiple broad signals around δ 130 for the aromatic carbons of the TRIP moiety (Figure 6b). In the ^{29}Si CP/MAS NMR spectrum (Figure 6c), a weak signal at δ –36 was assigned to the bridgehead Si atom of the TRIP moiety (^{29}Si NMR for **5**; δ –38.9).

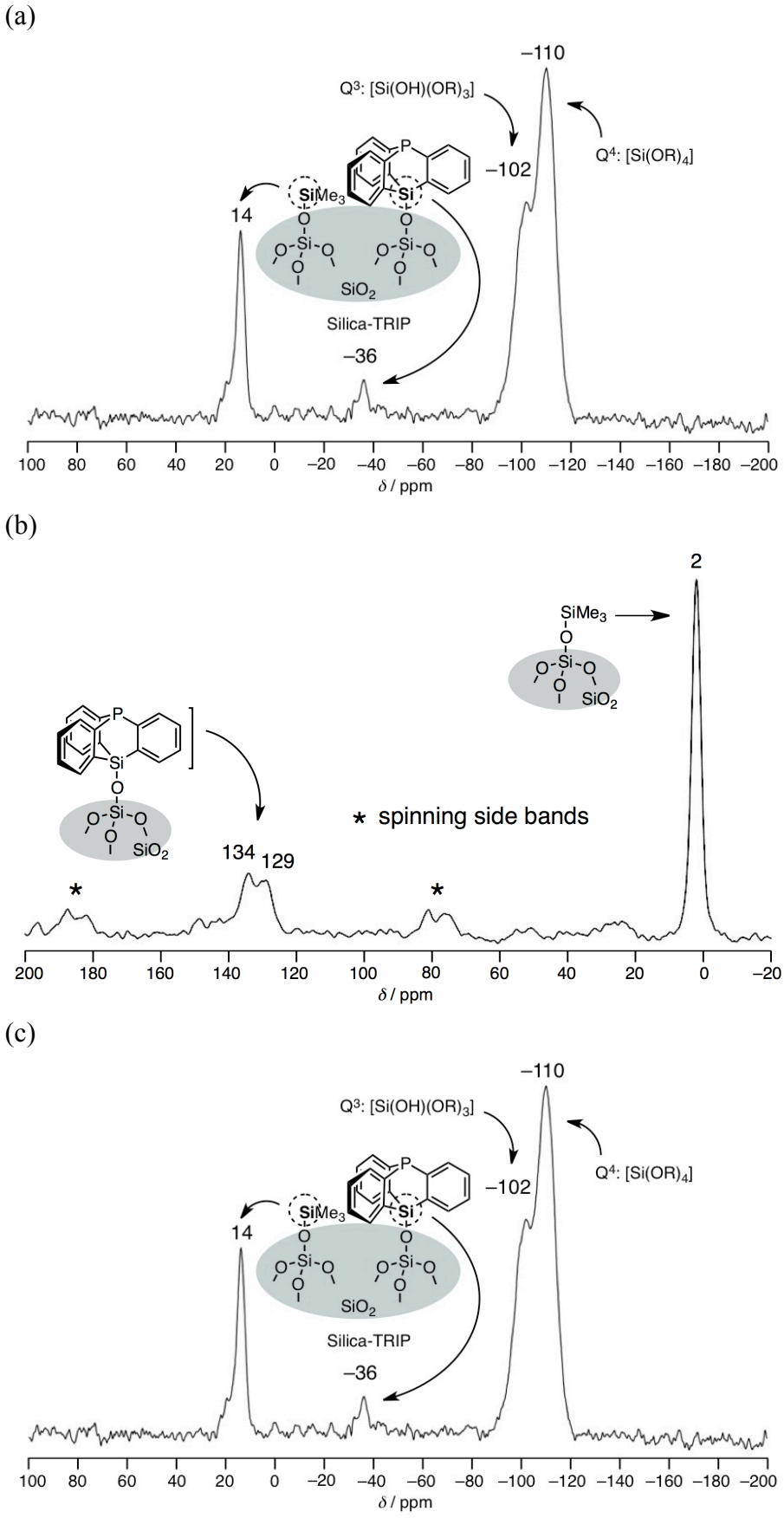

Figure 6. CP/MAS NMR spectra of Silica-TRIP for (a) ^{31}P (b) ^{13}C and (c) ^{29}Si nuclei.

The coordination property of Silica-TRIP in the reaction with $[PdCl_2(py)_2]$ (py = pyridine) was investigated. Specifically, the reaction of Silica-TRIP with an excess amount of $[PdCl_2(py)_2]$ (Pd/P 2:1) in CH_2Cl_2 at room temperature for 0.5 h produced pale yellow silica gel, indicating that Pd atoms were bound to the gel. Unreacted $[PdCl_2(py)_2]$ was recovered from the filtrate, and its weight was measured. This procedure allowed us to estimate the amount of P loading on the silica gel, which was calculated to be 0.078 mmol/g under the assumption of selective formation of [$PdCl_2$(py)(Silica-TRIP)] with a Pd/P stoichiometry of 1:1 (*vide infra* for the structure assignment). On the other hand, the inductively coupled plasma-atomic emission spectroscopic (ICP-AES) analysis of [$PdCl_2$(py)(Silica-TRIP)] gave P and Pd loading values of 0.063 and 0.072 mmol/g, respectively. For convenience, the value of 0.07 mmol/g was used for P loading in metal complexations and catalytic applications (*vide infra*)

The ^{31}P CP/MAS NMR spectrum of the silica-supported Pd complex obtained in this manner showed a singlet peak at –5 ppm (Figure 7a). The comparison of this chemical shift value with those of homogeneous Pd complexes prepared from TMSO-TRIP (**5**) (Pd/P 0:1, 1:1, 1:2 in Figure 8) is consisted with the formation of mono-P-ligated Pd complex [$PdCl_2$(py)(Silica-TRIP)] without forming a bis-P-ligated Pd complex $PdCl_2$(Silica-TRIP)$_2$ [^{31}P NMR in $CDCl_3$ for [$PdCl_2$(py)(**5**)] δ –6.5; for [$PdCl_2$(**5**)$_2$] δ –19.5]. Notably, the mono-P-ligated Pd complex was formed selectively even when excess P was present (Pd/P 1:2, in CH_2Cl_2 at room temperature for 0.5 h) (Figure 7b).

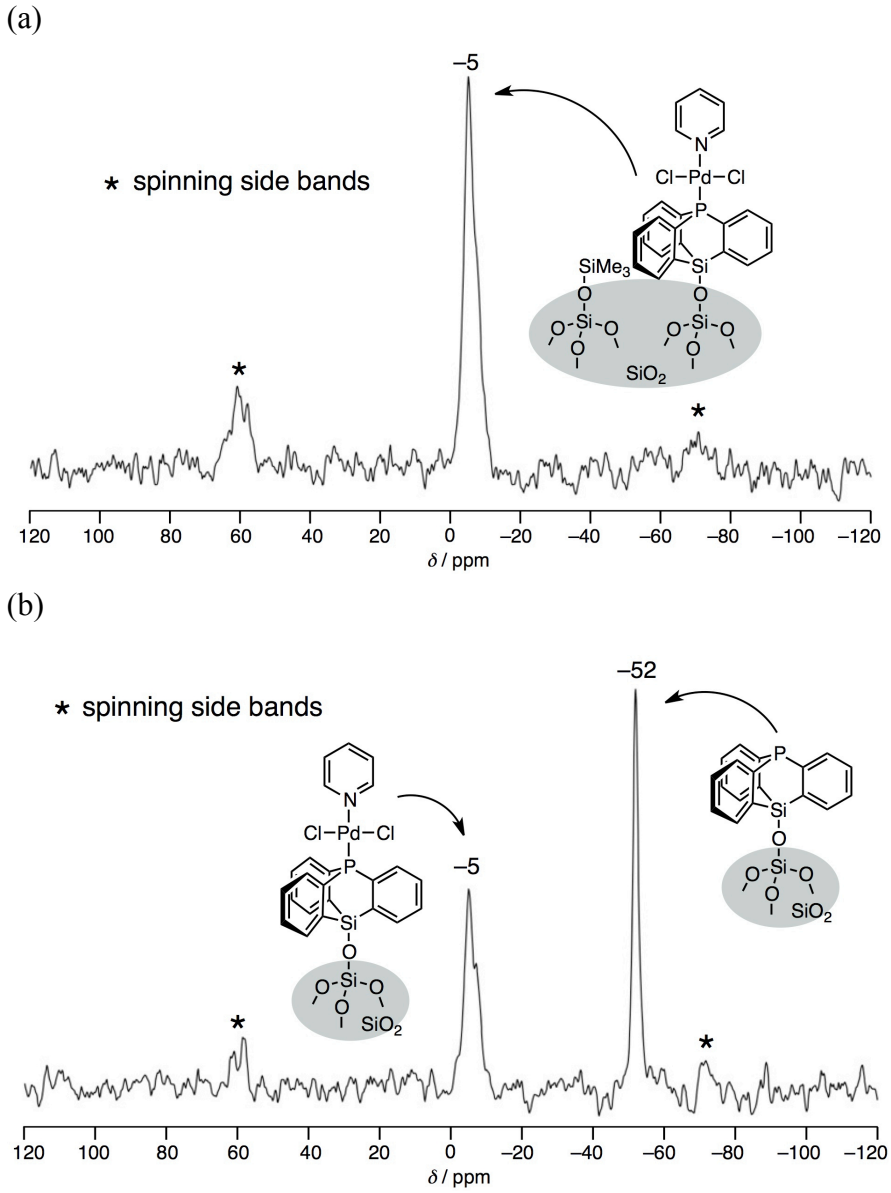

Figure 7. ^{31}P CP/MAS NMR spectra obtained from (a) $PdCl_2(py)_2$/Silica-TRIP (Pd/P 2:1) and (b) $PdCl_2(py)_2$/Silica-TRIP (Pd/P 1:2).

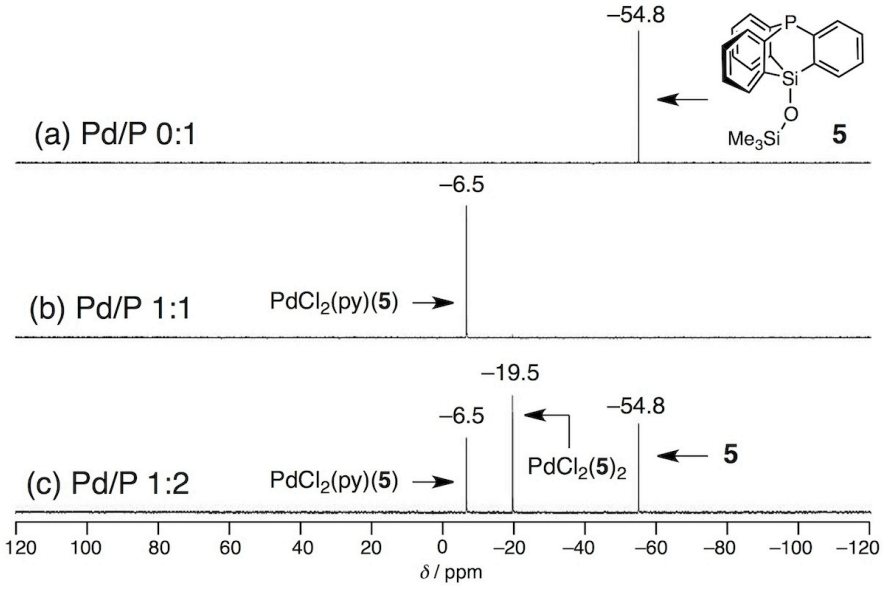

Figure 8. ^{31}P NMR spectra obtained from $PdCl_2(py)_2$ and TMSO-TRIP (**5**) [in $CDCl_3$, Pd/P (a) 0:1; (b) 1:1; (c) 1:2].

In contrast, the reaction of $PdCl_2(py)_2$ with silica-supported non-cage-type triarylphosphine Silica-1p-TPP[4h,15b] (Pd/P 1:2, in CH_2Cl_2 at room temperature for 1 h) gave well-separated two ^{31}P signals at δ 29 and δ 23, which were assignable to a 1:1 Pd/P complex $PdCl_2$(py)(Silica-1p-TPP) and a 1:2 Pd/P complex $PdCl_2$(Silica-1p-TPP)$_2$, respectively, on the basis of the ^{31}P NMR studies using the corresponding soluble phosphine PPh_2[4-Me_2(*i*PrO)Si-C_6H_4] (**6**)[15b] (Pd/P 0:1, 1:1 or 1:2; in $CDCl_3$, Figure 10), along with a signal for the free phosphine at δ –4 (Figure 9).[19] Comparison of the Pd coordination properties of Silica-TRIP and Silica-1p-TPP indicated that the cage-to-surface direct immobilization was an effective means for site isolation of the P centers to allow selective mono-P-ligation.

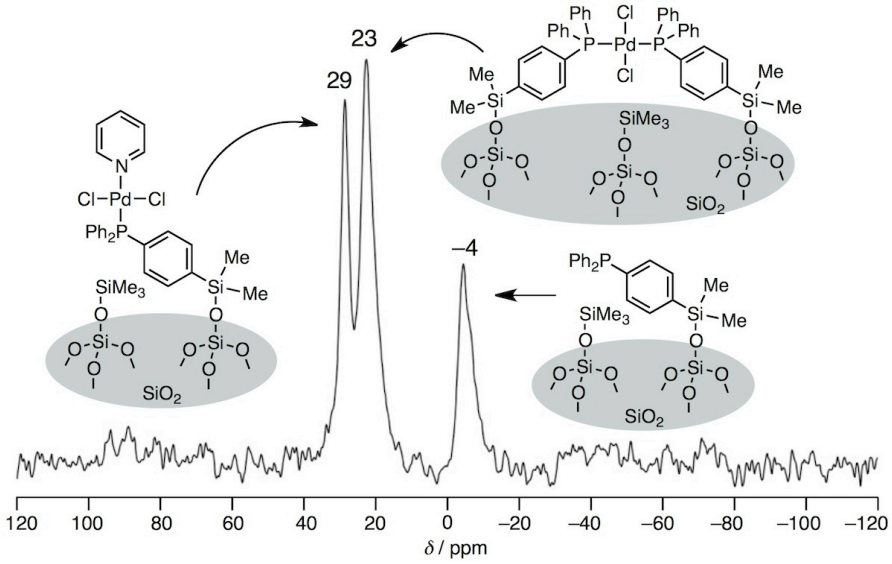

Figure 9. ^{31}P CP/MAS NMR spectra obtained from $PdCl_2(py)_2$/Silica-1p-TPP (Pd/P 1:2).

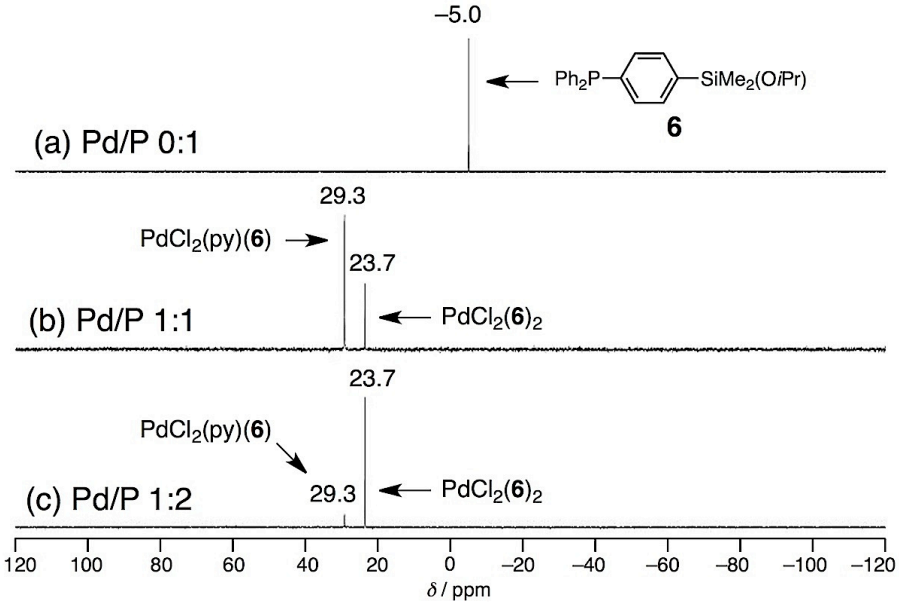

Figure 10. ^{31}P NMR spectra obtained from $PdCl_2(py)_2$ and $PPh_2[4\text{-}Me_2(iPrO)Si\text{-}C_6H_4]$ [in $CDCl_3$, Pd/P (a) 0:1; (b) 1:1; (c) 1:2].

To demonstrate ligand characteristics of Silica-TRIP for catalytic applications, we examined Pd-catalyzed Suzuki–Miyaura coupling of chloroarenes, in which mono-ligation of two-electron donor ligands is important for high catalytic activity.[10–12] Specifically, the reaction of 4-chlorotoluene (**7a**, 0.5 mmol) and phenylboronic acid (**8a**, 0.6 mmol) was conducted at 60 °C for 12 h in the presence of K_3PO_4 as a base and a palladium source (0.5 mol%). The results are summarized in Table 2.

The pre-formed immobilized mono-P-ligated Pd complex $PdCl_2(py)$(Silica-TRIP)

initiated the coupling reaction to give the desired product **9a** in 56% yield, regardless of the moderate electron-donor power of Silica-TRIP as a triarylphosphine (Table 2, entry 1). However, the heterogeneous catalyst prepared *in-situ* from $PdCl_2(py)_2$ and Silica-TRIP were less efficient (5%, entry 2). In both cases, their solution phases changed from colorless to dark brown during the reactions probably due to leaching of Pd. More active catalyst was produced by a combination of Silica-TRIP and commercially available $Pd(OAc)_2$ (93%, entry 3). The supernatant was colorless; however, 3% Pd leaching into solution was observed by the ICP-AES analysis (*vide infra*). Using unmodified silica gel CARiACT Q10 or TMS-endcapped CARiACT Q10 in place of Silica-TRIP under the conditions of entry 3 caused no reaction, indicating that $Pd(OAc)_2$ directly bound to silica gel was not effective (entries 4 and 5).

Table 2. Pd-catalyzed Suzuki–Miyaura cross-coupling between **7a** and **8a**.[a]

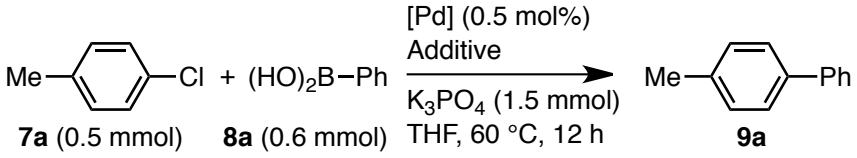

entry	Pd source [Pd]	additive	yield (%)[b]
1	$PdCl_2(py)$(Silica-TRIP)	none	56
2[c]	$PdCl_2(py)_2$	Silica-TRIP	5
3[c]	$Pd(OAc)_2$	Silica-TRIP	93 (88)
4[d]	$Pd(OAc)_2$	CARiACT Q10 (unmodified)	0
5[d]	$Pd(OAc)_2$	CARiACT Q10 (TMS-endcapped)	0

[a] Conditions: **7a** (0.5 mmol), **8a** (0.6 mmol), [Pd] (0.0025 mmol, 0.5 mol%), K_3PO_4 (1.5 mmol), THF (1.5 mL), 60 °C, 12 h. [b] Yields of **9a** were determined by ^{1}H NMR. Isolated yield is given in parentheses. [c] Silica-TRIP (0.030 mmol, 0.6 mol%). [d] CARiACT Q10 (42.9 mg).

Effects of phosphine ligands shown in Figure 11 were investigated in the presence of a catalytic amount of $Pd(OAc)_2$ (0.5 mol%, Table 3). Cage-type trialkylphosphine Silica-SMAP[4] and tripodally immobilized triarylphosphine Silica-3p-TPP,[15b] which possess mono-P-ligating features toward transition metals, promoted the coupling reaction, but their

reaction efficacies were slightly less than that of Silica-TRIP (Table 2, entry 3 *vs*. Table 3, entries 1 and 2). The conventional monopodally silica-immobilized ligand Silica-1p-TPP, in which site-isolation of the P center was not enough as shown in Figure 9, was much less effective (9% yield, entry 3). In contrast to the silica-supported catalyst systems, their homogeneous counterparts TMSO-TRIP (**5**), Ph-TRIP,[4h] Ph-SMAP,[5] or PPh_3 induced no or trace of coupling reactions (entries 4–7). These results indicated that immobilization of ligands for obtaining a mono-P-ligating feature (e.g., cage-to-surface or tripod), which was supported by NMR studies of Pd-P coordination (Figure 7), is crucial for the high catalytic activities obtained with Silica-TRIP. Under the present reaction conditions, sterically demanding homogeneous trialkylphosphines such as PCy_3 and P*t*Bu_3 were not as effective as Silica-TRIP (entries 8 and 9), while a (dicyclohexylphosphino)biphenyl-type ligand XPhos,[10a] which is one of the most efficient ligands reported to date in the cross-coupling reactions, gave **9a** quantitatively (entry 10)

Table 3. Ligand effects in Pd-catalyzed Suzuki–Miyaura cross-coupling between **7a** and **8a**.[a]

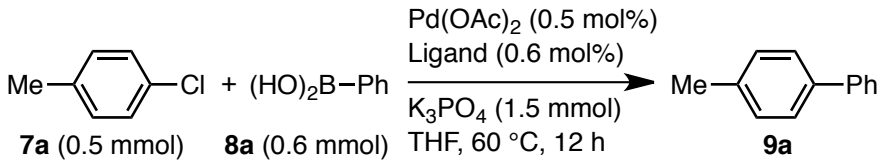

entry	ligand	yield (%)[b]
1[c]	Silica-SMAP	82[d]
2	Silica-3p-TPP	83
3	Silica-1p-TPP	9
4	TMSO-TRIP (**5**)	1
5	Ph-TRIP	0
6	Ph-SMAP	0
7	PPh_3	<1
8	PCy_3	51
9	P*t*Bu_3	14
10	XPhos	>99

[a] Conditions: **7a** (0.5 mmol), **8a** (0.6 mmol), $Pd(OAc)_2$ (0.0025 mmol, 0.5 mol%), ligand (0.003 mmol, 0.6 mol%), K_3PO_4 (1.5 mmol), THF (1.5 mL), 60 °C, 12 h. [b] Yields of **9a** were determined by ^1H NMR. [c] 0.5 mol% of ligand, for 10 h. [d] Data were taken from ref. 4g.

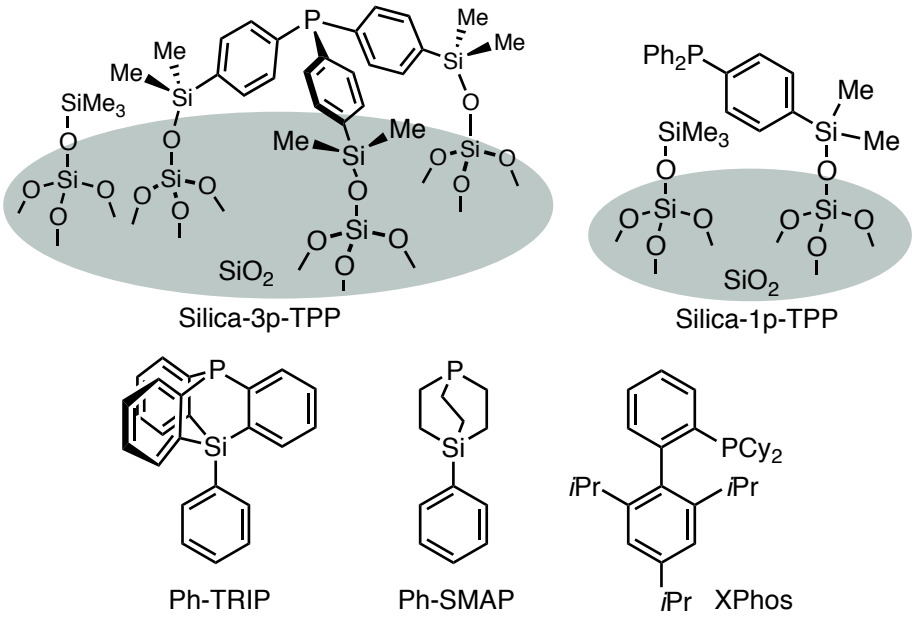

Figure 11. Heterogeneous and homogeneous phosphine ligands employed in Table 3.

The heterogeneous Silica-TRIP-Pd catalyst has the advantage of catalyst-product separation over homogeneous molecular catalyst systems. Thus, after the reaction between **7a** and **8a** in the presence of the Silica-TRIP/$Pd(OAc)_2$ catalyst system (Table 2, entry 3), the reaction mixture was filtered through Celite®. The ICP-AES analysis indicated that Pd residues in the filtrate were 3% of the loaded Pd. This value was much less than the corresponding value (58% of the loaded Pd) in the experiment for the homogeneous system with the XPhos ligand (Table 3, entry 10).

Unfortunately, reusability of the Silica-TRIP/$Pd(OAc)_2$ catalyst system was unsatisfactory under the present conditions. Specifically, the reaction of **7a** (0.5 mmol) and **8a** (0.75 mmol) with K_3PO_4 (1.5 mmol) in THF (1 mL) at 60 °C for 1 h in the presence of a heterogeneous catalyst prepared from $Pd(OAc)_2$ (1 mol%) and Silica-TRIP (1.5 mol%) gave **9a** in 97% yield (^{1}H NMR). Insoluble solids were recovered by filtration through a cotton plug followed by washing successively with H_2O, THF, and Et_2O. The catalysts recovered in this way gave decreased product yields with the increasing of the reuse (2nd run, 28%; 3rd run, 3%). The black color of the solid phase was supportive of the formation of inactive Pd species in the solid phase. Gradual Pd leaching was also observed during the catalyst reuse experiment; during the second run, the solution phase turned dark brown. This Pd leaching may be due to the moderate coordination ability of the triarylphosphine center of Silica-TRIP.

The ^{31}P CP/MAS NMR spectrum of the silica gel Pd-Silica-TRIP recovered after the coupling reaction on a larger scale (**7a**; 2.5 mmol) showed a distinct major signal at δ 4

together with minor signals at δ −52 (Silica-TRIP) and −8 (overlapped with Silica-TRIP oxide) (Figure 12).

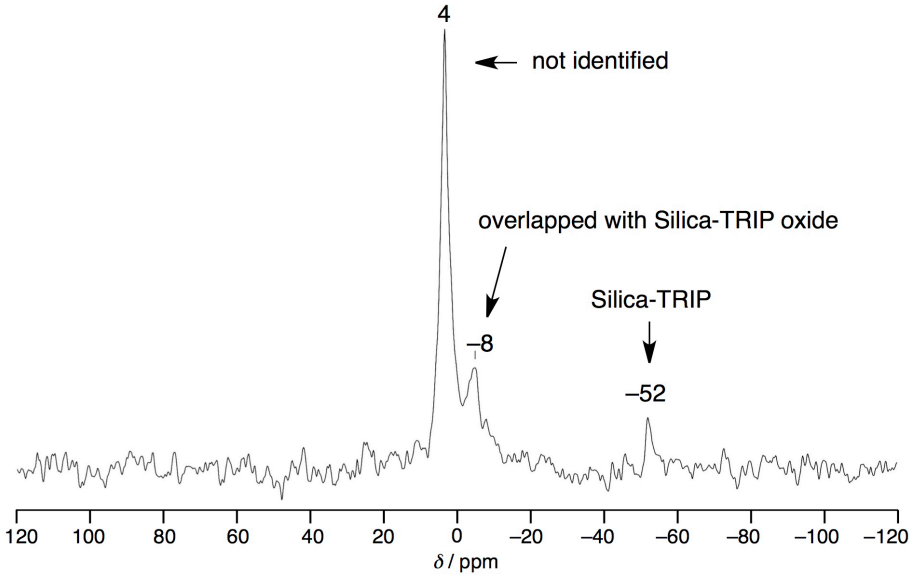

Figure 12. ^{31}P CP/MAS NMR spectra of the recovered silica gel after the reaction of **7a** and **8a** with the Silica-TRIP/$Pd(OAc)_2$ catalyst system.

On the other hand, a sample obtained from the solution phase of the reaction mixture showed no signal in ^{31}P NMR spectroscopy (in $CDCl_3$). These results indicate that at least most of the phosphine moiety remained bound to the solid surface. However, partial degradation of the Silica-TRIP structure during the catalytic reaction cannot be ruled out.

3. Conclusion

A silica-supported triptycene-type phosphine Silica-TRIP, comprising a 9-phospha-10-silatriptycene (TRIP) and silica gel as a coordinating moiety and a solid support, respectively, was synthesized. This material was characterized by nitrogen adsorption measurements and ^{13}C, ^{29}Si and ^{31}P CP/MAS NMR spectroscopies. Because of the cage-to-surface direct immobilization, Silica-TRIP exhibited a mono-P-ligating feature toward a Pd(II) complex, resulting in selective formation of a 1:1 Pd-P species even with the P-ligand in excess. This coordination behavior was confirmed by ^{31}P CP/MAS NMR spectroscopy. The use of Silica-TRIP as a ligand enabled the Pd-catalyzed Suzuki–Miyaura cross-coupling reaction with chloroarenes under mild conditions, regardless of the moderate electron-donating nature of the triarylphosphine-based ligand. The facile catalyst-product separation by filtration was demonstrated as the merit of the heterogeneous Pd catalyst system over homogeneous systems. However, catalyst deactivation in the Suzuki–Miyaura

coupling hampered the efficient reuse of the Pd catalyst.

4. Experimental Section

4.1. Instrumentation and Chemicals

All reactions were carried out under nitrogen or argon atmosphere. Materials were obtained from commercial suppliers or prepared according to standard procedures unless otherwise noted. Although Silica-SMAP[4a,c] and Silica-TRIP[4h] are commercially available, the silica-supported ligands for this work were prepared according to the reported procedure or the modified procedure described below, respectively. CARiACT Q-10 silica gel (Catalyst grade, 75–150 μm, Fuji Silysia Chemical, Ltd.) was dehydrated by heating at 120 °C under vacuum for 10 h and stored in a glove box before use. Silica-3p-TPP,[15b] Silica-1p-TPP,[15b] Ph-SMAP,[5] and Ph-TRIP[4h] were prepared according to the reported procedure. $Pd(OAc)_2$ was purchased from Aldrich Co., Ltd., and $PdCl_2(py)_2$ was prepared according to the literature.[20] Phenylboronic acid (**8a**) was purchased from TCI Co., Ltd., and was recrystallized from hot water before use. K_3PO_4 was purchased from Junsei Chemicals Co., Ltd., and dried at 150 °C for 10 h under vacuum. All solvents for catalytic reactions were degassed via three freeze–pump–thaw cycles.

Solution NMR spectra were recorded on a JEOL ECX-II (400 MHz for ^{1}H NMR, 100.5 MHz for ^{13}C NMR, 79.4 MHz for ^{29}Si NMR and 161.8 MHz for ^{31}P NMR). Chemical shift values are referenced to Me_4Si (^{1}H and ^{29}Si), the residual solvent (^{13}C), and H_3PO_4 (^{31}P). Magic angle spinning (MAS) NMR spectra were recorded on a Bruker MSL-300 spectrometer, operating at 75.5 MHz for ^{13}C NMR, 59.6 MHz for ^{29}Si NMR, and 121.5 MHz for ^{31}P NMR. Combustion elemental analyses (J-SCIENCE Micro Corder JM10 or Yanako MT-6) and high-resolution mass spectra (Thermo Scientific Exactive or JEOL JMS-T100LC for ESI-MS, and JEOL JMS-T100GCv for EI-MS) were recorded at the Instrumental Analysis Division, Equipment Management Center, Creative Research Institution, Hokkaido University. N_2 adsorption (Quantachrome Autosorb-6) and ICP-AES analysis (Shimadzu ICPE-9000) were performed at Hokkaido University Sousei Hall. A microwave digestion system (Milestone, ETHOS One) was used to prepare samples for ICP-AES analysis. IR spectra were measured with a Perkin-Elmer Spectrum One. GLC analyses were conducted on a Shimadzu GC-14B equipped with a flame ionization detector. Melting points were determined on a micro melting point apparatus (Yanaco MP-500D).

4.2. Experimental Procedures

Preparation of Tris(2-bromophenyl)phosphine (2).[6a] A solution of *i*PrMgBr in THF (0.92 M, 38 mL, 35 mmol), which was freshly prepared from *i*PrBr and Mg, was added over 25 min to a solution of 1-bromo-2-iodobenzene (**1**, 9.90 g, 35 mmol) in THF (35 mL) at –20 °C. The reaction mixture turned into a gray slurry after stirring at –20 °C for an additional 3 h. After complete consumption of **1**, which was confirmed by GC analysis of a small aliquot of the reaction mixture, TMEDA (5.25 mL, 35 mmol) and PCl_3 (872 μL, 10 mmol) were added in a dropwise manner in that order at –20 °C. The resulting mixture was allowed to warm to 0 °C and stirred at this temperature for an additional 14 h to give a clear pale-yellow solution. After quenching with NH_4Cl aq. at 0 °C, the reaction mixture was extracted with EtOAc. The organic layer was washed with brine, dried over $MgSO_4$, filtered, and concentrated. The residue was passed through a short silica gel column with toluene as an eluting solvent, and the eluent was evaporated under vacuum. The residual solids were recrystallized from benzene/MeOH to give tris(2-bromophenyl)phosphine as a while solid (2.86 g, 57% yield).
^{1}H NMR ($CDCl_3$): δ 6.74–6.77 (m, 3H), 7.22–7.28 (m, 6H), 7.63–7.66 (m, 3H). ^{13}C NMR ($CDCl_3$): δ 127.78, 130.37 (d, J = 34.4 Hz), 130.73, 133.19 (d, J = 1.9 Hz), 134.69, 136.72 (d, J = 11.5 Hz). ^{31}P NMR ($CDCl_3$): δ –2.8.

Preparation of Silanol 3. For the preparation of **3**, Tsuji and Tamao's procedure for the synthesis of 10-chloro-9-phospha-10-silatriptycene[6a] was modified as follows. A solution of *t*BuLi in pentane (1.77 M, 5.1 mL, 9.0 mmol) was added over 15 min to a solution of **2** (748 mg, 1.5 mmol) in THF (4.5 mL) and Et_2O (23 mL) at –78 °C. After stirring for 4 h, $SiCl_4$ (172 μL, 1.5 mmol) was added in a dropwise manner at –78 °C, and the resulting mixture was stirred at this temperature for an additional 4 h. After quenching the excess organolithium species with Me_3SiCl (1.1 mL, 9 mmol) at –78 °C, the mixture was allowed to warm to room temperature and stirred for an additional 13 h. After evaporation of the volatiles, the residue was dissolved in toluene and filtered through a Celite® pad. The filtrate was concentrated, and the crude product was purified by silica gel column chromatography (hexane/EtOAc 100:0–80:20) followed by reprecipitation from CH_2Cl_2/hexane to give silanol **3** as a white solid (321 mg, 70% yield). Single crystals of **3** suitable for X-ray diffraction studies were obtained by recrystallization from a $CHCl_3$/hexane solution (CCDC: 1060983).
M.p.: 120 °C (decomp.). ^{1}H NMR ($CDCl_3$): δ 3.32 (s, 1H), 7.21–7.28 (m, 6H), 7.81 (d, J = 6.4 Hz, 3H), 7.87 (dd, J = 10.8, 7.2 Hz, 3H). ^{13}C NMR ($CDCl_3$): δ 127.86, 128.10 (d, J = 15.2 Hz), 131.56, 134.69 (d, J = 45.8 Hz), 141.13, 146.12 (d, J = 8.6 Hz). ^{29}Si NMR ($CDCl_3$): δ –30.6 (d, J = 8.5 Hz). ^{31}P NMR ($CDCl_3$): δ –54.0. IR (ATR): 3347 (br), 3052, 2964, 1688,

1572, 1430, 1260, 896, 755, 666 cm^{-1}. HRMS–ESI (*m/z*): $[M–H]^-$ calcd for $C_{18}H_{12}OPSi$, 303.04005; found, 303.04086.

Preparation of Disiloxane 4. Silanol **3** (30.0 mg, 0.1 mmol) and imidazole (1.4 mg, 0.02 mmol) were dissolved in benzene (0.5 mL), and the mixture was stirred at 80 °C for 10.5 h. After cooling to room temperature, the insoluble solids were filtered and washed with benzene to give the disiloxane **4** as a white solid (15.0 mg, 52% yield). Due to the low solubility of **4** into organic solvents, clear NMR data were not obtained.

White solid. M.p. 430 °C (decomp.). ^{1}H NMR ($CDCl_3$): δ 7.22–7.26 (m, 6H), 7.31 (t, J = 7.2 Hz, 6H), 7.91 (d, J = 6.4 Hz, 6H), 7.98 (dd, J = 11.2, 7.2 Hz, 6H). ^{13}C NMR ($CDCl_3$): δ 128.27, 128.47 (d, J = 15.3 Hz), 131.77, 134.98 (d, J = 45.8 Hz), 140.77, 146.31 (d, J = 9.6 Hz). ^{31}P NMR ($CDCl_3$): δ –55.1. HRMS-EI (*m/z*) Calcd for $[M]^+$ $C_{36}H_{24}OP_2Si_2$, 590.08409; found, 590.08389.

Preparation of TMSO-TRIP 5. A solution of silanol **3** (45.7 mg, 0.15 mmol) in CH_2Cl_2 (2 mL) was added dropwise to a solution of *N*-trimethylsilylimidazole (105 mg, 0.75 mmol) in CH_2Cl_2 (2 mL). After stirring at room temperature for 1 h, MeOH (2 mL) was added to quench the excess *N*-trimethylsilylimidazole, and then the mixture was stirred for additional 10 min. The volatiles were removed under reduced pressure. The crude product was purified by silica gel column chromatography (eluting with CH_2Cl_2) to give 10-{(trimethylsilyl)oxy}-9-phospha-10-silatriptycene (**5**) as a white solid (49.0 mg, 87% yield).

M.p.: 225–228 ºC. ^{1}H NMR ($CDCl_3$): δ 0.52 (s, 9H), 7.19–7.28 (m, 6H), 7.76 (dd, J = 6.8, 0.8 Hz, 3H), 7.85 (dd, J = 11.6, 6.8 Hz, 3H). ^{13}C NMR ($CDCl_3$): δ 2.48, 127.79–127.94 (m), 131.58, 134.61 (d, J = 45.8 Hz), 142.09, 146.12 (d, J = 7.6 Hz). ^{31}P NMR ($CDCl_3$): δ –54.9. ^{29}Si NMR ($CDCl_3$): δ –38.9 (d, J = 9.1 Hz), 14.4. HRMS-EI (*m/z*) Calcd for $[M]^+$ $C_{21}H_{21}OPSi_2$, 376.08685; found, 376.08541.

Preparation of Silica-TRIP. Silanol **3** (365 mg, 1.2 mmol), CARiACT Q-10 silica gel (10.6 g), imidazole (408 mg, 6.0 mmol), and anhydrous, degassed toluene (42 mL) were placed in a 200-mL three-necked flask equipped with a mechanical stirrer under argon atmosphere. The suspension was gently stirred at 100 °C for 16 h. After cooling to room temperature, the mixture was filtered, washed successively with degassed toluene, toluene-MeOH (1:1), and MeOH, and dried under vacuum at 120 °C overnight. Next, a solution of *N*-trimethylsilylimidazole (5.3 mL) in THF (30 mL) was added to the flask with the functionalized silica gel Silica-TRIP(SiOH). The suspension was stirred at 60 °C for 24 h under argon atmosphere. After cooling to room temperature, solids were collected by filtration through a glass filter, washed with MeOH, and dried under vacuum at 120 °C

overnight to give 9.4 g of Silica-TRIP.

^{13}C CP/MAS NMR: δ 2, 123–150 (br-m). ^{29}Si CP/MAS NMR: δ –110, −102, –36, 14. ^{31}P CP/MAS NMR: δ –52. Elemental Anal. found: C 5.33; H 1.19.

Reaction of $PdCl_2(py)_2$ and Silica-TRIP (Pd/P 2:1). Silica-TRIP (401.5 mg, 0.028 mmol, 0.07 mmol/g) and $PdCl_2(py)_2$ (18.8 mg, 0.056 mmol) were placed in a vial containing a magnetic stirring bar. Anhydrous, degassed CH_2Cl_2 (2 mL) was added, and the tube was sealed with a screw cap. The mixture was stirred at room temperature for 0.5 h. The suspension was filtered and washed with CH_2Cl_2. The filtrate was evaporated to recover unreacted $PdCl_2(py)_2$ (8.3 mg, 0.025 mmol). The pale yellow silica gel was dried under vacuum to give $PdCl_2(py)$(Silica-TRIP) (375.1 mg). Thus, P loading on Silica-TRIP was calculated to be 0.078 mmol/g based on a Pd to P stoichiometry of 1:1 [{(18.8–8.3)/335.53}/0.4015 = 0.078]. For convenience, the value of 0.07 mmol/g was used for P loading in metal complexations and catalytic applications.

^{13}C CP/MAS NMR: δ 3, 120–158 (br-m). ^{31}P CP/MAS NMR: δ –5.

Reaction of $PdCl_2(py)_2$ and Silica-TRIP (Pd/P 1:2). Silica-TRIP (399.2 mg, 0.028 mmol, 0.07 mmol/g) and $PdCl_2(py)_2$ (4.8 mg, 0.014 mmol) were placed in a vial containing a magnetic stirring bar. Anhydrous, degassed CH_2Cl_2 (2 mL) was added, and the tube was sealed with a screw cap. The mixture was stirred at room temperature for 0.5 h. The suspension was filtered and washed with CH_2Cl_2. The pale yellow silica was dried under vacuum to give a mixture of $PdCl_2(py)$(Silica-TRIP) and unreacted Silica-TRIP (363.5 mg).

^{31}P CP/MAS NMR: δ –52, –5.

Reaction of $PdCl_2(py)_2$ and TMSO-TRIP (Pd/P 1:1, 1:2). TMSO-TRIP (**5**) (0.02 mmol) and $PdCl_2(py)_2$ (0.02 mmol for Pd/P 1:1; 0.01 mmol for Pd/P 1:2) were placed in a 5-mL glass tube containing a magnetic stirring bar. $CDCl_3$ (0.7 mL) was added and stirred at room temperature for 5 min. The mixture was analyzed with ^{31}P NMR spectroscopy.

Preparation of $PdCl_2(py)$(5). A solution of **5** (18.8 mg, 0.05 mmol) in $CHCl_3$ (1.5 mL) was added dropwise to a solution of $PdCl_2(py)_2$ (17.8 mg, 0.05 mmol) in $CHCl_3$ (1.5 mL). The mixture was stirred at room temperature for 0.5 h. The volatiles were evaporated. The residue was extracted with benzene. After filtration, the solution was evaporated. The residue was recrystallized from $CHCl_3$/hexane to give $PdCl_2(py)$(**5**) as a yellow solid (22.8 mg, contaminated with 3% of $PdCl_2(py)_2$, 71% yield)

M.p.: 190 °C (decomp.). ^{1}H NMR ($CDCl_3$): δ 0.53 (s, 9H), 7.30–7.39 (m, 6H), 7.50 (t, J = 7.2 Hz, 2H), 7.71 (d, J = 6.8 Hz, 3H), 7.88 (t, J = 7.2 Hz, 1H), 9.12 (dd, J = 13.6, 7.3 Hz, 3H), 9.16–9.19 (m, 2H). ^{13}C NMR ($CDCl_3$): δ 2.37, 124.89 (d, J = 3.8 Hz), 127.96 (d, J = 13.4 Hz), 128.73, 130.49 (d, J = 7.6 Hz), 136.74 (d, J = 19.2 Hz), 138.57, 140.04 (d, J = 49.8 Hz),

140.99, 151.47. ^{31}P NMR ($CDCl_3$): δ –6.5. Attempts to obtain MS spectra (ESI or FAB) of $PdCl_2$(py)(**5**) were unsuccessful.

Preparation of $PdCl_2$(5)$_2$. The mixture of **5** (37.6 mg, 0.10 mmol), $PdCl_2(py)_2$ (17.8 mg, 0.05 mmol) and $CHCl_3$ (2 mL) was stirred at room temperature for 1 h. The volatiles were evaporated. The residue was washed with $CHCl_3$ to give $PdCl_2$(**5**)$_2$ as a yellow solid (39.6 mg, 43% yield).

M.p.: 310 ºC (decomp.). ^{1}H NMR ($CDCl_3$): δ 0.55 (s, 18H), 7.30–7.43 (m, 12 H), 7.78 (d, J = 7.6 Hz, 6H), 9.18–9.24 (m, 6H). ^{31}P NMR ($CDCl_3$): δ –19.5. HRMS-ESI (m/z) Calcd for $[M+Na]^+$ $C_{42}H_{42}Cl_2O_2P_2PdSi_4Na$, 953.00508; found 953.00236. ^{13}C NMR data are not available due to the low solubility of $PdCl_2$(**5**)$_2$ in organic solvents.

Reaction of $PdCl_2(py)_2$ and Silica-1p-TPP (Pd/P 1:2). Silica-1p-TPP (200 mg, 0.018 mmol, 0.09 mmol/g) and $PdCl_2(py)_2$ (3.0 mg, 0.0089 mmol) were placed in a vial containing a magnetic stirring bar. Anhydrous, degassed CH_2Cl_2 (2 mL) was added, and the tube was sealed with a screw cap. The mixture was stirred at room temperature for 1 h. The suspension was filtered and washed with CH_2Cl_2. The pale yellow silica was dried under vacuum to give a mixture of $PdCl_2$(py)(Silica-1p-TPP), $PdCl_2$(Silica-1p-TPP)$_2$ and unreacted Silica-TRIP (200 mg).

^{31}P CP/MAS NMR: δ –4, 23, 29.

Reaction of $PdCl_2(py)_2$ and PPh_2[4-Me$_2$(*i*PrO)Si-C$_6$H$_4$] (Pd/P 1:1, 1:2). PPh_2[4-Me$_2$(*i*PrO)Si-C$_6$H$_4$] (**6**) (0.02 mmol) and $PdCl_2(py)_2$ (0.02 mmol for Pd/P 1:1; 0.01 mmol for Pd/P 1:2) were placed in a 5-mL glass tube containing a magnetic stirring bar. $CDCl_3$ (0.7 mL) was added and stirred at room temperature for 5 min. The mixture was analyzed with ^{31}P NMR spectroscopy.

Preparation of $PdCl_2$(py)(6). A solution of **6** (18.9 mg, 0.05 mmol) in $CHCl_3$ (1.5 mL) was added dropwise to a solution of $PdCl_2(py)_2$ (17.8 mg, 0.05 mmol) in $CHCl_3$ (1.5 mL). The mixture was stirred at room temperature for 0.5 h. The volatiles were evaporated. The residue was extracted with benzene. After filtration, the solution was evaporated. The residue was recrystallized from benzene/hexane to give $PdCl_2$(py)(**6**) as a yellow solid (16.8 mg, contaminated with 6% of $PdCl_2(py)_2$, 51% yield)

M.p.: 210 °C (decomp.). ^{1}H NMR ($CDCl_3$): δ 0.37 (s, 6H), 1.15 (d, J = 6.4 Hz, 6H), 4.02 (sept, J = 6.4 Hz, 1H), 7.35–7.51 (m, 8H) 7.64 (dd, J = 8.4, 2.8 Hz, 2H), 7.76–7.84 (m, 7H), 8.99–9.01 (m, 2H). ^{13}C NMR ($CDCl_3$): δ –1.16, 25.68, 65.51, 124.59 (d, J = 2.8 Hz), 128.09 (d, J = 11.5 Hz), 129.21 (d, J = 58.4 Hz), 130.16 (d, J = 56.5 Hz), 131.02 (d, J = 2.8 Hz), 133.02 (d, J = 10.6 Hz), 133.90 (d, J = 9.5 Hz), 134.82 (d, J = 9.5 Hz), 138.20, 142.33 (d, J = 1.9 Hz), 151.60. ^{31}P NMR ($CDCl_3$): δ 29.3. Attempts to obtain MS spectra (ESI or FAB) of

$PdCl_2$(py)(**6**) were unsuccessful.

Preparation of $PdCl_2$(6)$_2$. The mixture of **6** (22.7 mg, 0.06 mmol), $PdCl_2(py)_2$ (10.1 mg, 0.03 mmol) and $CHCl_3$ (1 mL) was stirred at room temperature for 1 h. The volatiles were evaporated. The resulting residue was recrystallized from CH_2Cl_2/hexane to give $PdCl_2$(**6**)$_2$ as a yellow solid (26.5 mg, contaminated with traces of impurities, 47% yield,)

M.p.: 192–195 °C. ^{1}H NMR ($CDCl_3$): δ 0.36 (s, 12H), 1.14 (d, J = 6.4 Hz, 12H), 4.01 (sept, J = 6.4 Hz, 2H), 7.35–7.45 (m, 12H), 7.59 (d, J = 7.6 Hz, 4H), 7.68–7.73 (m, 12H). ^{13}C NMR ($CDCl_3$): δ –1.15, 25.68, 65.44, 128.03 (vt, J = 4.8 Hz), 129.51 (vt, J = 24.9 Hz), 130.48, 130.59 (vt, J = 23.9 Hz), 132.97 (vt, J = 4.8 Hz), 134.15 (vt, J = 5.7 Hz), 135.00 (vt, J = 6.7 Hz), 141.48. ^{31}P NMR ($CDCl_3$): δ 23.7. HRMS-ESI (m/z) Calcd for $[M+Na]^+$ $C_{46}H_{54}Cl_2O_2P_2PdSi_2Na$, 957.14513; found 957.14797.

Typical Procedure for the Suzuki–Miyaura Coupling Reaction. In a nitrogen-filled glove box, Silica-TRIP (0.07 mmol/g, 42.9 mg, 0.003 mmol) and a solution of $Pd(OAc)_2$ (0.56 mg, 0.0025 mmol) in anhydrous, degassed THF (0.5 mL) were placed in a 10-mL glass tube containing a magnetic stirring bar. After stirring at room temperature for 5 min, phenylboronic acid (**8a**, 73.1 mg, 0.6 mmol), K_3PO_4 (318 mg, 1.5 mmol), *p*-chlorotoluene (**7a**, 63.3 mg, 0.5 mmol), and THF (1 mL) were added successively. The tube was sealed with a screw cap and removed from the glove box. The mixture was stirred at 60 °C for 12 h. After cooling to room temperature, the mixture was diluted with Et_2O and filtered through a Celite® pad (eluting with Et_2O). The volatiles were evaporated, and an internal standard (1,1,2,2-tetrachloroethane) was added to determine the yield of 4-methylbiphenyl (**9a**, 93% yield). The crude product was purified by silica gel chromatography (eluting with hexane) to give **9a** (74.3 mg, 0.44 mmol, 88% yield).

ICP-AES Measurements for Pd Residue. After the reaction of **7a** (0.5 mmol) and **8a** (0.6 mmol) in the presence of 0.5 mol% the Silica-TRIP-Pd catalyst (Table 2, entry 3), the reaction mixture was diluted with Et_2O, and filtered through a Celite® pad (eluting with Et_2O). The volatiles were evaporated. A small aliquot of the residue (ca. 5 mg) was taken for a microwave-assisted acid digestion with aqua regia (1000 W, 220 °C) followed by a mixture of nitric acid and perchloric acid (1000 W, 220 °C). The resulting mixture was diluted in H_2O (20 mL). This solution was subjected to ICP-AES analysis.

X-ray Crystallographic Analysis of 3. Crystal data for 3{**3**·1/3($CHCl_3$)} (CCDC 1060983; recrystallization from $CHCl_3$/hexane). $C_{55}H_{40}Cl_3O_3P_3Si_3$, M = 1032.46, trigonal, space group $P\bar{3}c1$ (#165), a = 15.5297(5) Å, c = 24.1564(11) Å, V = 5045.3(4) Å^3, Z = 4, density (calc.) = 1.359, total reflections collected = 39823, unique reflections = 3860 (R_{int} = 0.0542), GOF = 1.139, $R1$ (I>2σ(I)) = 0.0461, $wR2$ = 0.1077.

Data were collected on a Rigaku Mercury 70 CCD diffractometer with graphite monochromated Mo-Kα radiation (λ = 0.71075 Å) at 150 K, and processed using the CrystalClear software.[21] Structures were solved by a direct method using SIR-2004,[22] and refined by full-matrix least-square method using SHELXL-97.[23] Non-hydrogen atoms were refined anisotropically. All hydrogen atoms except for the silanol protons were located on the calculated positions and refined using a riding model. The silanol protons (H1 and H2; disordered, 1:1) were located in the difference Fourier map and refined isotropically. All calculations were performed using the CrystalStructure software package.[24]

5. References

(1) (a) Lindner, E.; Schneller, T.; Auer, F.; Mayer, H. A. *Angew. Chem., Int. Ed.* **1999**, *38*, 2154–2174. (b) Wight, A. P.; Davis, M. E. *Chem. Rev.* **2002**, *102*, 3589–3614. (c) Corma, A.; Garcia, H. *Adv. Synth. Catal.* **2006**, *348*, 1391–1412. (d) Hoffmann, F.; Cornelius, M.; Morell, J.; Fröba, M. *Angew. Chem., Int. Ed.* **2006**, *45*, 3216–3251. (e) Opanasenko, M.; Štěpnička, P.; Čejka, J. *RSC Adv.* **2014**, *4*, 65137–65162.

(2) (a) *Recoverable and Recyclable Catalysts*; Benaglia, M. Ed.; Wiley: Chichester, 2009; (b) *Heterogenized Homogeneous Catalysts for Fine Chemicals Production: Materials and Processes*; Barbaro, P.; Liguori, F. Eds.; Springer: Dordrecht, 2010.

(3) Blümel, J. *Coord. Chem. Rev.* **2008**, *252*, 2410–2423.

(4) Hamasaka, G.; Ochida, A.; Hara, K.; Sawamura, M. *Angew. Chem., Int. Ed.* **2007**, *46*, 5381–5383. (b) Kawamorita, S.; Hamasaka, G.; Ohmiya, H.; Hara, K.; Fukuoka, A.; Sawamura, M. *Org. Lett.* **2008**, *10*, 4697–4700. (c) Hamasaka, G.; Kawamorita, S.; Ochida, A.; Akiyama, R.; Hara, K.; Fukuoka, A.; Asakura, K.; Chun, W. J.; Ohmiya, H.; Sawamura, M. *Organometallics* **2008**, *27*, 6495–6506. (d) Kawamorita, S.; Ohmiya, H; Hara, K.; Fukuoka, A.; Sawamura, M. *J. Am. Chem. Soc.* **2009**, *131*, 5058–5059. (e) Kawamorita, S.; Ohmiya, H.; Sawamura, M. *J. Org. Chem.* **2010**, *75*, 3855–3858. (f) Yamazaki, K.; Kawamorita, S.; Ohmiya, H.; Sawamura, M. *Org. Lett.* **2010**, *12*, 3978–3981. (g) Kawamorita, S.; Ohmiya, H.; Iwai, T.; Sawamura, M. *Angew. Chem., Int. Ed.* **2011**, *50*, 8363–8366. (h) Kawamorita, S.; Miyazaki, T.; Ohmiya, H.; Iwai, T.; Sawamura, M. *J. Am. Chem. Soc.* **2011**, *133*, 19310–19313. (i) Kawamorita, S.; Yamazaki, K.; Ohmiya, H.; Iwai, T.; Sawamura, M. *Adv. Synth. Catal.* **2012**, *354*, 3440–3444. (j) Kawamorita, S.; Murakami, R.; Iwai, T.; Sawamura, M. *J. Am. Chem. Soc.* **2013**, *135*, 2947–2950. (k) Konishi, S.; Kawamorita, S.; Iwai, T.; Steel, P. G.; Marder, T. B.; Sawamura, M. *Chem. Asian J.* **2014**, *9*, 434–438. (l) Murakami, R.; Tsunoda, K.; Iwai, T.; Sawamura, M. *Chem. Eur. J.* **2014**, *20*, 13127–13131.

(5) (a) Ochida, A.; Hara, K.; Ito, H.; Sawamura, M. *Org. Lett.* **2003**, *5*, 2671–2674. (b) Ochida, A.; Ito, S.; Miyahara, T.; Ito, H.; Sawamura, M. *Chem. Lett.* **2006**, *35*, 294–295. (c) Ochida, A.; Hamasaka, G.; Yamauchi, Y.; Kawamorita, S.; Oshima, N.; Hara, K.; Ohmiya, H.; Sawamura, M. *Organometallics* **2008**, *27*, 5494–5503.

(6) (a) Tsuji, H.; Inoue, T.; Kaneta, Y.; Sase, S.; Kawachi, A.; Tamao, K. *Organometallics* **2006**, *25*, 6142–6148. (b) Tsuji, H.; Inoue, T.; Sase, S.; Tamao, K. *Acta Cryst. E* **2006**, *62*, m535–m537.

(7) Kawamorita, S.; Miyazaki, T.; Iwai, T.; Ohmiya, H.; Sawamura, M. *J. Am. Chem. Soc.* **2012**, *134*, 12924–12927.

(8) Portions of this work on the synthesis of Silica-TRIP (ref. 4h) and its application to Pd-catalyzed Suzuki–Miyaura cross-coupling of chloroarenes (ref. 16b) have been reported.

(9) For selected reviews, see: Littke, A. F.; Fu, G. C. *Angew. Chem., Int. Ed.* **2002**, *41*, 4176–4211. (b) Suzuki, A. *Angew. Chem., Int. Ed.* **2011**, *50*, 6722–6737.

(10) For selected reviews, see: (a) Martin, R.; Buchwald, S. L. *Acc. Chem. Res.* **2008**, *41*, 1461–1473. (b) Fu, G. C. *Acc. Chem. Res.* **2008**, *41*, 1555–1564. (c) Fleckenstein, C. A.; Plenio, H. *Chem. Soc. Rev.* **2010**, *39*, 694–711. (d) Lundgren, R. J.; Hesp, K. D.; Stradiotto, M. *Synlett* **2011**, *2011*, 2443–2458. (e) Wong, S. M.; So, C. M.; Kwong, F. Y. *Synlett* **2012**, *2012*, 1132–1153.

(11) For selected reviews, see: (a) Kantchev, E. A. B.; O'Brien, C. J.; Organ, M. G. *Angew. Chem., Int. Ed.* **2007**, *46*, 2768–2813. (b) Fortman, G. C.; Nolan, S. P. *Chem. Soc. Rev.* **2011**, *40*, 5151–5169.

(12) For selected examples, see: (a) Iwasawa, T.; Komano, T.; Tajima, A.; Tokunaga, M.; Obora, Y.; Fujihara, T.; Tsuji, Y. *Organometallics* **2006**, *25*, 4665–4669. (b) Ohta, H.; Tokunaga, M.; Obora, Y.; Iwai, T.; Iwasawa, T.; Fujihara, T.; Tsuji, Y. *Org. Lett.* **2007**, *9*, 89–92. (c) Fujihara, T.; Yoshida, S.; Ohta, H.; Tsuji, Y. *Angew. Chem., Int. Ed.* **2008**, *47*, 8310–8314. (d) Snelders, D. J. M.; van Koten, G.; Gebbink, R. J. M. K. *J. Am. Chem. Soc.* **2009**, *131*, 11407–11416. (e) Mom, S.; Beaupérin, M.; Roy, D.; Royer, S.; Amardeil, R.; Cattey, H.; Doucet, H.; Hierso, J.-C. *Inorg. Chem.* **2011**, *50*, 11592–11603. (f) Chow, W. K.; Yuen, O. Y.; So, C. M.; Wong, W. T.; Kwong, F. Y. *J. Org. Chem.* **2012**, *77*, 3543–3548. (g) Zhnag, J.; Bellomo, A.; Trongsiriwat, N.; Jia, T.; Carroll, P. J.; Dreher, S. D.; Tudge, M. T.; Yin, H.; Robinson, J. R.; Schelter, E. J.; Walsh, P. J. *J. Am. Chem. Soc.* **2014**, *136*, 6276–6287.

(13) Li, B.; Guan, Z.; Wang, W.; Yang, X.; Hu, J.; Tan, B.; Li, T. *Adv. Mater.* **2012**, *24*, 3390–3395.

(14) For related studies using phosphine-containing organic polymers, which were effective for Pd-catalyzed Suzuki–Miyaura coupling of chloroarenes, see: (a) Hu, Q.-S.; Lu, Y.; Tang, Z.-Y.; Yu, H.-B. *J. Am. Chem. Soc.* **2003**, *125*, 2856–2857. (b) Yamamoto, T.; Akai, Y.; Nagata, Y.; Suginome, M. *Angew. Chem., Int. Ed.* **2011**, *50*, 8844–8847.

(15) (a) Iwai, T.; Harada, T.; Hara, K.; Sawamura, M. *Angew. Chem., Int. Ed.* **2013**, *52*, 12322–12326. (b) Iwai, T.; Tanaka, R.; Harada, T.; Sawamura, M. *Chem. Eur. J.* **2014**, *20*, 1057–1065. (c) Iwai, T.; Harada, T.; Tanaka, R.; Sawamura, M. *Chem. Lett.* **2014**, *43*, 584–586.

(16) Kowada, T.; Yamaguchi, S.; Ohe, K. *Org. Lett.* **2010**, *12*, 296–299.

(17) Single-crystal X-ray diffraction analysis of triorganosilanols with hydrogen-bonding network: Beckmann, J.; Duthie, A.; Reeske, G.; Schürmann, M. *Organometallics* **2004**, *23*, 4630–4635.

(18) Without imidazole as an additive, a significant amount of silanol **3** remained in the crude product (ca. 20% conversion of **3** after 12 h).

(19) The coordination behavior of Silica-1p-TPP toward a Pd(II) center using $PdCl_2(PhCN)_2$ was studied previously. See, ref 15b.

(20) Krogul, A.; Cedrowski, J.; Wiktorska, K.; Ozimiński, W. P.; Skupińska, J.; Litwinienko, G. *Dalton Trans.* **2012**, *41*, 658–666.

(21) *CrystalClear*: (a) Rigaku Corporation, 1999. (b) CrystalClear Software User's Guide, Molecular Structure Corporation, 2000. (c) Pflugrath, J. W. *Acta Cryst. D* **1999**, *55*, 1718–1725.

(22) *SIR-2004*: Burla, M. C.; Caliandro, R.; Camalli, M.; Carrozzini, B.; Cascarano, G. L.; De Caro, L.; Giacovazzo, C.; Polidori, G.; Spagna, R. *J. Appl. Cryst.* **2005**, *38*, 381–388.

(23) *SHELXL-97*: Sheldrick, G. M. *Acta Cryst. A* **2008**, *64*, 112–122.

(24) *CrystalStructure 4.0*: Crystal Structure Analysis Package; Rigaku Corporation: Tokyo, Japan, 2000–2010.

Chapter 3

Synthesis, Properties and Catalytic Application of a Triptycene-Type Anionic Borate-Phosphine Ligand

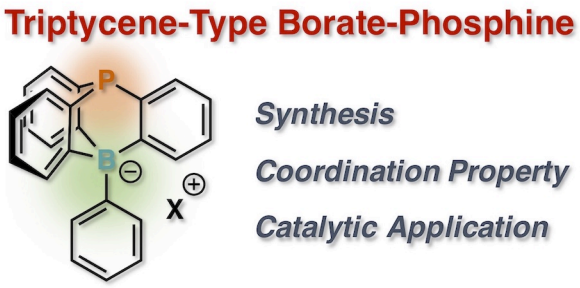

A borate-containing caged triarylphosphine **L-X** (X = Na or NBu_4), featuring a 9-phospha-10-boratriptycene framework, was synthesized and characterized by NMR spectroscopy and X-ray diffraction analysis. The NMR coupling constant of the corresponding phosphine selenide indicated a higher electron-donating property of borate-phosphine **L** compared to that of the 9-phospha-10-silatriptycene derivative (Ph-TRIP). The coordination property of **L-X** to [PdCl(η^3-allyl)] was dependent on the counter cation, giving a neutral Pd complex [PdCl(η^3-allyl)(**L-NBu$_4$**)] from **L-NBu$_4$** in CH_2Cl_2 or a zwitterionic Pd complex [Pd(η^3-allyl)(MeCN)(**L**)] from **L-Na** in MeCN/CH_2Cl_2. Utility of **L-X** as a ligand for metal catalysis was demonstrated in the Pd-catalyzed Suzuki–Miyaura cross-coupling of aryl chlorides.

1. Introduction

Caged phosphines with a bridgehead P atom are unique class of ligands in coordination and organometallics chemistries.[1,2] Due to their rigid structures, the P lone pair coordination is highly oriented. Sawamura *et al.* developed caged phosphine compounds containing a bridgehead silicon atom such as 1-phospha-4-silabicyclo[2.2.2]octanes (SMAP, named after *s*ilicon-constrained *m*onodentate tri*a*lkyl*p*hosphines, Figure 1a)[3] and 9-phospha-10-sila*trip*tycenes (TRIP, Figure 1b).[4,5] Substituents at the bridgehead Si atom of the SMAP derivatives had significant impact on electron-donor power of the P lone pair due to long range orbital interactions in the rigid cage system.[3b] Furthermore, the Si atoms of the caged phosphine molecules could be used as handles for immobilization of the phosphine molecules on solid supports such as silica gel[4,6] or gold surfaces.[7]

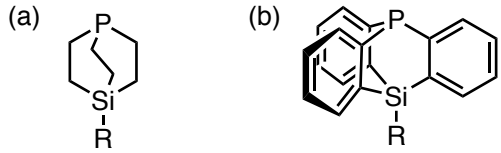

(R = Ph; Ph-SMAP) (R = Ph; Ph-TRIP)

Figure 1. (a) SMAP and (b) TRIP molecules

In this context, the Si atoms of these silicon-containing caged phosphines was replaced with a tetravalent B atom to produce *anionic* caged phosphine molecules[8,9] that increase the electron-donor power of the P lone pair.[10] It is also expected that such borate-phosphine hybrid ligands produce zwitterionic organometallic species with a well-defined location of cation and anion centers upon binding to cationic metal species.[11]

This chapter describes the synthesis and characterization of a borate-containing caged triarylphosphine (**L-X**) featuring a 9-phospha-10-boratriptycene framework (Figure 2). The P lone pair in the borate-phosphine **L-X** has a higher electron-donor power compared to the corresponding silicon-containing caged phosphine (Ph-TRIP, Figure 1). A zwitterionic Pd(II) complex with the cationic metal center and the anionic caged borate-phosphine (**L**) was also synthesized and characterized. The newly developed caged borate-phosphine **L-X** enabled the Pd-catalyzed Suzuki–Miyaura cross-coupling of aryl chlorides under mild conditions, for which neither the Si-analog Ph-TRAP nor a reported non-caged borate-phosphine were effective.

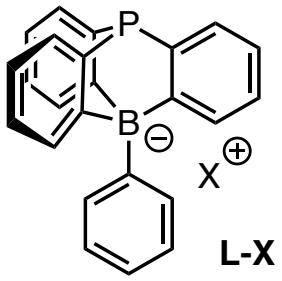

Figure 2. A triptycene-type borate-phosphine (**L-X**).

2. Results and Discussion

Synthesis. The 9-phospha-10-boratriptycene framework was constructed following to the synthetic route of the silicon-containing caged triarylphosphine TRIP derivatives, which was originally reported by Tsuji and Tamao's[5] and modified by Sawamura.[4] The route is summarized in Scheme 1. Commercially available 1-bromo-2-iodobenzene (**1**) was converted to tris(2-bromophenyl)phosphine (**2**) through the I–Mg exchange reaction followed by a Cu-catalyzed reaction with PCl_3. Three-fold Br–Li exchange reaction of **2** with *t*BuLi followed by reaction with $PhBF_3K$ gave, after treatment with 1 M aq. HCl and purification by silica gel column chromatography, a P-protonated borate-phosphine hybrid (**L-H**) in 72% yield as an air- and moisture-stable solid. Deprotonation of **L-H** with Na_2CO_3 in MeCN gave a sodium salt of free phosphine-borate (**L-Na**). The solubility of **L-Na** was good in coordinating organic solvents such as THF, MeCN, acetone, and DMF, but poor with non-polar hydrocarbon solvents such as toluene and hexane. The subsequent cation exchange with nBu$_4$NBr in MeCN/CH_2Cl_2 gave the corresponding tetrabutylammonium salt (**L-NBu$_4$**), which was also soluble in various organic solvents such as CH_2Cl_2, $CHCl_3$, THF, MeCN, acetone, and DMF. **L-K** and **L-Cs** could also be prepared by deprotonation of **L-H** with K_2CO_3 or Cs_2CO_3 (Scheme 2). Free phosphines **L-Na**, **L-K**, **L-Cs** and **L-NBu$_4$** were air-stable solids.

Scheme 1. Preparation of **L-Na** and **L-NBu$_4$**.

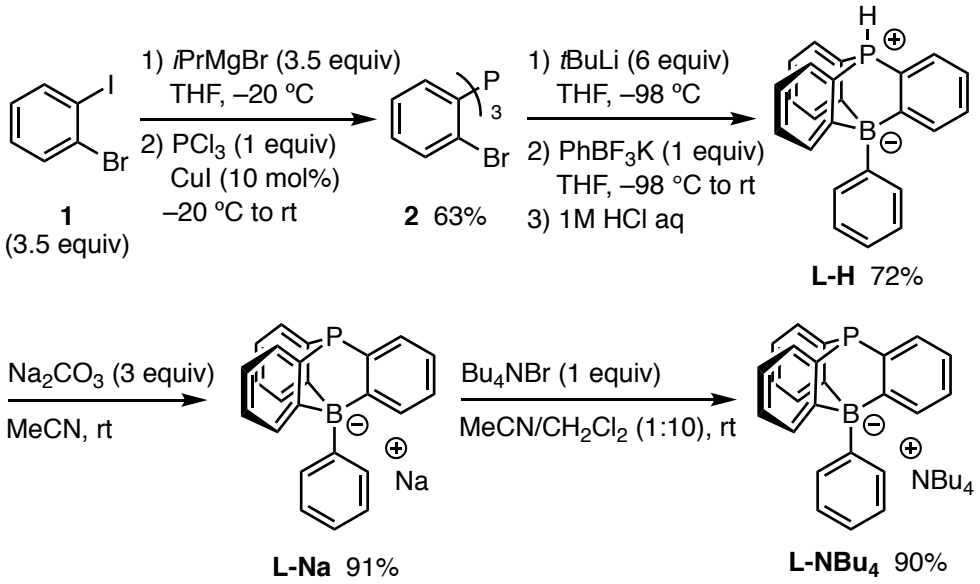

Scheme 2. Preparation of **L-K** and **L-Cs**

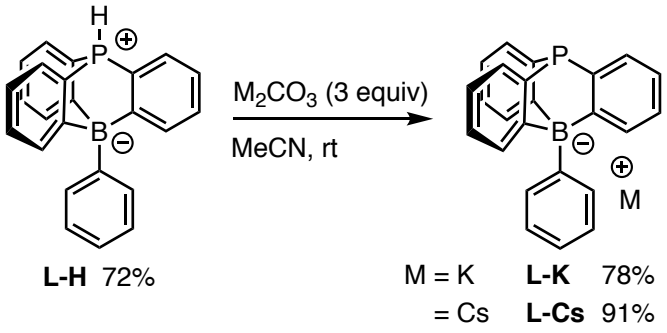

X-ray Crystal Structures. Single-crystal X-ray diffraction analysis of **L-H**, **L-Na** (1,2-dimethoxyethane adduct) and **L-NBu$_4$** confirmed their triptycene structures with bridgehead P and B atoms (Figure 3a-c). Comparison with the Si-analog Ph-TRIP indicated that **L-Na** [1.836 Å (avg.) and 96.1° (avg.)] and **L-NBu$_4$** [1.831 Å (avg.) and 95.9° (avg.)] had smaller P–C bond lengths and P–C–P angles than Ph-TRIP [1.845 Å (avg.) and 98.9° (avg.)]. These changes were due to the smaller size of the B atom compared to the Si atom. **L-H** had much shorter P–C bond lengths and larger C–P–C angles [1.778 Å (avg.) and 104.6° (avg.)] than the other borate-phosphine hybrids.

(a)

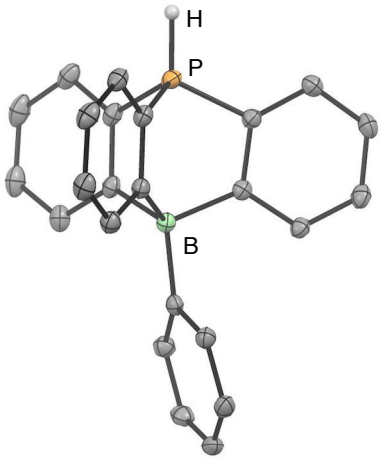

P–C length (ave.) 1.778 Å
C–P–C angle (ave.) 104.6°

(b)

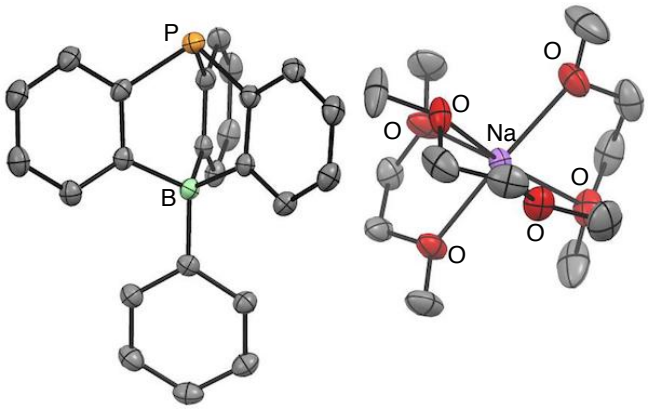

P–C length (ave.) 1.836 Å
C–P–C angle (ave.) 96.1°

(c)

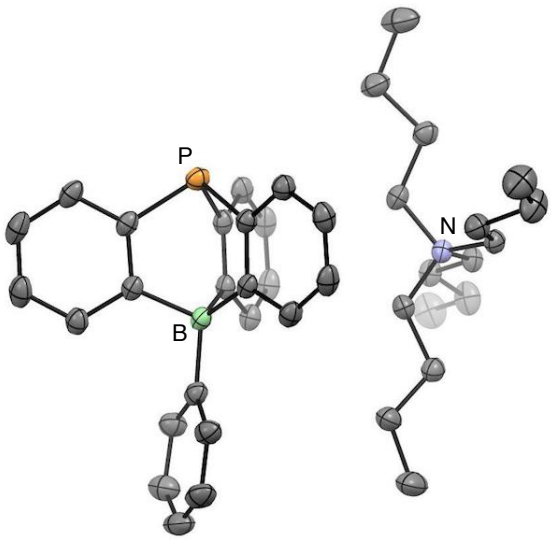

P–C length (ave.) 1.831 Å
C–P–C angle (ave.) 95.9°

Figure 3. ORTEP drawings of (a) L-H, (b) L-Na·3DME, and (c) L-NBu_4 with thermal ellipsoids drawn at the 30% probability level. Hydrogen atoms on the carbon atoms, except for the hydrogen atom on phosphorous atom of L-H, are omitted for clarity.

Electron-donor Power of L-X Phosphine Ligands. To evaluate the electron-donating ability of the borate-phosphine **L-X** as a phosphine ligand, a phosphine selenide (**Se-L-NBu$_4$**) of the tetrabutylammonium salt was prepared from **L-NBu$_4$** and Se by heating in $CHCl_3$ at 60 °C, and its $^1J_{P\text{-}Se}$ coupling constant was measured by ^{31}P NMR spectroscopy (Chart 1).[12] Phosphine selenide **Se-L-NBu$_4$** has a smaller $^1J_{P\text{-}Se}$ coupling constant than the selenide of the silicon-based phosphine selenide (**Se-Ph-TRIP**) (ΔJ = –74 Hz; Chart 1, top), indicating that the borate-phosphine is more basic. This borate effect in the caged system **L** was markedly more significant than the reported borate effect in the non-caged phosphine $[PPh_2(p\text{-}C_6H_4BPh_3)][PPh_4]$ (ΔJ = –28 Hz; Chart 1, bottom).[10j,13]

Chart 1. $^1J_{P\text{-}Se}$ Coupling Constants of Phosphine Selenides

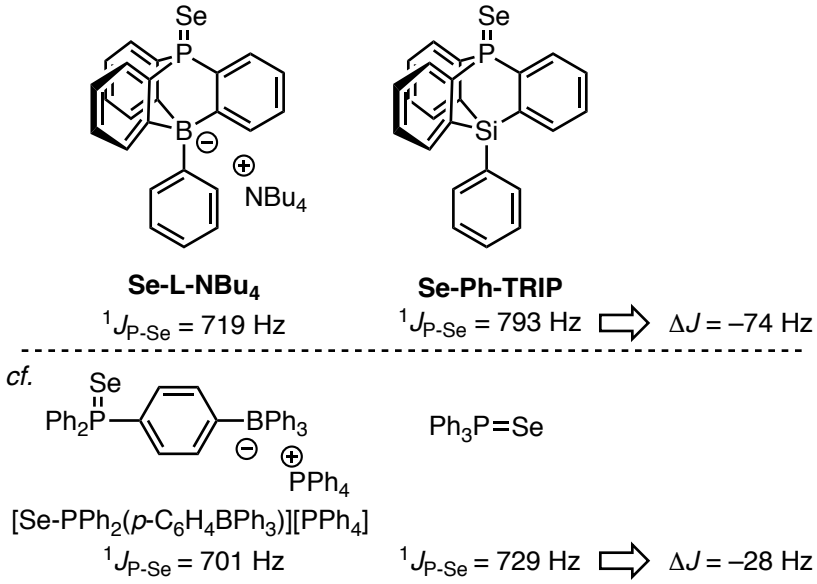

A molecular electrostatic potential map of the DFT-optimized borate-phosphine **L** shows that the boron-centered negative charge spreads out toward the four aromatic rings, and a resulting increase in P-electron density is suggested by comparing the map with that of the corresponding Si-based neutral phosphine Ph-TRIP (Figure 4).

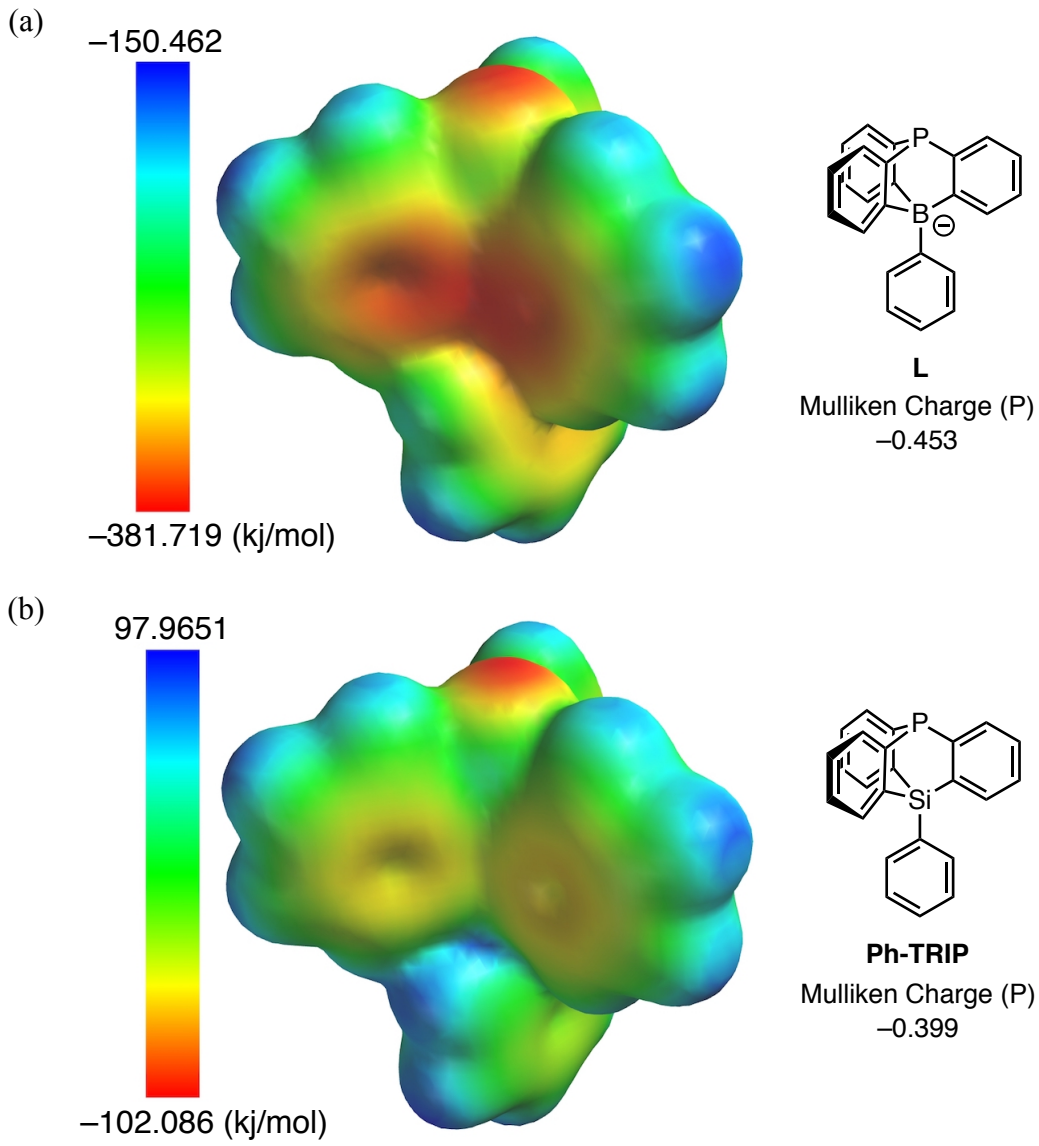

Figure 4. The molecular electrostatic potential map of (a) **L** and (b) Ph-TRIP [Spartan'14, B3LYP/6-311+G(2df,2p)]

Transition Metal Complexes. The effects of the counter cation of **L-X** (X = Na and NBu_4) on metal coordination were investigated through the synthesis of Pd(II) complexes. Specifically, the reaction between **L-NBu$_4$** and [PdCl(η^3-allyl)]$_2$ (P/Pd 1:1) in CH_2Cl_2 gave a square-planar Pd(II) complex [PdCl(η^3-allyl)(**L-NBu$_4$**)] with a neutral metal center as an air- and moisture-stable solid (Scheme 2 and Figure 5a). In contrast, the corresponding reaction with **L-Na** in CH_2Cl_2 failed to produce a well-defined compound due to its decomposition during the isolation process. However, when the reaction between **L-Na** and [PdCl(η^3-allyl)]$_2$ was conducted in a MeCN/CH_2Cl_2 mixed solvent system, a zwitterionic Pd complex [Pd(η^3-allyl)(MeCN)(**L**)] with a metal-centered positive formal charge was produced (Scheme 3 and Figure 5b). This complex could be isolated as a yellow-colored solid, but it

gradually decomposed in a CD_2Cl_2 solution to form Pd black and allylbenzene (detected by ^1H NMR spectroscopy). The phenyl group of the allylbenzene should be derived from the terminal phenyl substituent on the bridgehead B atom. Thus, this observation suggests that the C–B bond in the B-phenyl group was cleaved upon transmetalation with the cationic Pd center to form a Pd–Ph bond. The allylbenzene should be the product of reductive elimination of the allyl and phenyl ligands on the Pd(II) center. Observation of a postulated neutral 9-phospha-10-boratriptycene or its Pd complex has so far been unsuccessful.

Scheme 2. Preparation of [PdCl(η^3-allyl)(**L-NBu$_4$**)]

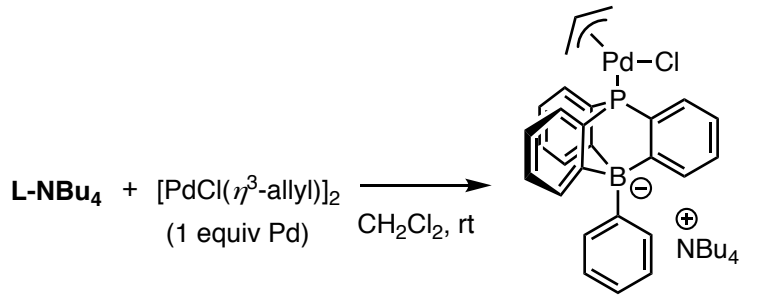

[PdCl(η^3-allyl)(**L-NBu$_4$**)]
43% (after recrystallization)

Scheme 3. Preparation of [Pd(η^3-allyl)(MeCN)(**L**)]

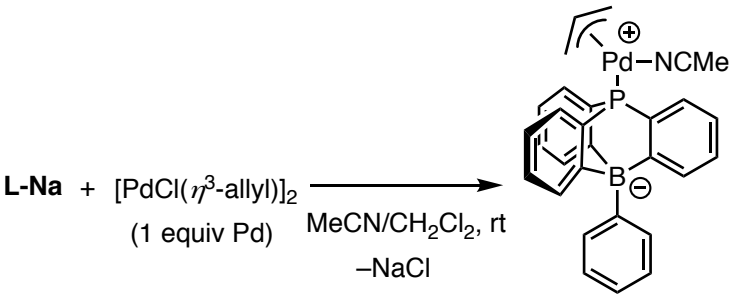

[Pd(η^3-allyl)(MeCN)(**L**)] 79%

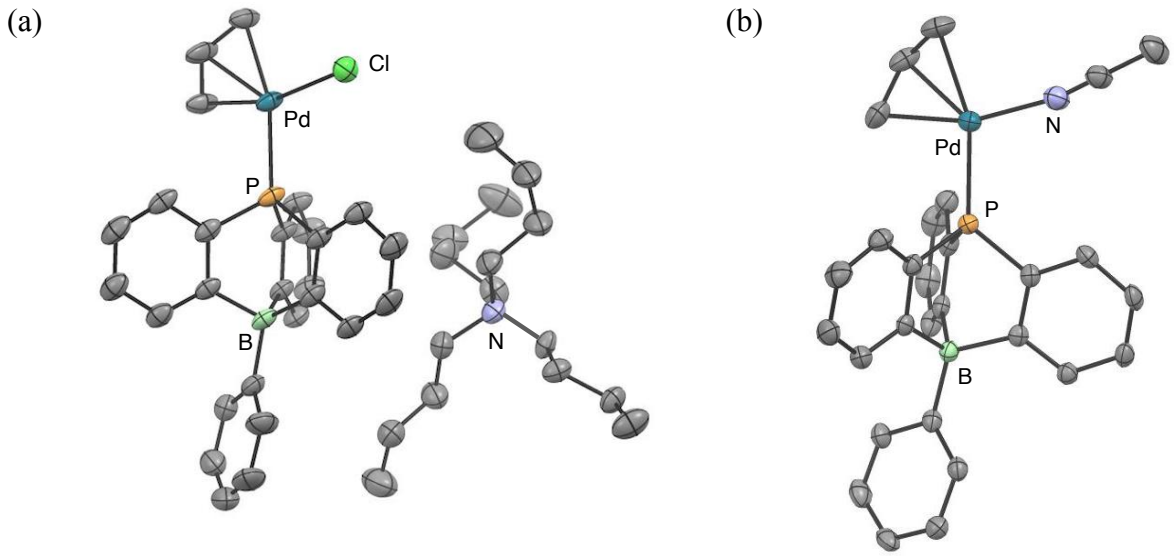

Figure 5. ORTEP drawings of (a) [PdCl(η^3-allyl)(**L-NBu$_4$**)] and (b) [Pd(η^3-allyl)(MeCN)(**L**)] with thermal ellipsoids drawn at the 30% and 50% probability level, respectively. For (a) hydrogen atoms on the carbon atoms are omitted for clarity. For (b), hydrogen atoms on the carbon atoms, the disordered π-allyl group and a solvent molecule MeCN are omitted for clarity.

Rhodium complexes were also synthesized by the reaction of **L–X** with [RhCl(cod)]$_2$. They showed similar reactivity by the change of counter cations. The reaction between **L-NBu$_4$** and [RhCl(cod)]$_2$ (P/Rh 1:1) in CH_2Cl_2 gave [RhCl(**L-NBu$_4$**)(cod)] (Scheme 4, Figure 6a). On the other hand, the reaction of **L-Na** and [RhCl(cod)]$_2$ in the presence of pyridine gave zwitterionic complex [Rh(**L**)(py)(cod)] (Scheme 5, Figure 6b).

Scheme 4. Preparation of [RhCl(**L-NBu$_4$**)(cod)].

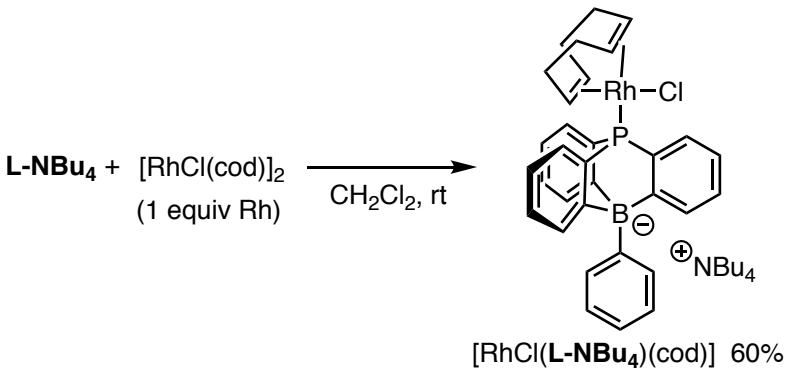

Scheme 5. Preparation of [Rh(**L**)(py)(cod)].

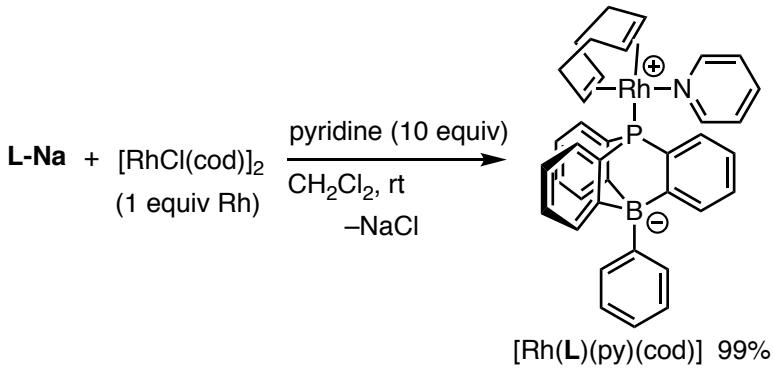

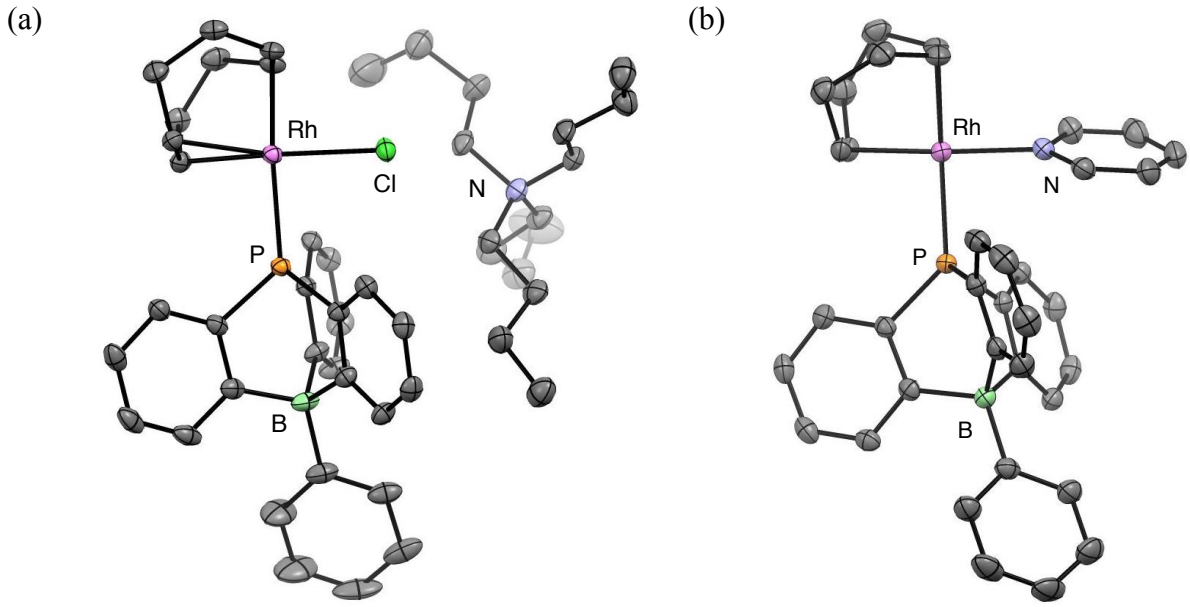

Figure 6. ORTEP drawings of (a) [RhCl(**L-NBu$_4$**)(cod)] and (b) [Rh(**L**)(py)(cod)] with thermal ellipsoids drawn at the 50% probability level. Hydrogen atoms on the carbon atoms are omitted for clarity.

Applications to Pd Catalysis. The synthetic utility of the borate-phosphine **L** was demonstrated in the Pd-catalyzed Suzuki–Miyaura cross-coupling of aryl chlorides, for which the effectiveness of bulky phosphines to produce catalytically active mono-P-ligated Pd species has already been established.[14] The efficiency of this reaction was influenced by the electron-donating property of the ligand, favoring stronger electron-donor power, which is demanded for cleavage of a C–Cl bond for oxidative addition to the Pd(0) center.[15] We envisaged that the borate-phosphine **L** might work favorably as a ligand for this transformation for the following two reasons. First, multiple ligation of **L** might cause electrostatic repulsion between the negative charges in the vicinity, resulting in favorable mono-P-ligation. Second, the electron-donor power of the P lone pair of **L** is significantly

increased due to the negative charge as indicated by the NMR spectroscopy of **Se-L-NBu$_4$** and by the electrostatic potential analysis. To our delight, a homogeneous **L**-Pd system appeared to be effective. Specifically, the coupling reaction between 1-butyl-4-chlorobenzene (**3a**) and phenylboronic acid (**4a**) occurred with 2 mol% loading of a catalyst prepared in situ from **L-NBu$_4$** and [$PdCl_2(PhCN)_2$] (P/Pd 2:1) in the presence of K_3PO_4 (3 equiv) at 60 °C in DMF over 12 h, giving the cross-coupling product **5a** in 92% yield (table 1, entry 1). The anionic ligand (**L-Na**) with a sodium counter cation also produced an active catalyst (entry 4, 93%), comparable to that with **L-NBu$_4$**. The effect of the P loading on the catalytic activity of the **L-NBu$_4$**-Pd system was significant (entry 2 and 3, 20% and 0%, respectively).

Other caged or non-caged phosphine ligands were used under the same conditions for comparison (Table 1). Neutral triarylphosphines such as PPh_3 (table 1, entry 5) and Ph-TRIP (entry 6) induced almost no reaction, indicating the crucial importance of the borate moiety of **L**. The previously reported PPh_3-based non-caged borate-phosphine [PPh_2(*p*-$C_6H_4BPh_3$)][PPh_4] was completely ineffective (entry 7). This suggests the importance of involving the borate group in the caged structure or at the position *ortho* to the P atom.[16] The ligand performance of the newly synthesized borate-phosphine **L** was comparable to that of the silica-supported triptycene-type phosphine Silica-TRIP (in THF, 98%, entry 8)[17] and the sterically bulky and electron-rich (dicyclohexylphosphino)biphenyl-type ligand XPhos (93%, entry 9). The usefulness of the former in the Suzuki–Miyaura coupling of aryl chlorides due to selective mono-P-ligation on a silica gel surface was demonstrated in our previous study.[4b]

Table 1. Ligand Effects in the Pd-Catalyzed Coupling between **3a** and **4a**[a]

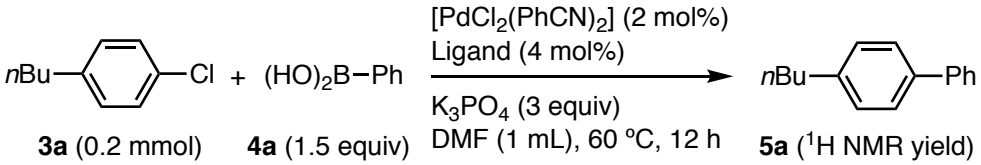

entry	ligand	yield (%)[b]
1	**L–NBu$_4$**	92 (92)
2	**L–NBu$_4$** (2 mol%, Pd:P 1:1)	20
3	**L–NBu$_4$** (6 mol%, Pd:P 1:3)	0
4	**L-Na**	93
5	PPh_3	3
6	Ph-TRIP	2
7	$[PPh_2(p\text{-}C_6H_4BPh_3)][PPh_4]$	0
8	Silica-TRIP (in THF)	98
9	XPhos	93

[a] Conditions: **3a** (0.2 mmol), **4a** (0.3 mmol), $[PdCl_2(PhCN)_2]$ (2 mol%), ligand (4 mol%), K_3PO_4 (0.6 mmol), DMF (1 mL), 60 °C, 12 h. [b] Yields are determined by ^1H NMR analysis. Isolated yields are in parentheses.

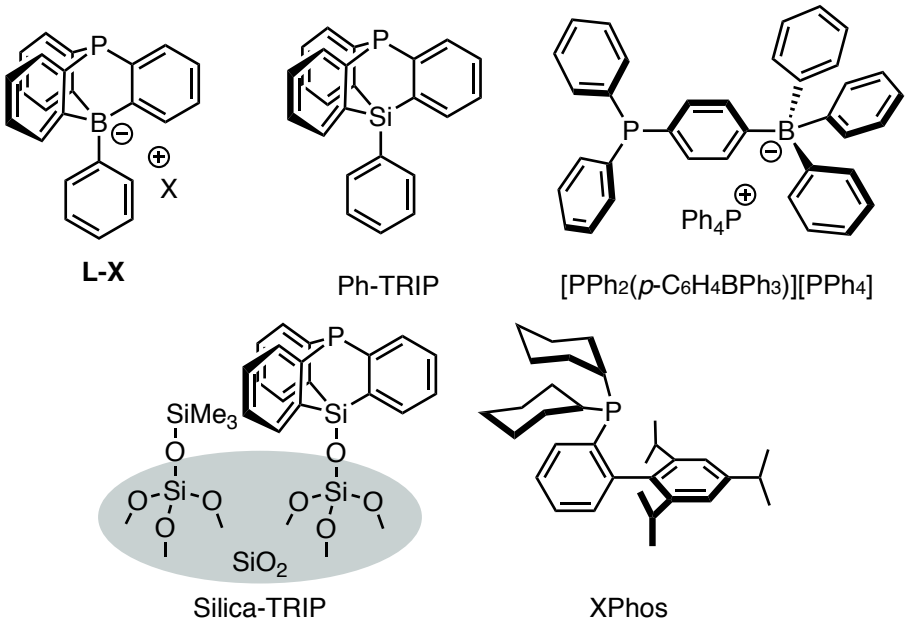

The use of other solvent systems with **L-NBu$_4$** was tested (Table 2). Non- or less-coordinating solvent such as toluene (0%) and 1,4-dioxane (0%) were ineffective due to the low solubility of the catalyst. Other coordinating solvents such as THF (12%), MeCN (12%) and MeOH (0%) were less effective than DMF.

Table 2. The effect of solvent on **L-NBu$_4$**–Pd catalyzed Suzuki-Miyaura cross-coupling between **3a** and **4a**[a]

entry	solvent	yield (%)[b]
1	DMF	92 (92)
2	toluene	0
3	1,4-dioxane	0
4	THF	12
5	MeCN	12
6	MeOH	0

[a] Conditions: **3a** (0.2 mmol), **4a** (0.3 mmol), [$PdCl_2(PhCN)_2$] (2 mol%), ligand (4 mol%), K_3PO_4 (0.6 mmol), solvent (1 mL), 60 °C, 12 h. [b] Yields are determined by ^{1}H NMR analysis. Isolated yields are in parentheses.

The **L-NBu$_4$**–Pd system (2 mol% Pd, P/Pd 2:1) catalyzed the cross-coupling between several aryl chlorides and arylboronic acids (Chart 2). The reactions of 4-chloroanisole or methyl 4-chlorobenzoate with **4a** proceeded smoothly at 60 °C, affording **5b** and **5c** in high yields. The same conditions were applicable to the reaction of a sterically demanding 2-chlorotoluene, albeit with a moderate yield (**5d**). The reactions of 4-chlorotoluene with 4-methoxy- or 4-acetyl-substituted phenyboronic acids gave the corresponding coupling products **5e** and **5f**, respectively, in good-to-high yields.

Chart 2. Suzuki–Miyaura Coupling Reactions between Aryl Chlorides (**3**) and Aryl Boronic Acids (**4**)

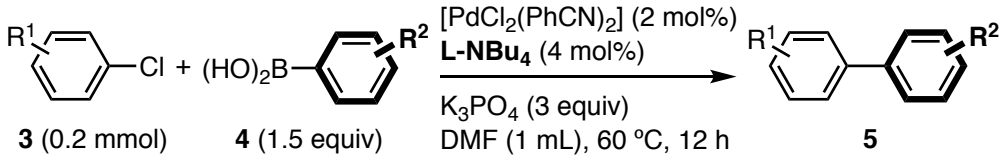

3 (0.2 mmol) **4** (1.5 equiv) **5**

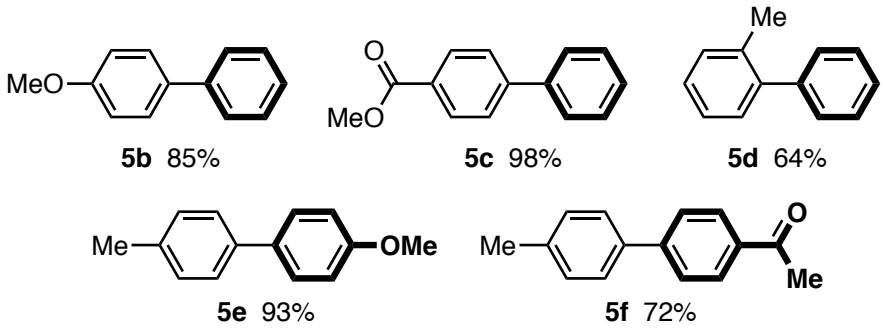

5b 85% **5c** 98% **5d** 64%

5e 93% **5f** 72%

[a] Conditions: **3** (0.2 mmol), **4** (0.3 mmol), $[PdCl_2(PhCN)_2]$ (2 mol%), **L-NBu$_4$** (4 mol%), K_3PO_4 (0.6 mmol), DMF (1 mL), 60 °C, 12 h. Isolated yields are given.

3. Conclusion

Borate-containing caged triarylphosphines **L-X**, featuring a 9-phospha-10-boratriptycene structure were developed. The coordination properties of **L-X** were dependent on the counter cation. In the reaction with $[PdCl(\eta^3\text{-allyl})]_2$, **L-NBu$_4$** provided the neutral Pd(II) complex [PdCl(η^3-allyl)(**L-NBu$_4$**)], while **L-Na** in MeCN/CH_2Cl_2 gave the zwitterionic Pd(II) complex [Pd(η^3-allyl)(MeCN)(**L**)]. The borate-phosphines **L-X** were applicable to the Pd-catalyzed Suzuki–Miyaura cross-coupling of aryl chlorides with arylboronic acids.

4. Experimental Section

4.1. Instrumental and Chemicals

All reactions were carried out under nitrogen or argon atmosphere. Materials were obtained from commercial suppliers or prepared according to standard procedures unless otherwise noted. $PhBF_3K$[18], $[PPh_2(p\text{-}C_6H_4BPh_3)][PPh_4]$[10j], Silica-TRIP[4b] and Ph-TRIP[4c] were prepared according to the reported procedure. Phenylboronic acid (**4a**), 4-methoxyphenylboronic acid (**4b**) and 4-acetylphenylboronic acid (**4c**) were recrystallized from hot water or water/acetone before use.

NMR spectra were recorded on a JEOL ECX-II (400 MHz for ^{1}H NMR, 100.5 MHz for ^{13}C NMR, 128.3 MHz for ^{11}B NMR, and 161.8 MHz for ^{31}P NMR). ^{1}H NMR and ^{13}C NMR chemical shift values are referenced to the residual solvent or Me_4Si (^{1}H; 0 ppm). ^{11}B NMR

and ^{31}P NMR chemical shift were referenced to $BF_3 \cdot OEt_2$ (^{11}B, 0 ppm) and H_3PO_4 (^{31}P; 0 ppm). High-resolution mass spectra (JEOL JMS-T100LP and Thermo Scientific Exactive for ESI-HRMS) and elemental analysis (EAI CE-440) were recorded at the Instrumental Analysis Division, Global Facility Center, Creative Research Institution, Hokkaido University. IR spectra were measured with a PerkinElmer Frontier instrument. Melting points were determined on a micro melting point apparatus using micro cover glass (Yanaco MP-500D). TLC analyses were performed on commercial glass plates bearing 0.25-mm layer of Merck Silica gel 60F_{254}. Silica gel (Kanto Chemical Co., Ltd., Silica gel 60 N, spherical, neutral) was used for column chromatography. GLC-analyses were conducted on a Shimadzu GC-14B equipped with a flame ionization detector. DFT calculations [B3LYP/6-311+G(2df,2p)] were performed with Spartan'16 v2.0.7 software (Wavefunction, Inc.).

4.2. Experimental Procedures

Preparation of 2. For the synthesis of **2**, previously reported procedure[4b] was slightly modified as follows. A mixture of 1-bromo-2-iodobenzene (39.6 g, 140 mmol,) in THF (140 mL) was cooled to –20 °C. A solution of *i*PrMgBr in THF (0.80 M, 175 mL, 140 mmol), which was freshly prepared from 2-bromopropane and Mg, was added over 10 min to the mixture. After stirring at –20 °C for 2 h, PCl_3 (3.79 mL, 40 mmol) and CuI (762 mg, 4 mmol) were added successively. The reaction mixture was allowed to warm gradually to room temperature, and then stirred overnight. After quenching with NH_4Cl aq., the reaction mixture was extracted with EtOAc. The organic layer was washed with brine, dried over $MgSO_4$, filtered, and concentrated under reduced pressure. The residue was passed through a short silica gel column with CH_2Cl_2 as an eluting solvent, and the volatiles was evaporated under vacuum. The residual solids were recrystallized from toluene/MeOH to give tris(2-bromophenyl)phosphine as a while solid (12.6 g, 63% yield). **^{1}H NMR** (400 MHz, $CDCl_3$): δ 6.74–6.77 (m, 3H), 7.22–7.28 (m, 6H), 7.63–7.66 (m, 3H). **^{13}C NMR** (100.5 MHz, $CDCl_3$): δ 127.77 (3C), 130.33 (d, J_{C-P} = 34.5 Hz, 3C), 130.72 (3C), 133.16 (d, J_{C-P} = 1.9 Hz, 3C), 134.67 (3C), 136.68 (d, J_{C-P} = 11.5 Hz, 3C). **^{31}P NMR** (161.8 MHz, $CDCl_3$): δ –2.8.

Preparation of L-H. A solution of *t*BuLi in pentane (1.64 M, 18.3 mL, 30 mmol) was added over 30 min to a solution of **2** (2.50 g, 5.0 mmol) in THF (50 mL) at –98 °C. After stirring for 1 h, $PhBF_3K$ (920 mg, 5.0 mmol) was added at –98 °C. The resulting mixture was allowed to warm gradually to room temperature over 4 h. After treatment with 1M HCl aq, the reaction mixture was extracted with EtOAc. The organic layer was washed with brine, dried over $MgSO_4$, filtered, and concentrated under reduced pressure. The crude product was

purified by silica gel column chromatography (hexane/CH_2Cl_2 100:0-to-0:100) followed by recrystallization from CH_2Cl_2/hexane to give **L-H** as a white solid (1.26 g, 72% yield). Single crystals of **L-H** suitable for X-ray diffraction studies were obtained by recrystallization from CH_2Cl_2/hexane. **M.p.** 220 °C (decomp.). **^{1}H NMR** (400 MHz, $CDCl_3$): δ 7.06 (tdd, J = 7.6, 4.8, 0.8 Hz, 3H), 7.22 (tt, J = 7.6, 1.2 Hz, 3H), 7.38 (tt, J = 7.6, 1.6 Hz, 1H), 7.54 (t, J = 7.6 Hz, 2H), 7.73 (dd, J = 15.2, 7.2 Hz, 3H), 7.81 (d, $J_{P–H}$ = 450 Hz, 1H), 7.82 (m, 3H), 8.08 (d, J = 7.6 Hz, 2H). **^{13}C NMR** (100.5 MHz, $CDCl_3$): δ 123.54 (d, $J_{C–P}$ = 15.4 Hz, 3C), 124.57, 124.64 (d, $J_{C–P}$ = 86.2 Hz, 3C), 127.39 (2C), 127.53 (d, $J_{C–P}$ = 12.4 Hz, 3C), 130.05 (3C), 132.92 (d, $J_{C–P}$ = 13.4 Hz, 3C), 135.99 (2C), 165.0–167.0 (m, 3C). One of signals for carbon directly attached to boron atom was not observed. **^{31}P NMR** (161.8 MHz, $CDCl_3$): δ –23.3 (partially relaxed 1:1:1:1 quartet, $J_{P–B}$ = ~20 Hz). **^{11}B NMR** (128.3 MHz, $CDCl_3$): δ –9.2 (d, $J_{B–P}$ = 23.4 Hz). **IR** (ATR): 3045.3, 1573.6, 1431.1, 1260.6, 1092.3, 889.2, 846.0, 816.0, 756.0, 706.1 cm^{-1}. **ESI-HRMS** (*m/z*): $[M–H]^-$ calcd. for $C_{24}H_{17}{}^{10}BP$, 346.12027; found, 346.12080. **Elem. Anal.** calcd for $C_{24}H_{18}BP$: C, 82.79; H, 5.21; found: C, 82.35; H, 5.17.

Preparation of L-Na. A mixture of **L-H** (174 mg, 0.5 mmol), finely grinded Na_2CO_3 (159 mg, 1.5 mmol) and MeCN (10 mL) was placed in a vial equipped with a magnetic stirring bar. The mixture was stirred at room temperature for 6 h. The resulting mixture was filtered through a pad of celite. The filtrate was concentrated to give pale yellow oil. The crude product was redissolved in CH_2Cl_2/Et_2O, and then evaporated. Repeating evaporation was carried out to remove MeCN until the residue became amorphous solid. The residue was washed with CH_2Cl_2/hexane to give **L-Na** as a white solid (167 mg, 91%). Single crystals of **L-Na·3DME** suitable for X-ray diffraction studies were obtained by recrystallization from DME/hexane. **M.p.** 316–319 °C. **^{1}H NMR** (400 MHz, acetone-d_6): δ 6.68 (t, J = 7.2 Hz, 3H), 6.76 (t, J = 7.2 Hz, 3H), 7.13 (t, J = 7.2 Hz, 1H), 7.34 (t, J = 7.2 Hz, 2H), 7.50 (br-s, 3H), 7.56 (dd, J = 11.2, 7.2 Hz, 3H), 8.12 (br-s, 2H). **^{13}C NMR** (100.5 MHz, acetone-d_6): δ 121.42 (d, $J_{C–P}$ = 14.4 Hz, 3C), 123.31, 125.45 (3C), 126.97 (2C), 131.72 (3C), 132.21 (d, $J_{C–P}$ = 43.1 Hz, 3C), 137.36 (2C), 147.08 (3C), 157.14 (q, $J_{C–B}$ = 57.6 Hz), 169.84 (q, $J_{C–B}$ = 44.0 Hz, 3C). **^{31}P NMR** (161.8 MHz, acetone-d_6): δ –44.2. **^{11}B NMR** (128.3 MHz, acetone-d_6): δ –7.4 (d, $J_{B–P}$ = 3.7 Hz). **IR** (ATR): 3045.6, 1574.0, 1426.2, 1256.4, 1186.7, 1024.6, 881.4, 747.4, 726.2, 689.2 cm^{-1}. **ESI-HRMS** (*m/z*): $[M–Na]^-$ calcd. for $C_{24}H_{17}{}^{10}BP$, 346.12027; found, 346.12092. **Elem. Anal.** calcd for $C_{24}H_{17}BNaP$: C, 77.87; H, 4.63 found: C, 74.13; H, 4.47 (although these results are outside the range viewed as establishing analytical purity, they are provided to illustrate the best values obtained to date).

Preparation of L-K. A mixture of **L-H** (69.6 mg, 0.2 mmol), K_2CO_3 (82.9 mg, 0.6 mmol) and MeCN (4 mL) was placed in a vial equipped with a magnetic stirring bar. The

mixture was stirred at room temperature for 6 h. The resulting mixture was filtered through a pad of celite. The filtrate was concentrated to give pale yellow oil. The crude product was redissolved in CH_2Cl_2/Et_2O, and then evaporated. Repeating evaporation was carried out to remove MeCN until the residue became amorphous solid. The residue was washed with CH_2Cl_2/hexane to give **L-K** as a white solid (60.3 mg, 78%). **M.p.** decomp. **(**350 °C). **^{1}H NMR** (400 MHz, acetone-d_6): δ 6.67 (t, J = 7.2 Hz, 3H), 6.75 (t, J = 7.2 Hz, 3H), 7.12 (t, J = 6.8 Hz, 1H), 7.33 (t, J = 6.8 Hz, 2H), 7.50 (br-s, 3H), 7.55 (dd, J = 11.2, 7.2 Hz, 3H), 8.11 (br-s, 2H). **^{13}C NMR** (100.5 MHz, acetone-d_6): δ 121.44 (d, $J_{C–P}$ = 15.3 Hz, 3C), 123.32, 125.47 (3C), 126.95 (2C), 131.73 (3C), 132.22 (d, $J_{C–P}$ = 44.1 Hz, 3C), 137.38 (2C), 147.10 (3C), 157.16 (q, $J_{C–B}$ = 57.5 Hz), 169.85 (q, $J_{C–B}$ = 44.1 Hz, 3C). **^{31}P NMR** (161.8 MHz, acetone-d_6): δ –44.2. **^{11}B NMR** (128.3 MHz, acetone-d_6): δ –7.4 (d, $J_{B–P}$ = 3.6 Hz). **ESI-HRMS** (*m/z*): $[M–K]^-$ calcd. for $C_{24}H_{17}{}^{10}BP$, 346.12027; found, 346.12092.

Preparation of L-Cs. A mixture of **L-H** (69.6 mg, 0.2 mmol), Cs_2CO_3 (195.5 mg, 0.6 mmol) and MeCN (4 mL) was placed in a vial equipped with a magnetic stirring bar. The mixture was stirred at room temperature for 6 h. The resulting mixture was filtered through a pad of celite. The filtrate was concentrated to give pale yellow oil. The crude product was redissolved in CH_2Cl_2/Et_2O, and then evaporated. Repeating evaporation was carried out to remove MeCN until the residue became amorphous solid. The residue was washed with CH_2Cl_2/hexane to give **L-Cs** as a white solid (87.5 mg, 91%). **M.p.** decomp. **(**345 °C). **^{1}H NMR** (400 MHz, acetone-d_6): δ 6.74 (t, J = 7.2 Hz, 3H), 6.82 (t, J = 7.2 Hz, 3H), 7.17 (t, J = 7.2 Hz, 1H), 7.38 (t, J = 7.2 Hz, 2H), 7.53 (br-d, J = 7.2 Hz, 3H), 7.60 (dd, J = 10.8, 7.2 Hz, 3H), 8.10 (br-s, 2H). **^{13}C NMR** (100.5 MHz, acetone-d_6): δ 120.94 (d, $J_{C–P}$ = 14.4 Hz, 3C), 122.70, 124.94 (3C), 126.30 (2C), 131.15 (3C), 131.74 (d, $J_{C–P}$ = 43.1 Hz, 3C), 136.55 (2C), 146.21 (3C), 155.97 (q, $J_{C–B}$ = 57.5 Hz), 168.96 (q, $J_{C–B}$ = 47.9 Hz, 3C). **^{31}P NMR** (161.8 MHz, acetone-d_6): δ –44.6. **^{11}B NMR** (128.3 MHz, acetone-d_6): δ –7.4 (d, $J_{B–P}$ = 3.7 Hz). **ESI-HRMS** (*m/z*): $[M–K]^-$ calcd. for $C_{24}H_{17}{}^{10}BP$, 346.12027; found, 346.12068.

Preparation of L-NBu$_4$. To a solution of **L-Na** (74.0 mg, 0.2 mmol) in MeCN (400 μL) and CH_2Cl_2 (4 mL) was added dropwise a solution of tetrabutylammonium bromide (64.5 mg, 0.2 mmol) in CH_2Cl_2 (1 mL). Upon addition, white precipitate was immediately formed. After stirring for 1 h, the precipitate was filtered off. The filtrate was concentrated under reduced pressure. Recrystallization of the residue from CH_2Cl_2/Et_2O gave **L-NBu$_4$** as a white solid (106 mg, 90%). **M.p.** 227–228 °C. **^{1}H NMR** (400 MHz, $CDCl_3$): δ 0.60–0.75 (m, 8H), 0.88 (t, J = 7.2 Hz, 12H), 0.95–1.09 (m, 8H), 1.45–1.61 (m, 8H), 6.72 (t, J = 6.8 Hz, 3H), 6.80 (t, J = 6.8 Hz, 3H), 7.22 (t, J = 6.8 Hz, 1H), 7.38 (t, J = 6.8 Hz, 2H), 7.52 (d, J = 6.8 Hz, 3H), 7.57–7.63 (m, 3H), 8.06 (br-d, J = 6.8 Hz, 2H). **^{13}C NMR** (100.5 MHz, $CDCl_3$): δ 13.80

(4C), 19.49 (4C), 23.66 (4C), 56.78 (4C), 121.30 (d, J_{C-P} = 15.4 Hz, 3C), 123.04, 125.49 (3C), 126.28 (2C), 131.25 (3C), 131.99 (d, J_{C-P} = 43.1 Hz, 3C), 136.60 (2C), 145.60 (3C), 168.85 (q, J_{C-B} = 46.9 Hz, 3C). One of signals for carbon directly attached to boron atom was not observed. **^{31}P NMR** (161.8 MHz, $CDCl_3$): δ –45.2. **^{11}B NMR** (128.3 MHz, $CDCl_3$): δ –8.6. **IR** (ATR): 2961.4, 2873.8, 1478.0, 1456.9, 1427.4, 1378.5, 1027.6, 878.4, 755.5, 737.3, 707.2, 688.2 cm^{-1}. **ESI-HRMS** (*m/z*): $[M–NBu_4]^-$ calcd. for $C_{24}H_{17}{}^{10}BP$, 346.12027; found, 346.12086. **Elem. Anal.** calcd for $C_{40}H_{53}BNP$: C, 81.48; H, 9.06; N, 2.38; found: C, 81.52; H, 9.09; N, 2.39.

Preparation of Se-L-NBu$_4$. A mixture of **L-NBu$_4$** (59.0 mg, 0.1 mmol), selenium (23.7 mg, 0.3 mmol) and $CHCl_3$ (1 mL) was stirred at 60 °C for 3 h. The resulting mixture was filtered through a pad of celite. Evaporation of volatiles gave **Se-L-NBu$_4$** as a white solid (54.6 mg, 82%). **M.p.** 224–225 °C. **^{1}H NMR** (400 MHz, $CDCl_3$): δ 0.80–1.07 (m, 28H), 1.98–2.12 (m, 8H), 6.86–6.98 (m, 6H), 7.29 (t, *J* = 7.2 Hz, 1H), 7.45 (t, *J* = 7.2 Hz, 2H), 7.56–7.63 (m, 3H), 7.98–8.08 (m, 5H). **^{13}C NMR** (100.5 MHz, $CDCl_3$): δ 13.71 (4C), 19.41 (4C), 23.65 (4C), 57.51 (4C), 121.12 (d, J_{C-P} = 14.3 Hz, 3C), 123.65, 126.69 (3C), 126.91 (2C), 127.69 (d, J_{C-P} = 14.3 Hz, 3C), 130.80 (d, J_{C-P} = 11.6 Hz, 3C), 135.79 (d, J_{C-P} = 73.9 Hz, 3C), 136.35 (2C), 151.0–153.5 (m), 165.3–167.0 (m, 3C). **^{31}P NMR** (161.8 MHz, $CDCl_3$): δ 12.2 [partially relaxed 1:1:1:1 quartet, J_{P-B} = ~25 Hz (satellite d, J_{P-Se} = 719 Hz)]. **^{11}B NMR** (128.3 MHz, $CDCl_3$): δ –10.6 (d, J_{B-P} = 14.8 Hz). **IR** (ATR): 2962.2, 1429.4, 1254.2, 1058.0, 883.2, 761.7, 704.3 cm^{-1}. **ESI-HRMS** (*m/z*): $[M–NBu_4]^-$ calcd for $C_{24}H_{17}BPSe$, 427.03316; found, 427.03421. **Elem. Anal.** calcd for $C_{40}H_{53}BNPSe$: C, 71.86; H, 7.99; N, 2.09; found: C, 71.47; H, 8.01; N, 2.11.

Preparation of Se-Ph-TRIP. A mixture of **Ph-TRIP** (36.4 mg, 0.1 mmol), selenium (23.7 mg, 0.3 mmol) and $CHCl_3$ (1 mL) was stirred at 60 °C for 3 h. The resulting mixture was filtered through a pad of celite. Evaporation of volatiles gave **Se-Ph-TRIP** as a white solid (43.8 mg, 99%). **M.p.** 320–321 °C. **^{1}H NMR** (400 MHz, $CDCl_3$): δ 7.32 (t, *J* = 7.2 Hz, 3H), 7.42 (tdd, *J* = 7.2, 3.2, 1.2 Hz, 3H), 7.70–7.81 (m, 6H), 8.27 (dd, *J* = 7.6, 1.6 Hz, 2H), 8.52 (dd, *J* = 15.6, 7.6 Hz, 3H). **^{13}C NMR** (100.5 MHz, $CDCl_3$): δ 124.06, 128.45 (d, J_{C-P} = 14.4 Hz, 3C), 129.01 (d, J_{C-P} = 2.9 Hz, 3C), 129.19 (2C), 131.70 (d, J_{C-P} = 14.4 Hz, 3C), 131.87, 132.07 (d, J_{C-P} = 9.5 Hz, 3C), 136.45 (2C), 138.70 (d, J_{C-P} = 71.0 Hz, 3C), 139.89 (d, J_{C-P}= 8.6 Hz, 3C). **^{31}P NMR** (161.8 MHz, $CDCl_3$): δ 13.3 (satellite d, J_{P-Se} = 793 Hz). **IR** (ATR): 2965.8, 1430.0, 1258.2, 1092.4, 883.9, 760.5, 736.3, 697.6, 667.7 cm^{-1}. **ESI-HRMS** (*m/z*): $[M+H]^+$ calcd for $C_{24}H_{18}PSeSi$, 445.00751; found, 445.00888. **Elem. Anal.** calcd for $C_{24}H_{17}PSeSi$: C, 65.01; H, 3.86; found: C, 64.15; H, 3.71. (although these results are outside the range viewed as establishing analytical purity, they are provided to illustrate the best

values obtained to date).

Preparation of [PdCl(η^3-allyl)(L-NBu$_4$)]. A mixture of **L-NBu$_4$** (47.2 mg, 0.08 mmol), [PdCl(η^3-allyl)]$_2$ (14.6 mg, 0.04 mmol) and CH_2Cl_2 (2 mL) was stirred at room temperature for 2 h. The volatiles were evaporated. The residue was recrystallized from CH_2Cl_2/Et_2O to give [PdCl(η^3-allyl)(**L-NBu$_4$**)] as a pale yellow solid (39.6 mg, 43% yield). Single crystals of [PdCl(η^3-allyl)(**L-NBu$_4$**)] suitable for X-ray diffraction studies were obtained by recrystallization from CH_2Cl_2/hexane. **M.p.** 193 °C (decomp.). **^{1}H NMR** (400 MHz, CD_2Cl_2): δ 0.93 (t, 7.2 Hz, 12H), 1.14–1.31 (m, 16H), 2.54–2.65 (m, 8H), 3.05 (d, J = 12.4 Hz, 1H), 3.91–4.02 (m, 2H), 4.86 (t, J = 6.8 Hz, 1H), 5.74–5.85 (m, 1H), 6.89 (td, J = 7.2, 3.2 Hz, 3H), 6.97 (t, J = 7.2 Hz, 3H), 7.27 (t, J = 7.2 Hz, 1H), 7.44 (t, J = 7.2 Hz, 2H), 7.56 (d, J = 7.2 Hz, 3H), 8.04–8.12 (m, 5H). **^{13}C NMR** (100.5 MHz, CD_2Cl_2): δ 13.75 (4C), 19.94 (4C), 24.02 (4C), 55.24, 58.63 (4C), 82.17 (d, $J_{C–P}$ = 30.7 Hz), 116.60 (d, $J_{C–P}$ = 4.7 Hz), 122.02 (d, $J_{C–P}$ = 17.4 Hz, 3C), 123.70, 126.71 (3C), 126.98 (2C), 131.38 (d, $J_{C–P}$ = 5.8 Hz, 3C), 132.41 (d, $J_{C–P}$ = 25.9 Hz, 3C), 136.83 (2C), 140.70 (d, $J_{C–P}$ = 43.1 Hz, 3C), 154.02 (q, $J_{C–B}$ = 60.4 Hz), 167.80 (q, $J_{C–B}$ = 45.9 Hz, 3C). **^{31}P NMR** (161.8 MHz, CD_2Cl_2): δ –6.8 (partially relaxed 1:1:1:1 quartet, $J_{P–B}$ = ~15 Hz). **^{11}B NMR** (128.3 MHz, CD_2Cl_2): δ –9.3 (d, $J_{B–P}$ = 12.3 Hz). **IR** (ATR): 3040.0, 2961.7, 2872.1, 1485.8, 1427.5, 1381.7, 879.8, 756.4, 709.1, 695.3 cm^{-1}. **ESI-HRMS** (*m/z*): [M–NBu$_4$]$^-$ calcd for $C_{27}H_{22}BClPPd$, 529.02874; found, 529.02667. **Elem. Anal.** calcd for $C_{43}H_{58}BClNPPd$: C, 66.85; H, 7.57; N, 1.81; found: C, 66.62; H, 7.58; N, 1.80.

Preparation of [Pd(η^3-allyl)(MeCN)(L)]. A mixture of **L-Na** (29.6 mg, 0.08 mmol), [PdCl(η^3-allyl)]$_2$ (14.6 mg, 0.04 mmol), MeCN (1 mL) and CH_2Cl_2 (1 mL) was stirred at room temperature for 30 min. The pale-yellow suspension was filtered through a pad of celite. The filtrate was concentrated to ca. 1 mL. White crystals formed upon concentration. The crystals were collected by filtration to give [Pd(η^3-allyl)(MeCN)(**L**)] acetonitrile monosolvate as a white solid (33.8 mg, 79% yield). Single crystals of [Pd(η^3-allyl)(MeCN)(**L**)]·(MeCN) suitable for X-ray diffraction studies were obtained by recrystallization from CH_2Cl_2/MeCN. **M.p.** 170 °C (decomp.). **^{1}H NMR** (400 MHz, CD_2Cl_2/CD_3CN = 10:1): δ 3.31 (br-s, 1H), 4.11 (dd, J = 14.0, 8.4 Hz, 1H), 4.33 (br-s, 1H), 5.24 (t, J = 6.8 Hz, 1H), 5.92 (m, 1H), 6.92 (tdd, J = 7.2, 3.2, 1.6 Hz, 3H), 7.01 (tt, J = 7.2, 1.2 Hz, 3H), 7.26 (t, J = 7.2 Hz, 1H), 7.44 (t, J = 7.2 Hz, 2H), 7.58 (br-d, J = 7.2 Hz, 3H), 7.67 (ddd, J = 9.6, 7.2, 1.2 Hz, 3H), 8.03 (br-d, J = 7.2 Hz, 2H). **^{13}C NMR** (100.5 MHz, CD_2Cl_2/CD_3CN = 10:1): δ 84.37 (d, $J_{C–P}$ = 24.0 Hz), 120.09, 122.33 (d, $J_{C–P}$ = 14.4 Hz, 3C), 123.84, 127.07 (2C), 127.29 (3C), 131.05 (d, $J_{C–P}$ = 24.9 Hz, 3C), 131.75 (d, $J_{C–P}$ = 7.6 Hz, 3C), 136.51 (2C), 138.65 (d, $J_{C–P}$ = 47.0 Hz, 3C), 167.50 (q, $J_{C–B}$ = 40.2 Hz, 3C). One of

signals for carbon directly attached to boron atom was not observed. Signals for one of carbons of the π-allyl moiety and for carbons of the coordinating MeCN ligand were overlapping to solvent signals. **^{31}P NMR** (161.8 MHz, CD_2Cl_2/CD_3CN = 10:1): δ –3.2 (partially relaxed 1:1:1:1 quartet, $J_{P–B}$ = ~10 Hz). **^{11}B NMR** (128.3 MHz, CD_2Cl_2/CD_3CN = 10:1): δ –9.2 (d, $J_{B–P}$ = 12.3 Hz). **IR** (ATR): 2964.6, 1428.0, 1255.0, 1025.8, 882.4, 756.2, 742.3, 719.8, 698.0 cm^{-1}. **ESI-HRMS** (*m/z*): $[M+Na]^+$ calcd. for $C_{29}H_{25}BNPPd$, 558.07656; found, 558.07728. **Elem. Anal.** calcd for $C_{31}H_{28}BN_2PPd$: C, 64.55; H, 4.89; N, 4.86; found: C, 63.68; H, 4.78; N, 4.81. (although these results are outside the range viewed as establishing analytical purity, they are provided to illustrate the best values obtained to date).

Preparation of [RhCl(L-NBu$_4$)(cod)]. A mixture of **L-NBu$_4$** (23.6 mg, 0.04 mmol), $[RhCl(cod)]_2$ (9.9 mg, 0.02 mmol) and CH_2Cl_2 (1 mL) was stirred at room temperature for 15 min. The mixture was added Et_2O (ca. 3 mL) to form yellow crystalline precipitate. The crystals were collected by filtration to give [RhCl(**L-NBu$_4$**)(cod)] (26.4 mg, 79% yield). Single crystals of [RhCl(**L-NBu$_4$**)(cod)] suitable for X-ray diffraction studies were obtained by recrystallization from CH_2Cl_2/Et_2O. **M.p.** 165 °C (decomp.). **^{1}H NMR** (400 MHz, CD_2Cl_2): δ 0.93 (t, 7.2 Hz, 12H), 1.14–1.31 (m, 16H), 2.09–2.25 (m, 4H), 2.50–2.70 (m, 12H), 5.24 (br-s, 2H), 5.49 (br-s, 2H), 6.85 (td, *J* = 7.2, 1.2 Hz, 3H), 6.90 (t, *J* = 7.2 Hz, 3H), 7.23 (t, *J* = 7.2 Hz, 1H), 7.41 (t, *J* = 7.2 Hz, 2H), 7.47 (d, *J* = 6.8 Hz, 3H), 8.03 (d, *J* = 6.8 Hz, 2H), 8.03 (dd, *J* = 10.8, 6.8 Hz, 3H). **^{13}C NMR** (100.5 MHz, CD_2Cl_2): δ 13.74 (4C), 19.96 (4C), 24.06 (4C), 29.00 (2C), 34.33 (2C), 58.69 (4C), 67.22 (d, $J_{C–Rh}$ = 12.5 Hz, 2C) 101.74 (dd, $J_{C–Rh}$ = 12.5 Hz, $J_{C–P}$ = 7.6 Hz, 2C), 121.49 (d, $J_{C–P}$ = 13.5 Hz, 3C), 123.54, 126.08 (3C), 126.85 (2C), 130.84 (d, $J_{C–P}$ = 5.7 Hz, 3C), 133.48 (d, $J_{C–P}$ = 23.0 Hz, 3C), 136.94 (2C), 141.32 (d, $J_{C–P}$ = 41.2 Hz, 3C), 154.59 (q, $J_{C–B}$ = 61.3 Hz), 168.34 (q, $J_{C–B}$ = 45.0 Hz, 3C). **^{31}P NMR** (161.8 MHz, CD_2Cl_2): δ –1.73 (partially relaxed dq, $J_{P–Rh}$ = 143 Hz, $J_{P–B}$ = ~15 Hz). **^{11}B NMR** (128.3 MHz, CD_2Cl_2): δ –9.5 (d, $J_{B–P}$ = 11.2 Hz). **ESI-HRMS** (*m/z*): $[M–NBu_4]^-$ calcd. for $C_{32}H_{29}{}^{10}BClPRh$, 592.08798; found, 592.08680.

Preparation of [Rh(L)(py)(cod)]. A mixture of **L-Na** (14.8 mg, 0.04 mmol), $[RhCl(cod)]_2$ (9.9 mg, 0.02 mmol), CH_2Cl_2 (1 mL) and pyridine (32.2 μL, 0.4 mmol) was stirred at room temperature for 40 min. The resulting mixture was filtrated through a pad of celite. The filtrate was concentrated under reduced pressure. The residue was recrystallized from CH_2Cl_2/Et_2O to give [Rh(**L**)(py)(cod)] as a yellow solid (22.0 mg, 98% yield). Single crystals of [Rh(**L**)(py)(cod)] suitable for X-ray diffraction studies were obtained by recrystallization from CH_2Cl_2/ Et_2O. **M.p.** 210 °C (decomp.). **^{1}H NMR** (400 MHz, CD_2Cl_2): δ 2.18–2.36 (m, 4H), 2.69–2.85 (m, 4H), 4.76 (s, 2H), 5.62 (s, 2H), 6.78–6.84 (m, 3H), 6.94 (t, *J* = 6.8 Hz, 3H), 7.20–7.28 (m, 3H) 7.42 (t, *J* = 6.8 Hz, 2H), 7.44 (t, *J* = 7.2 Hz, 3H), 7.61

(d, J = 7.6 Hz, 1H), 7.92 (dd, J = 11.6, 7.2 Hz, 3H), 7.61 (d, J = 7.2 Hz, 2H), 8.91 (d, J = 4.8 Hz, 2H). **^{13}C NMR** (100.5 MHz, CD_2Cl_2): δ 29.50 (2C), 33.16 (2C), 78.81 (d, $J_{C–Rh}$ = 11.5 Hz, 2C), 99.76 (2C), 121.9–122.2 (m, 5C), 123.88, 126.10 (3C), 127.14 (2C), 130.88 (d, $J_{C–P}$ = 24.0 Hz, 3C), 132.01 (3C), 136.72 (2C), 138.33, 138.53 (d, $J_{C–P}$ = 41.6 Hz, 3C), 152.50. signals for carbon directly attached to boron atom was not observed. **^{31}P NMR** (161.8 MHz, CD_2Cl_2): δ –18.8 (partially relaxed dq, $J_{P–Rh}$ = 147 Hz, $J_{P–B}$ = ~15 Hz). **^{11}B NMR** (128.3 MHz, CD_2Cl_2): δ –9.4 (d, $J_{B–P}$ = 12.3 Hz). Attempts to obtain MS spectra (ESI or FAB) of [Rh(**L**)(py)(cod)] were unsuccessful.

Typical Procedure for Pd-Catalyzed Suzuki–Miyaura Cross-Coupling of Aryl Chlorides. In a nitrogen-filled glove box, a mixture of **L-NBu$_4$** (4.7 mg, 0.008 mmol) and DMF (850 μL) was placed in a 10 mL screw-capped glass tube containing magnetic stirring bar. A solution of [$PdCl_2(PhCN)_2$] (1.5 mg, 0.004 mmol) in DMF (150 μL) was added to the mixture. After stirring for 5 min, 1-butyl-4-chlorobenzene (**3a**, 33.5 mg, 0.20 mmol), phenylboronic acid (**4a**, 36.6 mg, 0.30 mmol), K_3PO_4 (127.4 mg, 0.6 mmol) were added successively. The tube was sealed with a screw cap and removed from the glove box. The mixture was stirred at 60 °C for 12 h. After cooling to room temperature, the consumption of the starting material was determined by gas chromatography (1,4-dimethoxybenzene as internal standard). The mixture was diluted with Et_2O and filtered through a Celite pad (eluting with Et_2O). The volatiles were evaporated, and an internal standard (1,3,5-trimethoxybenzene) was added to determine the yield of 4-butyl-1,1'-biphenyl (**5a**, 92% yield) by ^{1}H NMR. The crude product was purified by silica gel chromatography (hexane/EtOAc, 100:0-to-97:3) to give **5a** as a colorless oil (0.20 mmol scale, 38.6 mg, 92% yield). **^{1}H NMR** (400 MHz, $CDCl_3$): δ 0.94 (t, J = 7.2 Hz, 3H), 1.33–1.44 (m, 2H), 1.59–1.68 (m, 2H), 2.64 (t, J = 7.6 Hz, 2H), 7.22–7.26 (m, 2H), 7.31 (t, J = 7.2 Hz, 1H), 7.41 (t, J = 7.2 Hz, 2H), 7.50 (d, J = 7.2 Hz, 2H), 7.55–7.60 (m, 2H). **^{13}C NMR** (100.5 MHz, $CDCl_3$): δ 13.99, 22.41, 33.65, 35.28, 126.8–127.1 (m, 5C), 128.67 (2C), 128.81 (2C), 138.49, 141.14, 142.03. The synthesis of **5a** was reported.[19]

4-Methoxy-1,1'-biphenyl (5b). The product **5b** was isolated by silica gel chromatography (hexane/EtOAc, 100:0-to-98:2) as a white solid (0.22 mmol scale, 33.9 mg, 85% yield). **^{1}H NMR** (400 MHz, $CDCl_3$): δ 3.82 (s, 3H), 6.96 (d, J = 8.8 Hz, 2H), 7.29 (t, J = 7.2 Hz, 1H), 7.40 (t, J = 7.2 Hz, 2H), 7.50–7.56 (m, 4H). **^{13}C NMR** (100.5 MHz, $CDCl_3$): δ 55.27, 114.13 (2C), 126.61, 126.69 (2C), 128.11 (2C), 128.69 (2C), 133.68, 140.75, 159.06. The synthesis of **5b** was reported.[20]

Methyl 4-phenylbenzoate (5c). The product **5c** was isolated by silica gel chromatography (hexane/CH_2Cl_2, 100:0-to-50:50) as a white solid (0.20 mmol scale, 42.1 mg,

98% yield). **^{1}H NMR** (400 MHz, $CDCl_3$): δ 3.92 (s, 3H), 7.38 (t, J = 7.2 Hz, 1H), 7.45 (t, J = 7.2 Hz, 2H), 7.58–7.67 (m, 4H), 8.09 (d, J = 8.8 Hz, 2H). **^{13}C NMR** (100.5 MHz, $CDCl_3$): δ 52.07, 126.96 (2C), 127.20 (2C), 128.07, 128.78, 128.85 (2C), 130.03 (2C), 139.88, 145.52, 166.91. The synthesis of **5c** was reported.[21]

2-Methyl-1,1'-biphenyl (5d). The product **5d** was isolated by silica gel chromatography (hexane) and following GPC as a pale-yellow oil (0.20 mmol scale, 20.9 mg, 64% yield). **^{1}H NMR** (400 MHz, $CDCl_3$): δ 2.27 (d, 3H), 7.22–7.28 (m, 4H), 7.30–7.36 (m, 3H), 7.38–7.43 (m, 2H). **^{13}C NMR** (100.5 MHz, $CDCl_3$): δ 20.47, 125.73, 126.71, 127.22, 128.01 (2C), 129.16 (2C), 129.78, 130.28, 135.31, 141.88, 141.91. The synthesis of **5d** was reported.[21]

4-Methoxy-4'-methyl-1,1'-biphenyl (5e). The product **5e** was isolated by silica gel chromatography (hexane/CH_2Cl_2, 80:20) as a white solid (0.22 mmol scale, 39.9 mg, 93% yield). **^{1}H NMR** (400 MHz, $CDCl_3$): δ 2.37 (s, 3H), 3.81 (s, 3H), 6.94 (d, J = 8.0 Hz, 2H), 7.21 (d, J = 8.0 Hz, 2H), 7.44 (d, J = 8.0 Hz, 2H), 7.50 (d, J = 8.0 Hz, 2H). **^{13}C NMR** (100.5 MHz, $CDCl_3$): δ 21.02, 55.25, 114.09 (2C), 126.52 (2C), 127.90 (2C), 129.40 (2C), 133.65, 136.29, 137.89, 158.85. The synthesis of **5e** was reported.[22]

4-Acetyl-4'-methyl-1,1'-biphenyl (5f). The product **5f** was isolated by silica gel chromatography (hexane/CH_2Cl_2, 70:30-to-50:50) as a white solid (0.21 mmol scale, 31.3 mg, 72% yield). **^{1}H NMR** (400 MHz, $CDCl_3$): δ 2.40 (s, 3H), 2.62 (s, 3H), 7.27 (d, J = 8.4 Hz, 2H), 7.52 (d, J = 8.4 Hz, 2H), 7.66 (d, J = 8.4 Hz, 2H), 8.01 (d, J = 8.4 Hz, 2H). **^{13}C NMR** (100.5 MHz, $CDCl_3$): δ 21.13, 26.61, 126.88 (2C), 127.04 (2C), 128.86 (2C), 129.63 (2C), 135.49, 136.85, 138.18, 145.63, 197.73. The synthesis of **5f** was reported.[23]

4.3. X-ray crystallographic studies

Data were collected on a Rigaku Mercury 70 CCD diffractometer with graphite monochromated Mo-Kα radiation (λ = 0.71075 Å, 50 kV, 200 mA), and processed using the CrystalClear software.[24] Structures were solved by a direct method using SIR-2011,[25] and refined by full-matrix least-square method using SHELXL-2014.[26] Non-hydrogen atoms were refined anisotropically. All hydrogen atoms were located on the calculated positions and refined using a riding model. All calculations were performed using the CrystalStructure software package.[27]

Crystal data for **L-H** (CCDC 1819398; recrystallization from CH_2Cl_2/hexane). Large accessible voids, which may host disordered solvent molecules, remained in the crystal structure. Thus, the SQUEEZE program in PLATON was employed for analysis.[28] $C_{24}H_{18}BP$, M = 348.19, triclinic, space group P-1 (#2), a = 10.6599(14) Å, b = 13.5205(18) Å, c =

14.248(2) Å, α = 83.895(6)°, β = 79.563(5)°, γ = 74.191(5)°, V = 1939.6(5) Å^3, T = 170 K, Z = 4, density (calc.) = 1.192 g/cm^3, total reflections collected = 14920, unique reflections = 7528 (R_{int} = 0.0242), $R1$ (I>2σ(I)) = 0.0389, $wR2$ (all data) = 0.1050, GOF = 1.064. A response for the following B-level alert in the CIF validation reports is shown below.

PLAT910_ALERT_3_B Missing # of FCF Reflection(s) Below Theta(Min)

12Note

Response: Theta min = 3.099 deg. Data completeness (0.991) and R1 factor (0.0389) were good enough for this structural assignment.

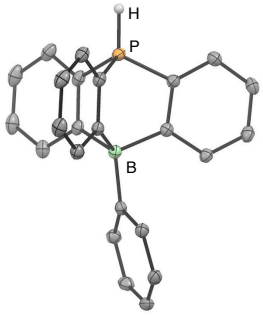

P–C length (ave.) 1.778 Å
C–P–C angle (ave.) 104.6°

Crystal data for **L-Na·3DME** (CCDC 1819399; recrystallization from 1,2-dimethoxyethane/hexane). $C_{36}H_{47}BNaO_6P$, M = 640.54, monoclinic, space group $P2_1/c$ (#14), a = 13.304(3) Å, b = 11.724(2) Å, c = 24.602(5) Å, β = 105.224(3)°, V = 3702.7(13) Å^3, T = 200 K, Z = 4, density (calc.) = 1.149 g/cm^3, total reflections collected = 27766, unique reflections = 7250 (R_{int} = 0.0407), $R1$ (I>2σ(I)) = 0.0583, $wR2$ (all data) = 0.1490, GOF = 1.072. A response for the following B-level alert in the CIF validation reports is shown below.

PLAT910_ALERT_3_B Missing # of FCF Reflection(s) Below Theta(Min)

12Note

Response: Theta min = 3.165 deg. Data completeness (0.995) and R1 factor (0.0583) were good enough for this structural assignment.

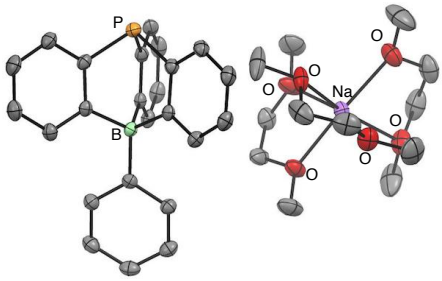

P–C length (ave.) 1.836 Å
C–P–C angle (ave.) 96.1°

Crystal data for **L-NBu$_4$** (CCDC 1819400; recrystallization from CH_2Cl_2/hexane). $C_{40}H_{53}BNP$, M = 589.65, orthorhombic, space group *Pbca* (#61), a = 17.892(4) Å, b = 19.303(5) Å, c = 20.596(5) Å, V = 7113(3) Å^3, T = 200 K, Z = 8, density (calc.) = 1.101 g/cm^3, total reflections collected = 52557, unique reflections = 6979 (R_{int} = 0.0648), $R1$ (I>2σ(I)) = 0.0698, $wR2$ (all data) = 0.1612, GOF = 1.127. A response for the following B-level alert in the CIF validation reports is shown below.

PLAT910_ALERT_3_B Missing # of FCF Reflection(s) Below Theta(Min) 12Note

Response: Theta min = 3.016 deg. Data completeness (0.998) and R1 factor (0.0689) were good enough for this structural assignment.

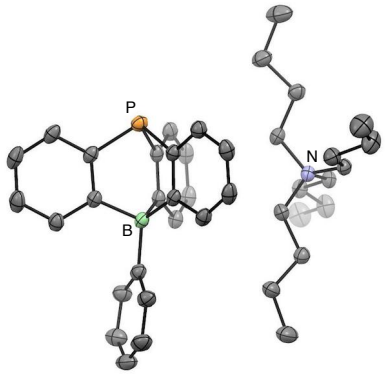

Crystal data for **Ph-TRIP** (CCDC 1819401; recrystallization from CH_2Cl_2/hexane). $C_{24}H_{17}PSi$, M = 364.46, orthorhombic, space group *Pnma* (#62), a = 21.485(5) Å, b = 10.455(3) Å, c = 8.335(2) Å, V = 1872.3(8) Å^3, T = 200 K, Z = 4, density (calc.) = 1.293 g/cm^3, total reflections collected = 13732, unique reflections = 1946 (R_{int} = 0.0253), $R1$ (I>2σ(I)) = 0.0433, $wR2$ (all data) = 0.1184, GOF = 1.087.

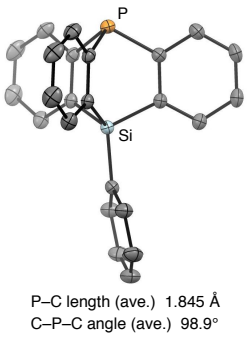

Crystal data for [PdCl(η^3-allyl)(**L-NBu$_4$**)] (CCDC 1819402; recrystallization from CH_2Cl_2/hexane). $C_{43}H_{40}BClNPPd$, M = 754.43, monoclinic, space group $P2_1/n$ (#14), a = 16.363(5) Å, b = 14.574(5) Å, c = 17.970(6) Å, β = 111.162(4)°, V = 3996(2) Å^3, T = 200 K, Z = 4, density (calc.) = 1.254 g/cm^3, total reflections collected = 30036, unique reflections = 7825 (R_{int} = 0.0280), $R1$ (I>2σ(I)) = 0.0564, $wR2$ (all data) = 0.1591, GOF = 1.051. A response for the following B-level alert in the CIF validation reports is shown below.

PLAT910_ALERT_3_B Missing # of FCF Reflection(s) Below Theta(Min) 13Note

Response: Theta min = 3.014 deg. Data completeness (0.997) and R1 factor (0.0564) were good enough for this structural assignment.

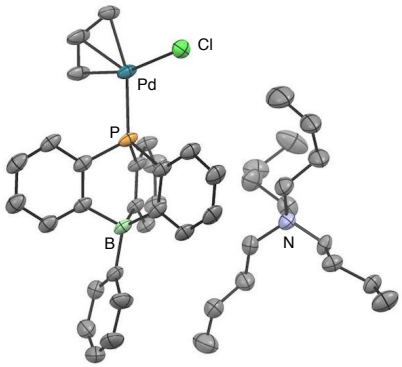

Crystal data for [Pd(η^3-allyl)(MeCN)(**L**)] (CCDC 1819403; recrystallization from CH_2Cl_2/MeCN). $C_{31}H_{28}BN_2PPd$, M = 576.76, orthorhombic, space group $P2_12_12_1$ (#19), a = 10.6478(5) Å, b = 13.6696(8) Å, c = 18.2916(8) Å, V = 2662.4(2) Å^3, T = 200 K, Z = 4, density (calc.) = 1.439 g/cm^3, total reflections collected = 20549, unique reflections = 5222 (R_{int} = 0.0197), $R1$ (I>2σ(I)) = 0.0222, $wR2$ (all data) = 0.0504, GOF = 1.048.

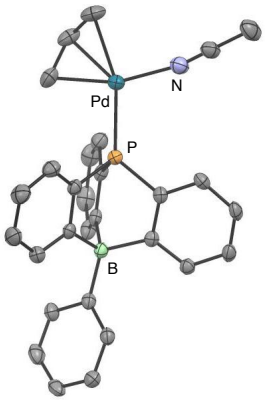

5. References

(1) For selected examples of caged phosphine ligands, see: (a) Agou, T.; Kobayashi, J.; Kawashima, T. *Chem. Lett.* **2004**, *33*, 1028–1029. (b) Pike, R. D.; Reinecke, B. A.; Dellinger, M. E.; Wiles, A. B.; Harper, J. D.; Cole, J. R.; Dendramis, K. A.; Borne, B. D.; Harris, J. L.; Pennington, W. T. *Organometallics* **2004**, *23*, 1986–1990. (c) Fuchs, E.; Keller, M.; Breit, B. *Chem. Eur. J.* **2006**, *12*, 6930–6939. (d) Lee, A.; Ahn, S.; Kang, K.; Seo, M.-S.; Kim, Y.; Kim, W. Y.; Kim, H. *Org. Lett.* **2014**, *16*, 5490–5493. (e) Ube, H.; Yasuda, Y.; Sato, H.; Shionoya, M. *Nat. Commun*. **2017**, *8*, 14296.

(2) For related reviews on caged phosphine ligands, see: (a) Phillips, A. D.; Gonsalvi, L.; Romerosa, A.; Vizza, F.; Peruzzini, M. *Coord. Chem. Rev.* **2004**, *248*, 955–993. (b) Zablocka, M.; Hameau, A.; Caminade, A.-M.; Majoral, J.-P. *Adv. Synth. Catal.* **2010**, *352*, 2341–2358.

(3) (a) Ochida, A.; Hara, K.; Ito, H.; Sawamura, M. *Org. Lett.* **2003**, *5*, 2671–2674. (b) Ochida, A.; Ito, S.; Miyahara, T.; Ito, H.; Sawamura, M. *Chem. Lett.* **2006**, *35*, 294–295. (c) Ochida, A.; Hamasaka, G.; Yamauchi, Y.; Kawamorita, S.; Oshima, N.; Hara, K.; Ohmiya, H.; Sawamura, M. *Organometallics* **2008**, *27*, 5494–5503.

(4) (a) Kawamorita, S.; Miyazaki, T.; Iwai, T.; Ohmiya, H.; Sawamura, M. *J. Am. Chem. Soc.* **2012**, *134*, 12924–12927. (b) Iwai, T.; Konishi, S.; Miyazaki, T.; Kawamorita, S.; Yokokawa, N.; Ohmiya, H.; Sawamura, M. *ACS Catal.* **2015**, *5*, 7254–7264. The synthesis of **Ph-TRIP** was described in the following paper. (c) Kawamorita, S.; Miyazaki, T.; Ohmiya, H.; Iwai, T.; Sawamura, M. *J. Am. Chem. Soc.* **2011**, *133*, 19310–19313.

(5) 9-Phospha-10-silatriptycenes were originally synthesized by Tsuji and Tamao et. al. Tsuji, H.; Inoue, T.; Kaneta, Y.; Sase, S.; Kawachi, A.; Tamao, K. *Organometallics* **2006**, *25*, 6142–6148.

(6) (a) Hamasaka, G.; Ochida, A.; Hara, K.; Sawamura, M. *Angew. Chem., Int. Ed.* **2007**, *46*, 5381–5383. (b) Hamasaka, G.; Kawamorita, S.; Ochida, A.; Akiyama, R.; Hara, K.; Fukuoka, A.; Asakura, K.; Chun, W.; Ohmiya, H.; Sawamura, M. *Organometallics* **2008**, *27*, 6495–6506.

(7) Hara, K.; Akiyama, R.; Takakusagi, S.; Uosaki, K.; Yoshino, T.; Kagi, H.; Sawamura, M. *Angew. Chem., Int. Ed.* **2008**, *47*, 5627–5630.

(8) For triolborate-containing caged phosphines, see: (a) Ignat'eva, S. N.; Nikonov, G. N.; Erastov. O. A.; Arbuzov, B. A. *Russ. Chem. Bull.* **1985**, *34*, 1005–1009. (b) Nikonov, G. N.; Litvinov, I. A.; Ignat'eva, S. N.; Erastov, O. A.; Arbuzov, B. A. *Russ. Chem. Bull.* **1988**, *37*, 147–150. (c) Huang, W.; Xu, N. *Synth. Commun.* **2016**, *46*, 1182–1186.

(9) For tris(pyrazolyl)borate-containing caged phosphines, see: Gu, L.; Gopakumar, G.; Gualco, P.; Thiel, W.; Alcarazo, M. *Chem. Eur. J.* **2014**, *20*, 8575–8578.

(10) For selected examples of borate-phosphine hybrids, see: (a) Hoic, D. A.; Davis, W. M.; Fu, G. C. *J. Am. Chem. Soc.* **1996**, *118*, 8176–8177. (b) Barney, A. A.; Heyduk, A. F.; Nocera, D. G. *Chem. Commun.* **1999**, 2379–2380. (c) Peters, J. C.; Feldman, J. D.; Tilley, T. D. *J. Am. Chem. Soc.*, **1999**, *121*, 9871–9872. (d) Thomas, J. C.; Peters, J. C. *J. Am. Chem. Soc.* **2001**, *123*, 5100–5101. (e) Jaska, C. A.; Dorn, H.; Lough, A. J.; Manners, I. *Chem. Eur. J.* **2003**, *9*, 271–281. (f) Thomas, C. M.; Peters, J. C. *Inorg. Chem.* **2004**, *43*, 8–10. (g) Granville, S. L.; Welch, G. C.; Stephan, D. W. *Inorg. Chem.* **2012**, *51*, 4711–4721. (h) Kim, Y.; Jordan, R. F. *Organometallics* **2011**, *30*, 4250–4256. (i) Lavallo, V.; Wright, J. H.; Tham, F. S.; Quinlivan, S. *Angew. Chem., Int. Ed.* **2013**, *52*, 3172–3176. (j) Tassone, J. P.; Mawhinney, R. C.; Spivak, G. J. *J. Organomet. Chem.* **2015**, *776*, 153–156. (k) Jia, X.; Zhang, M.; Pan, F.; Babahan, I.; Ding, K.; Jia, L.; Crandall, L. A.; Ziegler, C. J. *Organometallics* **2015**, *34*, 4798–4801.

(11) For a review on zwitterionic metal complexes, see: Stradiotto, M.; Hesp, K. D.; Lundgren, R. J. *Angew. Chem., Int. Ed*. **2010**, *49*, 494–512.

(12) (a) Pinnell, R. P.; Megerle, C. A.; Manatt, S. L.; Kroon, P. A. *J. Am. Chem. Soc.* **1973**, *95*, 977–978. (b) Tolman, C. A. *Chem. Rev.* **1977**, *77*, 313–348. (c) Allen, D. W.; Taylor, B. F. *J. Chem. Soc., Dalton Trans.* **1982**, 51–54.

(13) The date of Ph_3P=Se ($^1J_{Se-P}$) was taken from the following paper. Muller, A.; Otto, S.; Roodt, A. *Dalton Trans.* **2008**, 650–657.

(14) For selected reviews, see: (a) Kantchev, E. A. B.; O'Brien, C. J.; Organ, M. G. *Angew. Chem., Int. Ed.* **2007**, *46*, 2768–2813. (b) Martin, R.; Buchwald, S. L. *Acc. Chem. Res.* **2008**, *41*, 1461–1473. (c) Fu, G. C. *Acc. Chem. Res.* **2008**, *41*, 1555–1564. (d) Fleckenstein, C. A.; Plenio, H. *Chem. Soc. Rev.* **2010**, *39*, 694–711. (e) Lundgren, R. J.; Hesp, K. D.; Stradiotto, M. *Synlett* **2011**, *2011*, 2443–2458. (f) Fortman, G. C.; Nolan, S. P. *Chem. Soc. Rev.* **2011**, *40*, 5151–5169. (g) Wong, S. M.; So, C. M.; Kwong, F. Y. *Synlett* **2012**, *2012*, 1132–1153.

(15) For selected examples of the use of moderately electron-donating triarylphosphine-based ligands in the Pd-catalyzed cross-coupling of aryl chlorides, see: (a) Iwasawa, T.; Komano, T.; Tajima, A.; Tokunaga, M.; Obora, Y.; Fujihara, T.; Tsuji, Y. *Organometallics* **2006**, *25*, 4665–4669. (b) Ohta, H.; Tokunaga, M.; Obora, Y.; Iwai, T.; Iwasawa, T.; Fujihara, T.; Tsuji, Y. *Org. Lett.* **2007**, *9*, 89–92. (c) Fujihara, T.; Yoshida, S.; Ohta, H.; Tsuji, Y. *Angew. Chem., Int. Ed.* **2008**, *47*, 8310–8314. (d) Snelders, D. J. M.; van Koten, G.; Gebbink, R. J. M. K. *J. Am. Chem. Soc.* **2009**, *131*,

11407–11416. (e) Mom, S.; Beaupérin, M.; Roy, D.; Royer, S.; Amardeil, R.; Cattey, H.; Doucet, H.; Hierso, J.-C. *Inorg. Chem.* **2011**, *50*, 11592–11603. (f) Chow, W. K.; Yuen, O. Y.; So, C. M.; Wong, W. T.; Kwong, F. Y. *J. Org. Chem.* **2012**, *77*, 3543–3548. (g) Zhang, J.; Bellomo, A.; Trongsiriwat, N.; Jia, T.; Carroll, P. J.; Dreher, S. D.; Tudge, M. T.; Yin, H.; Robinson, J. R.; Schelter, E. J.; Walsh, P. J. *J. Am. Chem. Soc.* **2014**, *136*, 6276–6287.

(16) Thomas and Petersreported a similar but smaller borate effect in the Pd-catalyzed cross-coupling of aryl chlorides with a bulky and electron-rich P^iPr_2Ph-based ligand $[P^iPr_2(m\text{-}C_6H_4BPh_3)][NR_4]$.

(17) The use of DMF as a solvent in the Silica-TRIP-Pd system was not effective, giving **5a** in only 6% yield under otherwise the same conditions.

(18) Liesen, A. P.; Silva, A. T.; Sousa, J. C.; Menezes, P. H.; Oliveira, R. A. *Tetrahedron Lett.* **2012**, *53*, 4240–4242.

(19) Pena, M. A.; Sestelo, J. P.; Sarandeses, L. A. *Synthesis* **2005**, *2005*, 485–492.

(20) Yamada, Y. M. A.; Sarkar, S. M.; Uozumi, Y. *J. Am. Chem. Soc.* **2012**, *134*, 3190–3198.

(21) Dai, Q.; Gao, W.; Liu, D.; Kapes, L. M.; Zhang, X. *J. Org. Chem.* **2006**, *71*, 3928–3934.

(22) Lü, B.; Fu, C.; Ma, S. *Tetrahedron Lett.* **2010**, *51*, 1284–1286.

(23) Molander, G. A.; Iannazzo, L. *J. Org. Chem.* **2011**, *76*, 9182–9187.

(24) Data Collection and Processing Software, Rigaku Corporation (1998-2015). Tokyo 196-8666, Japan.

(25) Burla, M. C.; Caliandro, R.; Camalli, M.; Carrozzini, B.; Cascarano, G. L.; Giacovazzo, C.; Mallamo, M.; Mazzone, A.; Polidori, G.; Spagna, R. *J. Appl. Cryst.* **2012**, *45*, 357–361.

(26) Sheldrick, G. M. *Acta Cryst.* **2008**, *A64*, 112–122.

(27) Analysis Package, Rigaku Corporation (2000-2015). Tokyo 196-8666, Japan.

(28) Spek, A. L. *Acta Crystallogr., Sect. D* **2009**, 65, 148–155.

Publication List

(1) "Site-selective C–H Borylation of Quinolines at the C-8 Position Catalyzed by a Silica-supported Phosphane-Iridium System."
Konishi, S.; Kawamorita, S.; Iwai, T.; Steel, P. G.; Marder, T. B.; Sawamura, M. *Chem. Asian J.* **2014**, *9*, 434–438.

(2) "Silica-supported Triptycene-type Phosphine. Synthesis, Characterization, and Application to Pd-Catalyzed Suzuki–Miyaura Cross-coupling of Chloroarenes."
Iwai, T.; Konishi, S.; Miyazaki, T.; Kawamorita, S.; Yokokawa, N.; Ohmiya, H.; Sawamura, M. *ACS Catal.* **2015**, *5*, 7254–7264.

(3) "Synthesis, Properties and Catalytic Application of a Triptycene-Type Borate-Phosphine Ligand."
Konishi, S.; Iwai, T.; Sawamura, M. *Organometallics* **2018**, in Press.

Acknowledgement

The study described in this thesis had been carried out under the direction of Professor Masaya Sawamura at Graduate School of Chemical Sciences and Engineering, Hokkaido University.

I would like to express my sincere gratitude to my supervisor, Professor Masaya Sawamura for providing me this precious study opportunity, kind guidance, enormous supports, insightful comments and invaluable discussion. I also wish to express my deepest appreciation to Assistant Professor Tomohiro Iwai for his elaborated guidance, and invaluable discussion, considerable encouragement and kind support. I am also very grateful to Professor Hirohisa Ohmiya for his helpful discussions, considerable encouragement and considerable suggestions. I wish to express my appreciation to Dr. Yohei Shimizu and Dr. Fernando Arteaga Arteaga for helpful discussions and suggestions.

Professor Keiji Tanino, Professor Takanori Suzuki, Professor Takeshi Ohkuma gave me insightful comment and considerate suggestions on this thesis.

Moreover, I am very grateful to my co-workers. I especially wish to express my deepest appreciation to Dr. Soichiro Kawamorita for his elaborated guidance and supports. Mr. Tatsuya Miyazaki and Ms. Natsumi Yokokawa made a significant contribution to the study described in Chapter 2. I am also thankful to Dr. Kazunori Nagao, Dr. Tomoya Harada, Dr. Ryo Murakami, Dr. Yurie Takayama, Dr. Kentaro Hohjoh, Mr. Takamichi Wakamatsu, Mr. Ryotaro Tanaka and all other members in Prof. Sawamura's group for the helpful discussions and continuous encouragements.

Finally, I also like to express my gratitude to my family for their moral supports and continuous assistance.

Shota Konishi

June, 2018